A numerical investigation into natural ventilation of double skin façades and the improvement of energy efficiency in high rise buildings

by

NAIF OLAYAN ALHARBI

A thesis Submitted in partial fulfilment of the requirements for the degree of Doctor of Philosophy at the University of Central Lancashire

School of Engineering

August 2022

بسم الله الرحمن الرحيم

Statement of Original Authorship

The work contained in this thesis has not been previously submitted to meet requirements for an award at this or any other higher education institution. To the best of my knowledge and belief, the thesis contains no material previously published or written by another person except where due reference is made.

Signature: *Naif*

Date: $1 - 08 - 2022$

List of Publications

Alharbi, N. & Liu, W. 2015. A multi-scale method for large eddy simulation of

turbulence, 2015 ICMIDS conference, http://www.arl.psu.edu/ICMIDS/

Alharbi, N. & Liu, W. 2017. An investigation into solar double-skin Façades for

high rise buildings, Internal Engineering Conference & Exhibition

(IECE), in Riyadh KSA 4-7 December 2017

Abstract

Buildings consume a large amount of energy, around 40% of global energy use. Under keeping comfortable environments for building occupants, reduction of buildings' energy use is significant and also challenging. Passive techniques, such as natural ventilation, are promoted in certain climates to provide low energy cooling and ventilation. However, controlling natural ventilation in an effective manner to maintain occupant comfort can be a difficult task, particularly during warm periods.

One of the passive techniques is carefully designing building façade, e.g., 'double-skin façade', one of the best options in managing the interaction between the outdoor and internal spaces. Double-skin façade (DSF) building is one of the energy conservation opportunities available through recent intelligent buildings. Not only does the façade constitute the architectural aesthetics of the building, but it is also of great importance due to its impact on energy performance and interior function. Therefore, the development of innovative façade technology continues to be one of the most active research areas for the built environment. In this work, an investigation into the optimal application of a double-skin façade (DSF) for high-rise buildings is presented using computational fluid dynamics (CFD) approaches.

The work firstly reviewed state-of-the-art research, technologies and applications for double-skin façades. Based on the review, the author then proposed some new and innovative forms of double-skin façade which are particularly

applicable to high-rise buildings. These façades offer natural ventilations for tall office buildings. The forces driving the ventilations, i.e., buoyancies, are produced from the solar energy. As CFD is applied, the effects of the wind and buoyancy are then investigated separately or in combination.

The overall objectives of the investigations are to determine whether the magnitude of airflow rates and the desired flow pattern through openings can be achieved over a range of specified conditions. Potential conditions where the design goals may not be ensured are identified. It is supposed that a seasonal control could be developed to provide the optimum desired flow pattern, sufficient flow rates for ventilated cooling and uniform airflow rates across floors. Segmented and non-segmented DSF cavity patterns with ventilated double façades are adopted as the main building configurations for coping with the potential magnitude of wind at high levels. The ducts between cavities are designed to control the natural ventilations in tall office buildings. Steady state condition approaches are adopted for investigating these cases. The results show that segmentation has tends to create relatively uniform air pressure, airflow and temperature at various elevations within the building, and therefore has the best performance.

In order to quantitatively assess the performance of the proposed double-skin façades, various CFD models were developed. These models are involved in turbulence calculations with kappa-epsilon model heat transfer. Various validations of the CFD models show that the models are able to produce precise

results. Ultimately, the CFD, CFX5 codes were applied to estimate and investigate the performance of the proposed DSFs and produce the optimal application of double-skin façades for high-rise buildings.

Table of Contents

List of Tables

List of Figures

List of Nomenclature and Abbreviations

ACH: Air change per hour

CFD: Computational fluid dynamics

DNS: Direct numerical simulation

DSF: Double-skin façade

DSFD: Double-skin façade with duct

FCU: Fan coil unit

HVAC: Heating, ventilation and air conditioning

IAQ: Indoor air quality

IEQ: Indoor environmental quality

LES: Large Eddy Simulations Model

NPL: Neutral pressure line

PDEs: Partial differential equations

SBS: Sick building syndrome

WWR: Wall opening ratio

CHAPTER 1 Introduction

1.1 Background

Energy consumption in heating, ventilation and air conditioning (HVAC) constitutes a large part of the total energy use of buildings. In developed nations, the energy consumption in HVAC is approximately 40% of the total energy used in buildings (Perez-Lombard et al., 2005), while in Europe, approximately 76% of this consumption is for HVAC (Laustsen, 2008). Therefore, innovation of traditional HVAC technology and reduction of energy consumption is of significance in modern building developments.

There are various strategies for minimising HVAC energy consumption, for example, making buildings more airtight, insulating them to avoid heat transfer with the exterior, producing higher efficiency appliances, passively ventilating the building and achieving better control. It will raise various issues of energy use during implementing these strategies effectively.

The issue of energy use of a building, indoor environmental quality (IEQ) and its effects on the people who live in the building is the subject of increasing research (ASHRAE, 2013). IEQ is defined as environmental quality within a building in terms of impact on the occupants' wellbeing and health (Center for Disease Control and Prevention, 2013), and includes factors such as light, temperature, quality of air and contamination. Each of these, except for light, is strongly

influenced by ventilation. That means that ventilation systems have central significance in IEQ.

Naturally ventilated designs rely on air flowing into and out of the building via placement of openings in the envelope of the building. This flow can result from stack effects and from wind (Awbi, 2003). In the past 30 years, a large body of research has developed on natural ventilation, since the ability of this approach can offer good IEQ and satisfy occupants while energy consumption and effects on the environment are far lower than for mechanically ventilated buildings (Awbi, 2008; Ghiaus and Allard, 2005).

Naturally ventilated designs are considered to perform well within hot and humid climates in passively cooling to increase comfort, that is, mechanical ventilation is less needed in such environments (Haase and Amato, 2006; Aynsley, 2007; Nguyen and Reiter, 2014). Nonetheless, control of natural ventilations is a key and challenging element to achieving acceptable IEQ without lower energy consumption.

According to Nicol et al. (2012), inappropriate building envelopes which disconnect the inside of the building from the outside surroundings are an important source of poor IEQ, reducing comfort for occupants (Sadineni et al., 2011; Ochoa and Capeluto, 2009; IEA, 2013a, b). This envelope is the main heat barrier from outside to inside, and is therefore significant for both ventilation and comfort, besides defining the building aesthetically (Sadineni et al., 2011).

The use of a double-skin façade (DSF) is becoming more acceptable as a tool for passive ventilation which, in addition to allowing a modern office aesthetic with transparent finishes, has a moderating effect on temperature inside the building, which can lower energy consumption for HVAC. DSFs contain an external skin consisting of full glazing, which is applied on top of the main façade to create a gap for airflow: sun shading tools are frequently utilised for protection of the inside of the building against excess heat from the sun which causes the interior to overheat (Oesterle et al., 2001).

1.1.1 Development of the double-skin façade

Designs for double-skin façades were first recorded in 1849 by Jean-Baptist Jobard (Streicher, 2005), who was director of the Brussels Industrial Museum. The design was proposed as a thermal control solution whereby warm air could circulate in the gap between the two façades in the colder seasons. Some types of non-ventilation DSFs forming a buffer came into use in temperate zones. In the early twentieth century, a German building, Steiff Machine Hall, was built with a controllable opening into the cavity, constituting one of the first examples of DSFs for natural ventilation. In the late 1920s, the La Cité de Refuge designed by Le Corbusier included a DSF with ventilation to the cavity with the intention of preventing heat from passing through the façade, making the interior more comfortable in terms of temperature (Saelens, 2002).

In the 1970s-80s, global energy supply reached crisis state, and the resultant moves within Europe to address energy consumption included a rise in the

number of façades using mechanical ventilation (Saelens, 2002). Following this, growing attention to threats to the environment and the desire to present new buildings as 'green' motivated a rapid rise in DSF use. One of the earlier designs to use shade-creating tools in the southern cavity was for the Brussels-based UCB Centre, and this feature was intended to avoid gaining large amounts of heat during sunny periods, while maintaining a transparent effect in the façade (Kragh, 2001).

DSF design has developed continuously since its introduction, fulfilling the aesthetic demand for transparency while also considering environmental functions. Currently, over half of DSFs are in northern and continental Europe: among these, Germany, which was an early implementer of the DSF, has 20% of such buildings. Elsewhere, Japan has around 13% of the global total, while others are in the USA, Australia and Canada, as well as other countries globally (Anđelković et al., 2015).

1.1.2 Application of double-skin façade in warm climates

DSF designs for reduced energy use in buildings within temperate zones have developed certain characteristics, including skins with a high level of insulation, and being glazed with quality glass which has a low U-value, performing well in winter as well as reducing heat loads. On the other hand, there are various examples where buildings have been shown to perform poorly in summer, with increased cooling requirements due to production of excess heat (Darkwa et al., 2014). This leads to more extensive air-conditioning systems which may consume

more energy than what is saved on heating in winter due to the DSF. This demonstrates that DSFs may make a building more or less energy efficient and that passively collected solar energy may have different effects (Streicher et al., 2007; Marques da Silva et al., 2015). The disadvantages of the DSF have led to the addition of features to protect against the sun, and to modified ventilating systems and geometrical façade designs which allow the building to function more effectively in the summer (Gratia and De Herde, 2004b; Eicker et al., 2008). Based on this, the seasonal mode of operation of the DSF is considered (Mingotti et al., 2011; Gratia and De Herde, 2007).

DSF designs offer a potential reduction in the need for cooling of buildings with extensive glazing in the warmer seasons, and this has led to these designs being implemented in urban settings in warm–hot climates to create buildings which present an image of business success in line with sustainable aims. Based on this, a large body of experimental and theoretical research has been conducted to explore whether DSF technologies can be effective in warm countries, as for example, in Spain (Torres et al., 2007), Singapore (Chou et al., 2009), China (Zhang et al., 2010), India (Singh et al., 2011), Malaysia (Rahmani et al., 2012), and the United Arab Emirates (Radhi et al., 2013).

While the majority of the DSF studies for warmer countries consider designs involving air conditioning, some recent research has begun to consider the use of DSFs to naturally ventilate the interior areas used by occupants. Naturally

ventilated buildings offer significant savings in energy consumption and mitigation of impact on the environment in comparison with mechanically ventilated ones, as well as being more satisfying to users while reducing the cost of operation (Day and Gunderson, 2015; Aflaki et al., 2015; Wood and Salib, 2013).

Natural ventilation using DSFs relies upon airflow in the cavity, which results from thermal buoyancy based on the differential in temperature between the cavity air and the comparatively less warm air which surrounds it. The warm air of the cavity creates a thermal chimney effect in which cooler external air is continuously sucked in, resulting in convection of air throughout the construction. In this model, greater temperature differentials lead to greater flows of air internally, leading to greater satisfaction for those within the building. However, this process is complicated by the manner in which the façade and building interact; meaning that, for hotter climates, additional features may need to be designed into the building to achieve this cooling function, including solar control features to avoid the building accumulating too much heat, as well as the choice of suitable shapes and forms of buildings by architects and properly-orienting buildings in line with exposure to wind and sun (CIBSE, 2005).

DSF technologies may potentially offer sustainability as an option for corporate buildings in countries where climatic conditions are warm or hot. However, these designs are currently inefficient and frequently cause excessive heat

accumulation, with major temperature increases within the cavity forming an essential obstacle for such designs in warmer conditions. Warm/hot climates do not offer extensive potential for cooling, whereas occupants expect a comfortable temperature when using a building (CIBSE, 2005). The heating effect inside the cavity may contribute to cooling through thermal buoyancy effects which cause vertical airflow; when DSF openings are not operated properly, this can cause thermal discomfort (Hamza, 2004; Gratia and De Herde, 2007a). Anecdotal evidence points to thermal discomfort occurring in such buildings during periods of very hot weather, but no studies were found that explore the implementation of the design features to decrease the danger of overheating in this context.

DSFs have been put forward as an approach to passively enhancing thermal performance in buildings using natural ventilation in hotter climates, dependent on appropriate designs being developed (CIBSE, 2005; Nasrollahi and Salehi, 2015). Despite the large amount of recent research conducted on DSF technologies, there is little research as applied to buildings with natural ventilation. In addition, there is a need to develop basic principles to underpin the way DSFs can be designed and operated in various climates (Mingotti et al., 2011; Darkwa et al., 2014).

1.2 Statement of Problems

The primary aspect of integrating natural ventilation into building design is that it does not only decrease energy use and costs, but it also creates pleasant, safe,

and efficient environments. Air movement occurs as a result of pressure differences between the inside of the building and outside conditions, which are caused by factors such as wind and buoyancy forces. In moderate climates, double skin facades are commonly used to allow office spaces to be naturally ventilated more effectively; Thermally buoyant forces in the gap between the facades are responsible for this. The forces created by these shafts promote natural air ventilation (Blaser, 2004). Furthermore, according to Irwin et al. (2008), the DSF protects opening windows in a tall building from strong winds. These features are absent from buildings that do not have a DSF. Building segmentation alongside DSF allows full control over the airflow inside the building as opposed to other methods such as single facade building or building segmentation without DSF (Etheridge and Ford, 2008). These features of DSF with segmentation of building make them the focus of this study without the other patterns of natural ventilation in high rise buildings.

Good design of DSF is highly complex work which requires buildings to reflect the contemporary desire for transparency but may also potentially contribute to the way the building performs thermally, through the use of suitable designs. For such designs to be developed, the complex thermal behaviours which underlie the operation of DSFs and the factors which affect these, including the shape and materials chosen for the construction, need to be comprehensively studied. Moreover, most previous research considers thermal performance for buildings

with air-conditioning and in cooler climates, as the majority of DSFs are located in such climates.

Mechanical ventilation systems are in widespread use within tall buildings, because the DSF performance, airflow control, and high building segmentation are issues that still need more investigation to enhance natural ventilation in high rise buildings. This research will study these issues to acquire more knowledge for natural ventilation strategies in high buildings to promote sustainability, decrease energy consumption and reduce operational costs, innovative designs are needed. This study puts forward novel concepts for naturally ventilated high-rise buildings, utilising a DSF and atrium design. It will develop a basic understanding regarding the application of natural ventilation designs to fulfil a range of criteria and reduce the energy consumed to operate the high-rise building.

Furthermore, the investigations presented here also contribute by developing designs to increase the accuracy with which design case studies are analysed. To consider the potential of varied DSF design approaches for enhancing efficiency in the thermal performance of buildings, a hypothesis is put forward, as follows:

Improving natural ventilation systems by applying an appropriate double-skin façade can enhance thermal performance in office-type buildings across a range of climates.

Therefore, this study assumes a pattern of DSF design which will help promote the application of natural ventilation in buildings, and then conducts the necessary tests for this design in order to ascertain its effectiveness and more of the obstacles and advantages of this modern design, in expectation of a qualitative shift in natural ventilation through patterns of DSF.

1.3   Aim and Objectives

Systems of natural ventilation are far more complex than mechanical systems in airflow behaviours and processes. This presents challenges for the use of natural ventilation in high-rise buildings. As mentioned above, however, there is a huge potential to improve HVAC performance in modern tall buildings through utilising DSFs. This thesis will, therefore, investigate the basic flow processes within naturally-ventilated tall buildings using a computational fluid dynamics approach, so as to contribute to a better understanding of the fundamental issues of applying DSFs in high-rise buildings, thereby improving control over airflow therein:

More specifically, the project will address the flow issues below:

1) To investigate flow structure and behaviour in a DSF cavity with a range of openings and compartments—In this study, DSF is being introduced to a building, with a novel solar energy collection source constructed surrounding the building, causing natural convection patterns within the

building to be modified. The study seeks to understand the changed patterns, and therefore studies it as objective 1.

2) To comprehensively investigate transfers of mass and heat caused by natural convection—Airflow within a building directly affects such transfers. Thermal transfer leads to effects on thermal comfort for building occupants, and mass transfer relates to the way in which pollutants are dispersed. Both transfers are an essential part of measuring the impact of the DSF on the performance of the chosen building and are therefore the focus of objective 2.

3) To investigate the effectiveness of segmentation in conjunction with DSF in high-rise buildings—This is to increase the understanding of how DSF and segmentation can complement one another to improve airflow within a space in a high-rise building. This combination of strategies is the topic of objective 3.

4) To investigate the impact of varied weather conditions on within-cavity airflow—Surrounding temperatures and other factors depend upon climate and specific weather patterns and form an significant influence on natural convection within buildings. Therefore, convection is studied across a range of seasonal weather conditions, including summer and winter, including assessing wind as a factor which influences ventilation, etc. The study will contribute to knowledge of the way in which

ventilation systems perform in general. This impact is analysed in objective 4.

1.4 Scope of the Research in this Thesis

In addition to thermal performance, various factors should be considered as part of DSF design, including acoustic behaviours (Oesterle et al., 2001), ventilation during the night (Gratia and De Herde, 2004b), maintaining solar shading features, structural weight, impacts upon floor space and fire regulations (Torres et al., 2007). Designing building and maintaining a DSF also has cost implications, being more costly than conventional single façade buildings (Oesterle et al., 2001; Poirazis, 2006), and this raises issues for implementing this technology.

While each of these factors should be investigated before taking a decision to implement a DSF design, they fall outside the scope of this research project which investigates thermal performance and airflow only.

1.5 Structure of the Thesis

CHAPTER 1. Introduction

This chapter gives a background to the development of double-skin façades as well as their use in warm-climate areas. The rationale for the study is provided, along with its scope, aims and main objectives.

CHAPTER 2. Literature Review

This chapter reviews the literature to investigate current understanding of DSFs' thermal performance and discusses the principles on which natural ventilation

via DSFs is based. Key findings from the literature are assessed and categorised into 3 types of parameters with an influence on the heat performance of DSF-clad buildings. Finally, guidance for designing natural ventilation through DSFs is formulated.

CHAPTER 3. Mathematical and Turbulence Modelling

Three principles or fundamental conservation laws are the basis of this research. They are the laws of conservation of mass, momentum and energy. By applying these principles, one can derive a set of partial differential equations which are called basic equations. The basic equations, i.e., the Navier-Stokes equations, are equivalently mathematical expressions of the conservation laws. Another complex aspect of solving the basic equations is turbulence. As is known, when a fluid flows quickly, i.e., Reynolds number is large, the flow will be turbulent. Turbulence leads to difficulties in obtaining the solutions to the basic equations. This chapter will address the basic equations and turbulence modelling.

CHAPTER 4. Numerical Models and Validation

This chapter outlines the fundamental knowledge of numerical modelling in CFD, in which the fluid governing equations, turbulence modelling, natural ventilation modelling, Boussinesq approximation and boundary conditions are

described in detail. The turbulence modelling technique of CFD used to model natural and forced convection in building ventilation is also presented. This is the approach followed in the current study.

CHAPTER 5. Validation

This chapter provides the necessary validation works for the proposed solution method.

CHAPTER 6. Buoyancy-driven (stack) ventilation

This chapter explores the two most important factors in the performance of double skin façades, namely thermal buoyancy and wind pressure. This is done by studying their effects on air behaviour within a part of a building, as a foundation for use in larger buildings. The results will be analysed and discussed in the context of the findings of previous studies. This is with a view to fulfilling objectives 1 and 2 of the study.

CHAPTER 7. Ventilation into the Segmentation of a tall building

In this chapter, the proposed pattern for applying DSF is studied for its performance in high-rise buildings. This pattern involves a multi-storey double-skin façade with a duct at the top of each segment linking the DSF cavity to the atrium to transfer the undesired airflow and buoyancy overload away from the occupational spaces. The effects of segmenting the DSF cavity will also be studied. Moreover, the effects of the ambient factors of temperature and wind on

this pattern will be investigated. The results will be analysed and discussed. This is with a view to fulling objectives 3 and 4 of the study.

CHAPTER 8. Investigation into Natural Ventilation of (Bdaia **Tower)**

To fulfil the main aim of this study and after fulfilling the objectives, the proposed pattern will be studied for its performance in a part of the Bdaia Tower in Al Khobar, Saudi Arabia. This building is one of the most complicated in terms of its design. The region in which it is located has a climate consisting of hot and mild weather.

CHAPTER 9. Conclusions and Future Work

This chapter presents and discusses the most significant findings from the study and considers possible further research.

CHAPTER 2. Literature Review

This chapter discusses existing research on functions and performance of double-skin façades (DSF) applied in buildings, particularly those that are high-rise in nature. The knowledge related to is reviewed and summarised, forming a foundation for the work in this project.

The basic functions of DSF are to reduce building energy consumption, to improve the performance of heating, ventilation and air conditioning (HVAC) of buildings and to provide a better and more satisfactory environment. Behind these functions lies complex knowledge of aerodynamics, heat transfer and pollutant dispersion, which are, therefore, the key aspects of this chapter. Finally, the technical standards and codes pertaining to DSF that are widely used in practice will be addressed.

2.1 Introduction to Ventilation

Ventilating a building involves transferring fresh external air to the building's internal spaces, distributing it across the space. This allows the building's internal emissions to be dissipated and improves the quality of the air breathed by its occupants (Atkinson, 2009; Awbi, 2003). Various factors must be considered when designing and building ventilation systems to meet the aims set for them, including variability of climatic conditions, minimising power demands and consistent delivery across different urban conditions. Thus, significant complexity is involved in creating effective systems for ventilation (Awbi, 2003).

There are three main forms of ventilation system; natural, mechanical and a hybrid using natural and mechanical ventilation. A large number of current ventilation systems are mechanical, but the costs associated with this approach have risen significantly. Within high-rise buildings, these costs have come to represent a significant part of buildings' maintenance costs. To develop alternative solutions to this problem, the attention of research and design has been drawn to the development of naturally ventilated systems (Joe et al., 2014).

Mechanically ventilating buildings require mechanical fans to be used to create internal airflow. These may be positioned within walls, windows or within air ducts which take air into or out of internal rooms. In contrast, naturally ventilated buildings rely on designs that utilise natural forces such as the wind along with thermal buoyancy forces, which arise from a difference in density between internal and external air. These forces push external air into the building via specific apertures in the envelope, such as door and window openings, solar chimneys, trickle ventilators and wind towers. The way in which such systems perform is reliant on climatic conditions, human activities and architectural design (Atkinson, 2009), with hybrid systems using mixed modalities of natural and mechanical elements. These systems utilise naturally occurring forces to drive airflows under general conditions, moving to mechanical methods where sufficient airflows are not achieved (Atkinson, 2009).

While this thesis relates to natural ventilation, it is recognised that there are circumstances where natural approaches are not effective and mechanical ventilation is suitable. For example, low air quality or significant noise in the surroundings of the building could mean that it would not be practical to have windows open. Deep-plan and completely internal-wall rooms might also need to be mechanically ventilated. Furthermore, mechanical systems may be required to meet specific demands for narrowly controlled conditions or clean conditions (Atkinson, 2009). Moreover, thermal comfort levels may not be met through natural ventilation due to factors such as very hot weather, high density of occupants or equipment emitting high levels of heat. These issues can be addressed by employing hybrid methods of ventilation, such as using mechanical ventilation only when temperatures reach their highest levels, while naturally ventilating the building at other times. This can allow excess heat to be avoided using lower energy consumption than when mechanical ventilation is used.

Hybrid/mixed-mode approaches to ventilating buildings can, in theory, offer the benefits of each approach while lessening the impact of their drawbacks (Kleiven, 2003).

2.2 Natural Ventilation

Buildings must be ventilated in order to maintain the internal conditions of the building at a satisfactory standard of air quality by removing pollutants, as well as to maintain an appropriate temperature. Mechanical ventilation might involve

operating fans to extract and supply air, while natural methods utilise air exchange via louvres and window openings, using stack effects/thermal buoyancy and wind to drive this exchange. Mechanical systems of ventilating buildings sometimes have equipment for conditioning the external air entering the building prior to allowing it to flow into the rooms which require ventilation. Although mechanical approaches generally increase the extent of controls on the air conditions within a building, natural ventilation usually presents a lower cost burden when viewed on an annual basis (Bordass et al., 2001).

Until the 20th Century and the introduction of mechanical ventilation systems, buildings were exclusively naturally ventilated. However, from the second half of the 19th Century, various factors led to technological moves to improve air quality inside buildings. Importantly, from that time onwards, air quality in cities has been affected by heavy pollution, first from oil and coal being burnt for power, and then from engine emissions as cars were introduced and grew in number (Heinberg, 2009). Highly polluted external air was transferred into highly polluted air within buildings based on natural ventilation methods, and this led to technological innovations to enhance the quality of internal air despite external conditions. New York's Larkin building, constructed in 1906, is an early example of mechanical ventilation use for a large, non-residential construction. Frank Lloyd Wright used a mechanical ventilation system and sealed the building in order to minimise both noises coming from the railway close to the building and pollutants in the air within the building (Thomas, 2013).

As well as addressing the frequent external air pollution issues in the 20th Century, during most of this period, energy was comparatively low cost, meaning that the ongoing cost involved in mechanically ventilating buildings was not considered a major factor for design and there was, therefore, limited perceived need to develop different approaches to ventilation. Thomas. 2013, states that this situation has continued, although to a lesser extent, into the current time and that drives for lower energy consumption are more related to concerns for the environment than cost reduction.

The move towards mechanically ventilated buildings was also driven by the aesthetics of modernism and the symbolic 'glass box' appearance of tower blocks, which reflected the feeling of modernity and the futuristic outlook of society (Thomas, 2013) and was, therefore, pursued by both architects and their clients. Mechanical ventilation of such buildings is successful on many measures, such as reducing the ingress of external contaminants, lowering incoming noise and maintaining thermal comfort throughout hot weather. Nevertheless, it involves significant energy consumption.

Increase in the cost of energy has added significantly to the costs involved in mechanically ventilating buildings for user comfort (Popescu et al. 2012). In addition, climate change, environmental footprint and the need to conserve natural resources have become more pressing concerns, with organisations coming under pressure to reduce energy consumption.

However, it is important that moves to reduce energy demand and other impacts on the environment still address the need of the building's users for comfort, as IEQ (indoor environmental quality) is shown to significantly influence the health, productivity and satisfaction levels, as discussed in the sub-sections which follow. The objectives while designing and when managing buildings frequently conflict, and this can be the case when the objectives are to achieve both best comfort for occupants and reduced power demand.

2.2.1 User comfort

Current lifestyle patterns see many individuals spending long periods of time indoors, implying a need to prioritise internal comfort levels when designing buildings. IEQ includes a number of different factors, covering IAQ (indoor air quality), thermal comfort, light and acoustic conditions, visual comfort, ergonomic factors, and more. It is not practically possible to achieve satisfaction for every individual who uses the building, due to variations in individual preferences.

Much of the existing work related to mechanical ventilation of buildings aims to enhance the satisfaction levels of users while incurring the lowest achievable power costs (Aswani et al., 2012; Ferreira et al., 2012; Oldewurtel et al., 2012). However, the current thesis deals with natural ventilation systems, and its main aim is to enhance comfort for users of the building. Showing the potential for greater control increases the feasibility of natural ventilation systems being used

in place of mechanically ventilating different building designs, which could have an indirect impact on energy use.

2.2.2 Impacts of ventilation on productivity levels and health of occupants

In addition to considering the comfort and satisfaction of occupants, IEQ is associated with productivity and health. Historically, it was assumed that internal pollutants mainly came from the building's users, via biological emissions and smoke from tobacco (Awbi, 2003). Over the past several decades, however, knowledge in this area has progressed, and it is now understood that for modern buildings a range of features, including furniture, finished surfaces and equipment can release contaminating chemicals. Indoor pollution may also originate from biological sources; especially in poorly ventilated buildings, condensation may arise, allowing fungal and bacterial growth. The legionella bacterium, for instance, can multiply in conditions of warmth and moisture within hot water systems, as well as evaporation cooling systems and (HVAC) coolers (Edagawa et al., 2008; Nguyen et al., 2006). These pollutants can adversely affect the wellbeing and health of a building's users.

Sick building syndrome (SBS) is a term often used to include illnesses and health issues that are associated with a building and its internal conditions. Frequently reported symptoms in SBS are problems affecting breathing, headaches, tiredness and irritated skin, nose and eyes (Fisk 2000). SBS has reached significant levels in certain buildings which have come to be known as 'sick buildings', with

many occupants affected. Nevertheless, symptoms associated with SBS can also be reported due to high density of occupants within buildings that have not had such issues recorded previously (Nelson et al., 1995; Brightman et al., 1997).

Several studies report that buildings using natural ventilation have lower rates of SBS in comparison to those using mechanical ventilation. Muhič and Butala (2004) compared buildings using mechanical and natural ventilation in a 6-month study in which occupants were surveyed and set parameters were measured. The findings show that SBS levels are significantly increased for buildings with mechanical ventilation, with all associated symptoms apart from inflamed eyes and swelling of the eyelids showing greater levels in comparison to naturally ventilated buildings. In a similar study, Vincent et al. (1997) surveyed 1,144 individuals working in one naturally ventilated building, one building with air conditioning and one building with a fan coil unit (FCU) cooling system. For the buildings with FCU and air-conditioning, the occurrence of non-specific symptoms was slightly more than in the building with the natural ventilation system. It is clear, however, that natural ventilation is not appropriate in certain situations. Thus, where the external air has high levels of particulate matter, natural ventilation may reduce SBS but expose occupants to different health issues. Dutton et al. (2013) examined naturally ventilated office buildings in California, and report that, although symptoms of SBS were reduced, the increased ingress of pollutants into occupied spaces would increase health-related costs significantly.

In addition to influencing the occurrence of symptoms of illness, IEQ impacts the mental and physical performance of those using a building. Several works report that productivity is influenced to a significant extent by thermal comfort levels (Fisk, 2000a; Wyon, 1993, 1997; Wyon et al., 1979), and additionally by IAQ (Heerwagen, 2000; Wyon, 2004; Clements-Croome, 2006). Issues associated with insufficient ventilation or low IAQ are often found in schools, and many studies consider how academic attainment can be enhanced by improving IAQ (Clements-Croome et al., 2008; Daisey et al., 2003; Ole Fanger, 2006). Higher levels of CO_2 in particular are reported to influence health and learning performance (Myhrvold et al., 1996).

Implementation of higher ventilation rates to reduce cases of SBS as well as to increase occupants' productivity is reported in several works (Fisk et al., 2012; Sundell et al., 2011; Seppänen, 2006). Moreover, the effective control of thermal comfort levels is reported to be linked to more productive occupants (Fisk, 2000b). Developing greater control in natural approaches to ventilation, MPC, as considered in the current work, could potentially allow thermal comfort and IAQ to be enhanced.

Besides increasing satisfaction levels among users and benefiting productivity and health, organisations can benefit financially from enhanced-control natural ventilation systems, through both reduced power consumption and better

ventilated buildings, which can lead to harder to measure financial benefits due to improvements in occupant health and productivity.

2.2.3 Natural ventilation design

Naturally ventilated designs exploit heat differentials and wind forces in driving airflows, which has conventionally been done through the use of vents and/or windows operated by the user. Many different designs exist for the placing of windows/apertures, but most spaces employing natural ventilation fall into one of 3 categories of design; single-sided ventilation, stack ventilation or cross ventilation (see Table 2.1).

Table 2.1: Three main categories of naturally ventilated space (CIBSE 2005).

Design category	Principal driving force	Applications
Single	Wind or thermal buoyancy	Shallow plan
Cross	Wind	Shallow or deeper plan
Stack	Buoyancy	Larger spaces possible

Single-sided designs include apertures for ventilation on a single side of the space. Turbulence from wind is the main driver of airflows, while buoyancy can

become a driving force where the design includes an opening with adequate vertical height to allow this (CIBSE 2005). Where several apertures are installed vertically at various heights, buoyancy can be used to enhance airflows, with the enhancement in flow rates connected directly to the amount of vertical separation of each opening as well as the internal-external variation in temperature. However, even where several vertically distributed openings are used, single-sided ventilation is only suitable for shallow room plans, with CIBSE (2005) recommending depths of no more than 2-2.5 times the vertical distance from floor to ceiling as a general rule.

Cross-ventilated spaces have windows/vents on either side, and the main driver of airflows is wind. However, certain cross-ventilation designs also utilise buoyancy. Cross-ventilated designs allow deeper rooms, but the further the air travels across the room, the greater the temperature, and decreased air quality may also be an issue.

Based on the above, the possible depth of rooms is limited in designs using cross ventilation or single-sided ventilation. Moreover, as daylight can be exploited more fully in shallow room plans, buildings with natural ventilation are conventionally designed at shallow depths. For deeper designs to be used with natural ventilation, an alternative design is stack ventilation. This approach relies mainly on buoyancy to drive airflows. Stack ventilation draws air across the space as it enters and exits via a vertically oriented space, which may be an atrium

or a chimney for example. Chimneys, as wind towers, have been employed to improve room ventilation for several centuries in some Middle Eastern architectural designs, using buoyancy and wind to drive flows (Bahadori, 1978) (See Figure 2.1). Recent decades have seen solutions based on stack effects being applied within the UK and other countries globally for driving airflows.

Figure 2.1: Use of natural ventilation in the Middle East (Isa bin Ali: Wikipedia)

For cross- and single-sided ventilation, windows which are opened manually by users can be employed, while windows are likely to be automated to some extent in large buildings. Windows are often operated manually on the lower floors, and automated on the upper floors. When stack ventilation is used, windows are generally automated to some extent because of lack of access to exhaust apertures as well as linking together of resident spaces, which precludes the possibility of one user controlling ventilation.

2.2.4 Natural ventilation in high-rise buildings

The potential benefits, including reduction in energy consumption and therefore bills, are applicable to buildings of all heights and perhaps more pronounced in taller buildings. Nevertheless, the number of buildings with 25 or more than 25 storeys that are entirely naturally ventilated is remarkably small. There are, however, a number of noteworthy buildings with a mix of natural and mechanical, or hybrid, ventilation. This mix minimises the risk of relying on natural ventilation while affording the benefits of the natural approach. The high profile, important nature of many tall buildings means that people typically want to have full control over all the factors and conditions therein, which means an even bigger task for natural ventilation if it is to challenge its mechanical competitors.

All buildings use the same physical mechanisms for natural ventilation, such as pressure differences created by the wind and the effect of gravity on the differences in temperature inside and out. It is more difficult to control the ventilation of taller buildings entirely naturally due to the possible various magnitudes and relative magnitudes of wind and thermal buoyancy at high altitudes. This is coupled with the increase of the size of buildings, which necessitates better aerodynamics. At the same time, the greater size requires a greater range of possible controlling configurations of ventilation points.

One potential solution to the difficulties of ventilating a tall building is to segment it into isolated parts separated by open spaces (see Fig. 2.2). This now

means that designers must find the necessary flow magnitudes and directions for each individual part or 'segment', which is more difficult than for a comparable low-rise structure, due to the aerodynamic effects of each segment's outlets. The design problem is now to achieve the required flow directions and magnitudes for each segment. Original, creative solutions such as that of Daniels et al. (1993) are sometimes called upon here. The segmentation approach is most sensible for envelope design of commercial and other non-residential buildings, as long as the aerodynamic issues are adequately managed.
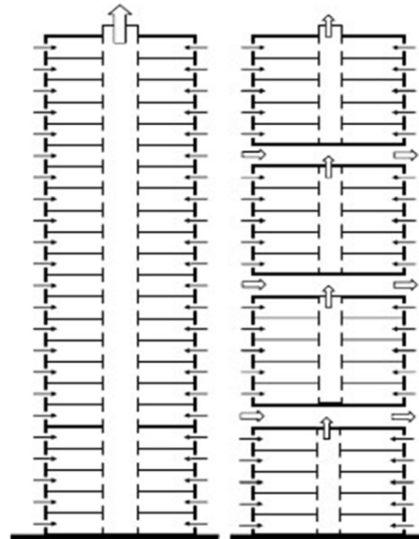
Figure 2.2. Illustration of segmentation of a tall building (Etheridge and Ford, 2008).

Certain varieties of double-skinned façades often suit tall buildings remarkably well, providing both thermal and acoustic buffering between the inside and outside of the building. This system has been widely employed in Germany in order to naturally ventilate the interior by way of the thermal buoyancy created in the glazed cavity.

The future of natural ventilation is therefore promising, provided that we have sufficient strategies to manage the wide range of conditions and factors that could be at play.

2.3 Double-Skin Façade

The DSF has an external and internal surface, between which is a space which may be centimetres or metres wide, depending on the design specifications. DSFs are principally used to enhance the way in which the building performs in terms of protection from noise, pollutants and climate externally, as well as making heating, ventilation and air-conditioning (HVAC) more efficient, while reducing the energy demands of the building. In order to achieve these objectives, smart design should be applied at a whole-building level, exploiting understanding of internal natural ventilation, with DSFs offering a solution to issues with airflows.
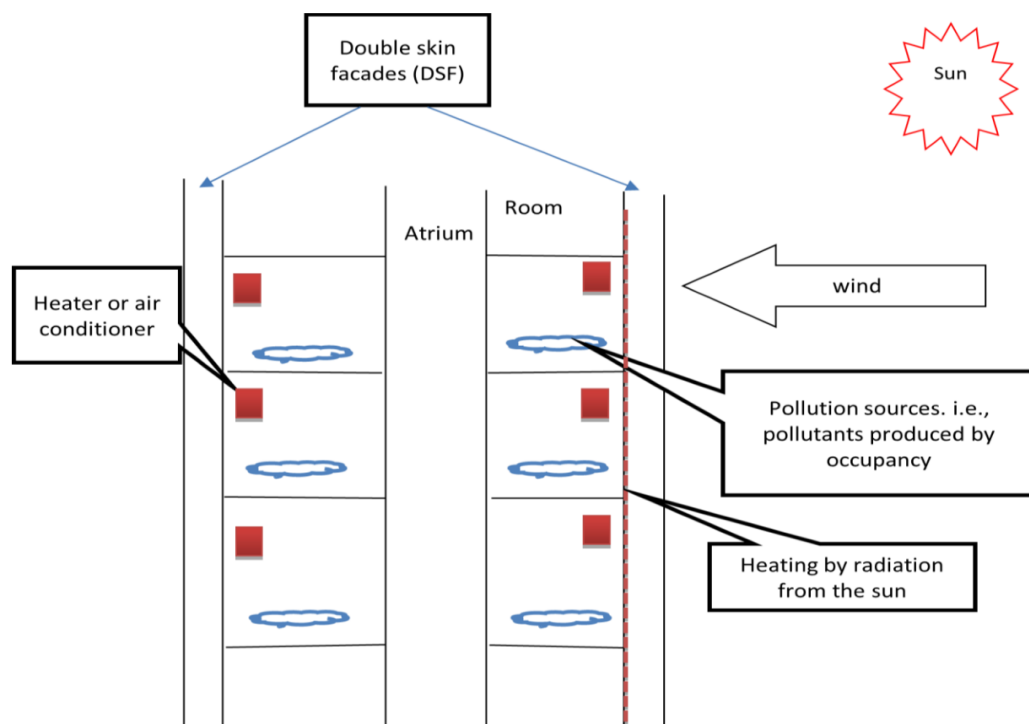
Figure 2.3: Schematic diagram showing a high-rise construction.

The schematic diagram in Figure 2.3 illustrates airflows for a DSF-clad high-rise construction. It demonstrates the driving forces operating for convection-produced airflow, such as: (a) internal air-conditioning/heating systems; (b) wind forces external to the building; and (c) buoyant air caused by solar radiation passing through the cavity of the DSF. The combination of these factors produces the building's airflow patterns, restricted by the structural features of the building, such as the DSF, and affecting mass and heat transfers both internally and bridging inside and outside spaces. Smart designs address airflow control in order to achieve thermal comfort for those using the building, as well as allowing pollutants to exit the structure, presenting an airflow problem of significant complexity. DSFs are mainly applied to achieve a reduction in the energy consumed and enhance HVAC functions, making the building more agreeable for its occupants. To achieve this, an in-depth understanding of heat transfer, dispersal of pollutants and aerodynamics is needed; these factors are the central focus of this chapter. In addition, commonly applied codes and technical standards related to DSFs are also reviewed.

2.3.1 Double-skin façade definition

Arons (2001) offers a simple definition of a double-skin façade as being:

> ''A façade that consists of two distinct planar elements that allows interior or exterior air to move through the system. This is sometimes referred to as a twin skin''.

Meanwhile, the Belgian Building Research Institute (2002) offers a more detailed definition and explanation of its working, stating the following:

> ''an active façade is a façade covering one or several storeys constructed with multiple glazed skins. The skins can be airtight or not. In this kind of façade, the air cavity situated between the skins is naturally or mechanically ventilated. The air cavity ventilation strategy may vary with time. Devices and systems are generally integrated in order to improve the indoor climate with active or passive techniques. Most of the time such systems are managed in semi-automatic way via control systems''.

Compagno (2002), on the other hand, adds detail about the materials used, describing a DSF as follows:

> ''an arrangement with a glass skin in front of the actual building façade. Solar control devices are placed in the cavity between these two skins, which protects them from the influences of the weather and air pollution a factor of particular importance in high rise buildings or ones situated in the vicinity of busy roads''.

2.3.2 Historical development of double-skin façade

Saelens (2002) cites Jean-Baptiste Jobard, who in 1849 was director of the Industrial Museum in Brussels, as describing a primitive, mechanically ventilated multiple-skin façade and that winter would see hot air circulated between two glazings, and summer would see the circulation of cold air.

Meanwhile, Santamouris (2013) cites Crespo and Neubert who both claim that a double-skin curtain wall was first employed in 1903 in the Steiff Factory, Germany, and was made of steel. The approach was deemed a success, so two more were built in 1904 and 1908 using the same system, but with wood due to financial constraints. These three buildings continue to be used to this day. According to Santamouris (2013), DSFs were being used during the late 1920s in communal housing in Russia. In 1929, Le Corbusier began designing the Cité de Refuge in Paris and the Immeuble Clarté in 1930, also in Paris; both were communal housing facilities.

There was then a lengthy period of minimal progress and development until the 1980s, when DSFs became increasingly popular, particularly on ecological grounds and due to the perceived aesthetics of multiple layers of glass. DSFs were used in many important commercial buildings, including Leslie and Godwin Ltd.'s offices. In the 1990s the environment became a hot topic in politics and society at large, pushing companies to seek buildings with DSF to improve their image as being environmentally friendly.

2.4 Basic Functions of Double-Skin Façade

Double-skin façades perform a thermal chimney function and can contribute to mechanisms for naturally ventilating buildings through differences in pressure and thermal buoyancy caused by wind and solar forces. The impacts of wind and thermal stacking are always combined with other forces, with the pattern and scale of naturally-occurring airflows within buildings being reliant upon how

strong the forces which drive these flows are, the way they are directed, and flow resistance.

The thermal buoyancy within the cavity is created primarily as a result of solar radiation reaching the DSF. In essence, a part of the total shortwave solar radiations incident on the outer layer of the DSF is reflected to the exterior, some is absorbed by the material and some directly transmitted into the cavity, according to the properties of the glazing used. A portion of the radiation absorbed is stored as thermal energy within the glazing, causing it to become hotter. Convection forces cause part of the thermal energy to move into the cavity, causing the temperature of the air to rise, while another part of the heat travels both outwards and inwards in the form of longwave radiation. Comparable processes of thermal exchange take place as radiation comes into contact with the inner skin of the façade.

When the radiation reaches an opaque surface, a portion of it is absorbed and a portion reflected, returning to the cavity. The increased thermal energy created by absorbing the radiation leads to heat convection in the direction of both the cavity and the adjacent room. In practice, there are repeated reflective processes across the cavity, and the rise in the temperature of each skin leads to temperature gain via in-cavity air convection (Pérez-Grande et al., 2005). The figure below presents a diagram to illustrate the heat exchange process.
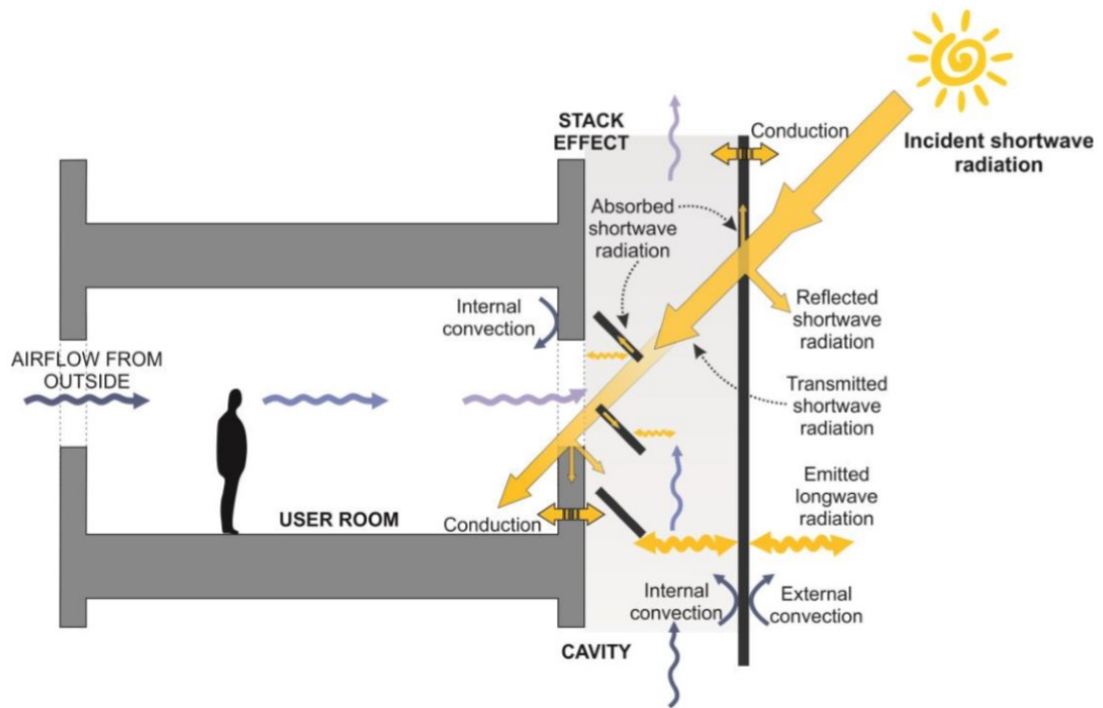
Figure 2.4: Airflow processes and transfer of heat for the double-skin façade and
the adjoining office space (Chan et al., 2014).

The cavity is frequently designed with shading mechanisms inside it to minimise radiation from the sun reaching the occupied space, and thereby minimise temperature increases in the room. Additionally, the shading devices may lead to increases in the within-cavity air temperature, as a portion of the radiation penetrating the external skin is absorbed within the shades, before convection transmits this into the DSF cavity (Pappas and Zhai, 2008).

Expansion of the warmed air in the cavity occurs, causing it to rise within the cavity as its density decreases, causing a stack effect to emerge. The temperature difference between the air outside the building and the air within the cavity makes the warmer air less dense and reduces pressure towards the top of the cavity in comparison with the bottom and the external air. This leads the internal

air to be drawn out via the upper cavity opening and external air to be drawn in through the lower opening (CIBSE, 2005).

For buildings designed with crossflow natural ventilation, air in the cavity is displaced, drawing in air from adjoining user space, thus drawing fresh, external air into that space through windows in the opposing side of the building. This air flows through the user space and is emitted into the DSF cavity. Continuous heating of the cavity air occurs when solar radiation hits the façade, causing continual convection-driven airflow within the DSF (Radhi et al., 2013; Ding et al., 2005). Figure 2.4 illustrates this process.

Lou et al. (2012) and Gratia and De Herde (2004a) report that the lowest airflow levels are observed in conditions where the wind blows parallel to the DSF, and higher levels are seen when the wind is at right angles to the façade, in particular where a DSF is on the building's leeward side, strengthening the stack effect within the cavity. The impact of wind can be used to increase the airflows between the occupants' space and the DSF cavity. At times, the scale of this effect can overcome the impact of thermal buoyancy, but strong pressure coefficient differences are not always achievable for every wind direction. Because of this, dependence on this factor may result in an ineffective design. Designs should, therefore, utilise thermal stack effect as their foundation, with wind effect included as a complement which can strengthen the forces which drive airflows (CIBSE, 2005).

The sections which follow provide a review of the literature to understand current knowledge regarding DSF designs and their implementation, considering the impact of both design and aspects of specific sites for the thermal performance of buildings. Three sets of factors are discussed here, which significantly affect the way in which DSFs perform, namely: parameters of the façade, including the cavity's and outer façade's characteristics; the physical features of the building, which include the properties of the DSF's internal layer; and finally, factors related to the site, including the impact of the external environment on thermal performance for the building. For each of these sets of factors, the key findings from case studies in the review are tabulated at the end of the relevant section.

2.5 Configurations of Double-skin Façade

This section explores the impact of the main features of façades for a building's thermal performance, considering the size of cavity apertures, structural features, depth and height as parameters which can strongly influence outcomes, including shading control, thermal exchange and ventilation magnitude (Shameri et al., 2011).

2.5.1 Cavity height

The height variance between the cavity's air outlets and inlets is a key factor for thermal buoyancy magnitude within the DSF, as this sets the pressure differential of the openings, in which the higher the cavity the greater the stack effect, with a higher level of airflow (Oesterle et al., 2001; Mingotti et al., 2011). Airflow level

inside the cavity is a key concern, particularly for climates with high temperatures and humidity levels, as there must be sufficient buoyancy to draw out excess thermal energy by cross-ventilating using occupant spaces.

The intersection between the external and internal hydrostatic pressure gradient is termed the neutral pressure line (NPL) and is illustrated in Figure 2.5. The NPL's location in relation to the cavity openings determines the size and direction of the building's ventilation flows. If the temperature of the air within the cavity is higher than in the external environment, air will enter the cavity through apertures nearer the bottom of the DSF and exit nearer the top. The NPL's position depends partly on the building's internal compartment layout. It is not always unique and is not always positioned at the median between the bottom and the top of the building. There can be local NPLs created, which cross an aperture vertically where windows interconnect an occupant space and the cavity of the DSF. Where this happens, air in the local area may recirculate, interfering with a DSF-building's air exchanges (CIBSE, 2005; ASHRAE, 2009).
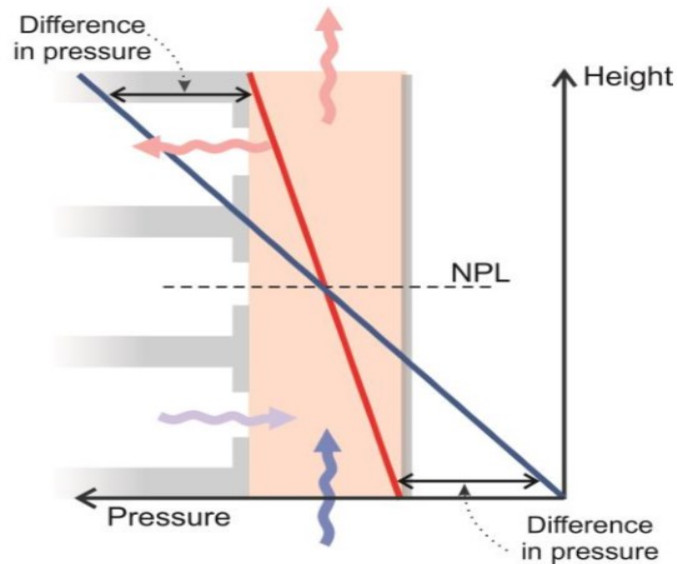
Figure 2.5: Schematic diagram showing within-cavity and external air pressure gradients: adapted from CIBSE (2005).

In principle, the higher the cavity the greater the pressure variation between the openings, with greater differences promoting greater airflow. Based on the literature, however, in practice, patterns of stratified heat within the cavity vary based on the type of building and the solar radiation pattern. Thus, each building requires an individual analysis of ventilation based on its geometric design and climatic considerations.

Moreover, Ding et al. (2005) show the impact on thermal performance of a natural ventilation design of including a chimney which is higher than the roof of the building, as in Figure 2.6. Their findings demonstrate that raising the cavity height raises the NPL higher than the level of the highest window. This increases the in-cavity airflow rate, leading to increased exchange of air on all floors, but particularly on the higher levels. The authors advise that the cavity be extended by 2 storeys or even more.
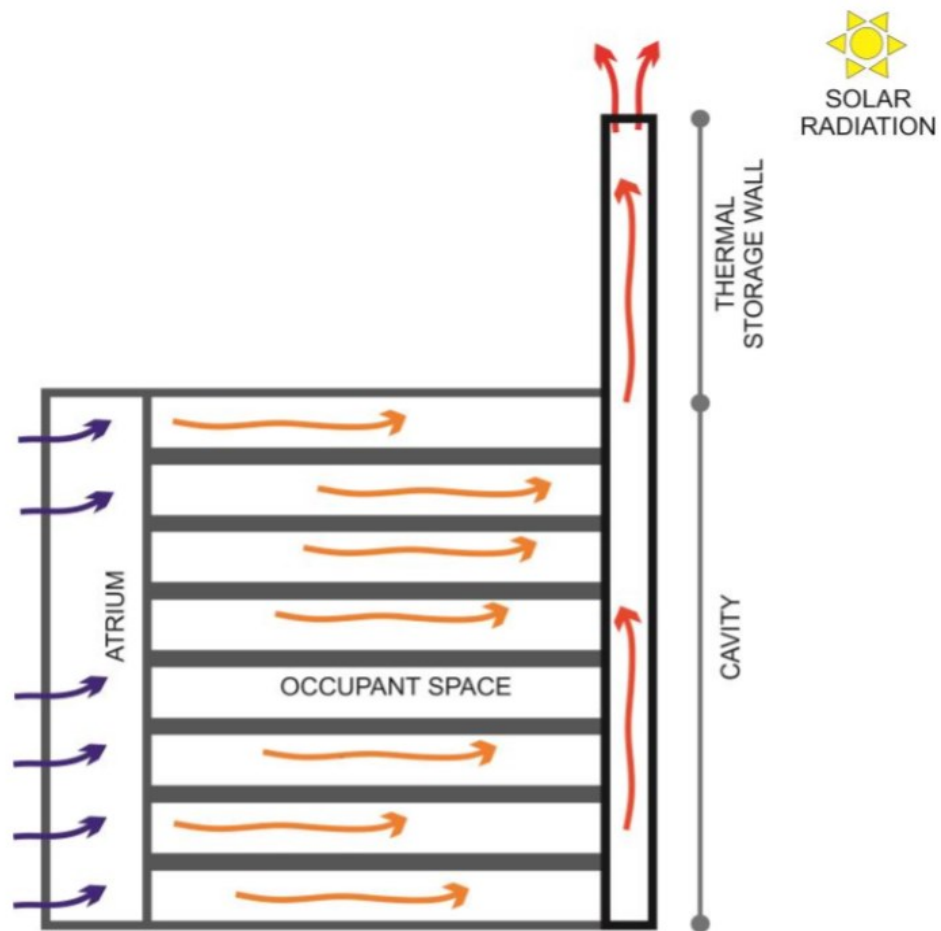
Figure 2.6: Proposed DSF design including a heat storage area above the main cavity (Ding et al., 2005)

It should be noted that the residual cavity height required could differ based on the geometry of the specific building. As a result, individualised calculations need to be made based on the area and quantity of opening windows, as well as the area of the aperture at the top end of the cavity. In addition, the ability to extend the cavity above the building's roof faces constraints in relation to building regulations, budget and safety considerations. Where such impediments exist, the building may be mechanically ventilated at the higher levels, with the part of the cavity extending above the area of the building using natural ventilation acting as an extended chimney. A novel chimney model is

proposed for connection to the top of the DSF to improve naturally ventilated performance, while avoiding the barriers related to chimneys extending above roof level.

The model proposed by (Ding et al., 2005) is further detailed, tested and the findings are discussed in Chapter 5. Validation of Numerical Methods.

2.5.2 Structure Of DSF

The internal divisions within the cavity are also a factor in calculating cavity height. DSFs may be constructed according to a range of models. Oesterle et al. (2001) categorise these structure types based on the compartment pattern of the intermediated cavity, as shown in Figure 2.7, with an evaluation and comparison of different types and their advantages. Four categories are presented:

a) Box window: In this structural form, the cavity is positioned between the outer and inner layers, with vertical and horizontal divisions positioned at the structural axes based on either individual rooms or window elements.

b) Shaft box: This form is a type of box window, where adjoining boxes create a shaft extending vertically across multiple floors producing stack effects.

c) Corridor: In this structural form, the cavity between the inner and outer layers is closed off for each floor, as well as being divided horizontally. Apertures for air to flow in and out are positioned close to floor and ceiling level on every floor, avoiding locations where air exiting the floor below is drawn into the next floor.

This design requires consideration of the increased risk of sound being transmitted from one room to the next.

d) Multi-storey: Here, multiple rooms are adjacent to a cavity which spans the whole of the façade, ventilated through large-scale apertures at the lower and upper ends. The NPL's location can lead to weakening or reversal of airflows at higher levels of the building, meaning that the upper storeys may need to be mechanically ventilated (Oesterle et al., 2001).
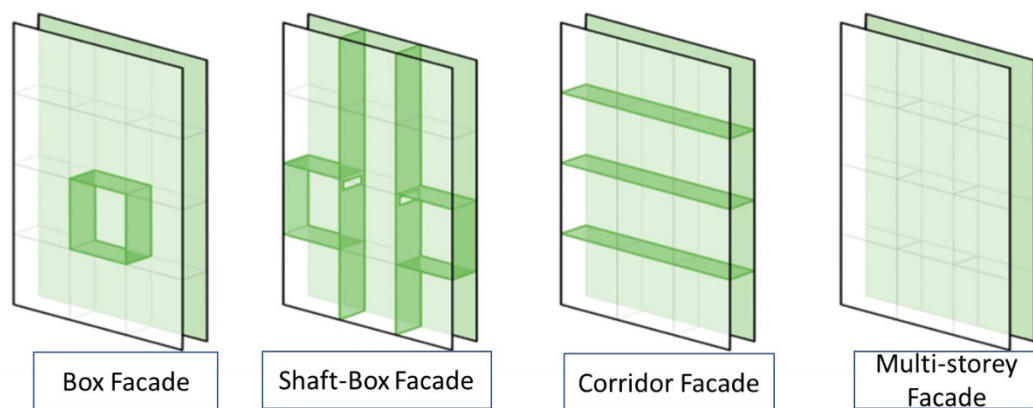
Figure 2.7: Categories of DSF structural types: Box, Shaft-box, Corridor and Multi-storey façades
(Brown,2016)

The multi-storey façade is investigated in depth in this study, because it is the only model that allows control over the entire façade of building. Hong et al. (2013) and Torres et al. (2007) compared thermal performance across various DSF forms and found that the largest thermal gradients through the cavity are afforded by multi-storey and shaft DSF designs, based on the height achieved. These forms create greater stack effects, increasing ventilation rates within the

cavity and causing the cavity air to be cooler, minimising thermal gain for user rooms.

Façade height is a key factor in the way a DSF performs because of its impact on buoyancy effects. Therefore, multi-storey and shaft-box DSF designs are appropriate options when using natural ventilation for a building. In contrast, the shorter vertical distance separating openings for incoming and outgoing airflows in box window and corridor DSFs reduces the effectiveness of natural ventilation for buildings following other designs.

2.5.3 Depth of the cavity

The depth of the cavity in DSF design has attracted extensive research attention, with designs ranging from 10cm to over 2m, based on varying space requirements for shade devices, access to maintain and clean the cavity and different design aims (Pappas and Zhai, 2008) (See Figure 2.8).
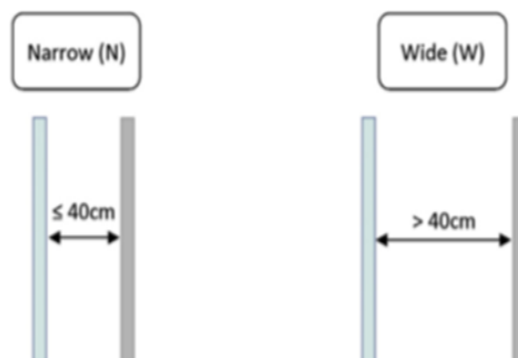
Figure 2.8: Narrow and wide depths of DSF (Pappas and Zhai, 2008).

The depth of the cavity affects the extent to which solar radiation transfers across the layers of the DSF, impacting temperature of the air and airflow rate, as

reported by a number of studies (Gratia and De Herde, 2007a; Torres et al., 2007; Rahmani et al., 2012; Radhi et al., 2013), which used various models but invariably found that temperatures were higher, airflow faster and stack effects stronger where smaller depths were used. Thus, narrow DSF cavities allowed for more warm air to be extracted, with lower thermal transfer inwards to the occupied space of the building, allowing lower energy use during periods of hot weather.

While stack effects are generally strengthened by narrower cavity space when using natural ventilation for buildings, airflow resistance also is greater. Moreover, as cooler air exits adjacent rooms into the cavity, airflow patterns and magnitude in both areas may be affected. Based on this, there is a need to evaluate the impact of airflows between the occupant space and the cavity, and appropriate cavity spacing may differ for buildings which are mechanically ventilated and those which use natural ventilation.

Other factors that may affect the dimensions of the cavity include cost considerations for extra materials, greater structural weight and provision of space to install shade devices (Torres et al., 2007). Moreover, the space necessary for maintenance access impacts cavity dimensions, with Torres et al. (2007) advising that a width of 40 cm or more is needed if access is required. Conversely, because the cavity is not generally used by occupants, its depth may be

constrained by the need for greater space within the building and is, therefore, generally less than 1 m in depth.

2.5.4 Cavity apertures

The depth of a cavity places constraints on the size of the cavity's upper and lower end openings. This has a significant impact on total thermal performance for DSF-implemented buildings. Aperture area has an effect on buoyancy forces and cavity air temperatures. A number of studies have investigated interactions between the size and form of apertures, and of airflows and temperatures (Gratia and De Herde, 2007a; Safer et al., 2005; Torres et al., 2007). The findings reveal that greater opening sizes tend to result in cooler air and greater airflows in comparison to lower opening areas, due to the greater resistance to airflow with smaller apertures. When the aperture dimensions were increased to 15% from 5%, this led to a 5.6% lower air temperature within a corridor-design DSF (Torres et al., 2007). Gratia and De Herde (2007a) found a 3x increase in airflows in the cavity when the upper aperture were increased from 8 % to 20%. While a number of authors report the advantages of larger-dimension openings to the cavity (Gratia and De Herde, 2007a; Safer et al., 2005; Torres et al., 2007), there is a lack of published evidence as to the effects of apertures that allow the lower and upper ends of the cavity to be completely open. Research in this area could lead to improvements in cavity ventilation, based on decreased airflow resistance with greater depth of cavity. The upper end of the cavity has particular significance for airflow where buildings are naturally ventilated, as this is

generally the single opening for outflow of air. Thus, a greater opening at the upper end of the cavity has the potential to improve ventilation in the building. Also, while no studies consider a closed lower end to the cavity, this could cause a rise in airflow rate coming from the opposing windows, with enhancement in rates of thermal comfort for buildings in warmer areas.

2.6 Factors of Characteristic Parameters in Buildings

Here, the literature regarding thermal performance of DSFs in relation to the parameters of the building is reviewed, including a discussion of material characteristics and the dimensions and location of the inside skin's apertures, as investigated further in the fourth chapter.

2.6.1 Proportion of walls to window apertures

Windows present advantages to occupants, as they allow daylight and direct sunshine to enter the building and connect occupants visually to the building's surroundings. However, issues can arise based on the ability of glass to transmit a high level of solar radiation, which can cause temperatures to rise excessively and result in asymmetrical heat radiation (Park et al., 2004). For DSF buildings with natural ventilation, as well as considering material use, the dimensions and location of window apertures can have an important impact on the thermal performance of the DSF.

Chou et al. (2009) and Manz et al. (2004) explored the impact that the window to wall opening ratio (WWR) has on transfer of solar radiation across the double-

skin façade. Their findings agree that the implementation of DSFs to minimise the building's thermal gain is impaired by a high WWR, meaning that a balance must be found in this area in order to decrease energy use during hot weather. Chou et al. (2009) report, from studying a building in Singapore, which lies at 1.1° North and 103.5° East, that increasing WWR from 50% to 70% decreased the building's yearly heat gain. In contrast, when investigating a model using a 90% WWR, thermal transfer was seen to be increased compared with lower ratios, with Haase et al. (2009) reporting that a 30% WWR allowed 26% reduction in energy use over the 90% WWR. Hence the overall building performance was better at a lower WWR.

Ding et al. (2005) investigated ventilation in a model of DSF using natural ventilation and reported an increase in first floor air change per hour (ACH) to 10 ACH with a 30% WWR, compared with 7 ACH with a 15% WWR. However, change in ventilation rate was seen to be smaller, at 60%, with the ACH reaching just 11. The authors concluded that a minimum of 30% WWR should be used for positive airflows across all floors of a building.

From the literature, it is clear that higher WWR positively impacts buildings with DSFs by increasing the airflow in occupied spaces, allowing heat gained to be removed at a faster rate. At the same time, high WWRs also increased accumulation of solar radiation, which is a disadvantage, leading to the

recommendation that WWRs should be balanced taking into consideration the parameters of the building as well as the climate in which it is located.

Research on office buildings that use natural ventilation (Zhang and Barrett, 2012; Herkel et al., 2008; Rijal et al., 2007) has shown that users' management of window opening/closing is significantly associated with the temperature of the external atmosphere. Changes in outside temperatures were found to be quickly followed by altered window-opening behaviours, which implies that users respond to temporary temperature changes. A further finding is that there is a range of approximately 4°C from having windows mostly closed to maximum opening behaviours, as at 16 °C, there is a 50% chance that windows will be opened, while by 20°C, window opening has reached its highest level.

The parameters of buildings and façades are among a range of factors which affect the functioning of DSF buildings. Environmental factors have an effect on the thermal performance of a building, and consequently, DSF designs should be assessed with the impact of climatic variations in mind.

2.7 Environmental Factors

The literature investigating important site parameters is discussed here and these are identified as; orientation of the façade, solar conditions, outdoor air temperature, wind and humidity levels (Poirazis, 2006), as addressed in the third case study.

2.7.1 Solar Irradiance

The difference in the temperature of the air in the cavity compared with external air is reported as a highly significant parameter for ventilating DSF buildings (Gratia and De Herde, 2007a; Kim et al., 2009). While the levels and orientation of solar radiation are central aspects in the temperature reached inside the cavity (Hazem et al., 2015), the direction of the façade orientation as well as shading provided by external features are also important. According to Mulyadi (2012), the proportion of solar radiation which glazing absorbs, reflects and transmits depends on the construction material as well as the angle of solar radiation to the façade (Figure 2.8). With an incidence angle of under 70°, a lower proportion of the radiation is absorbed and reflected, with more radiation being transmitted. The proportions of solar radiation reflected, absorbed and transmitted at different times for one day are illustrated in Figure 2.9, using a solar angle of 32°at 0800 hrs and 77° at 1100 hrs. Apart from the time of day, the season and the latitude of the building are also influential. The heat transferred from solar radiation has an impact on the temperature of the air in the cavity, and as a result on airflows as well.
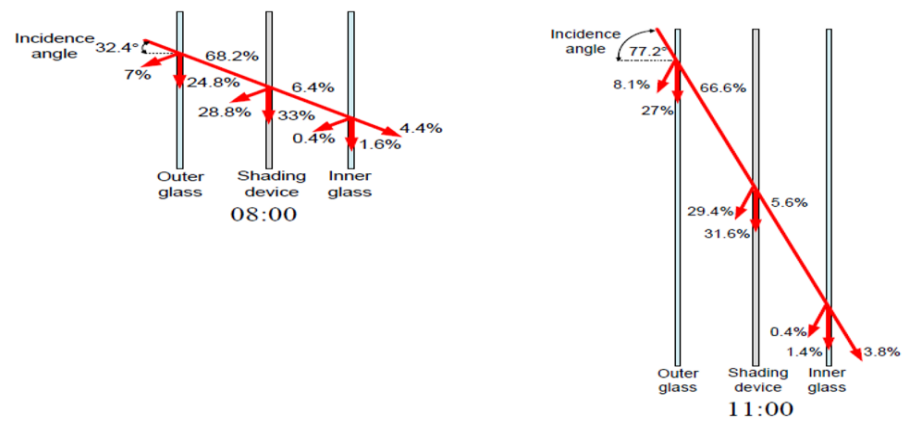
Figure 2.9: Proportions of solar radiation reflected, absorbed and transmitted under different solar incidence angles Source: Mulyadi, 2012.

Gratia and De Herde (2007a), Kim et al. (2009), and Stec and Paassen (2005) each investigated the impact of variance in solar radiation across different days, and report that, on days with more sunshine, air temperature within the cavities of DSFs oriented towards the south (in northern hemisphere-based studies) was on average 20°C higher than the surrounding air temperature where shading was not used. In comparison, on days with less direct sunshine, the differential achieved was 10°C on average.

Both Gratia and De Herde (2007a) and Hamza (2008) state that in buildings with air-conditioning the DSF was least useful when oriented in a west- or east-facing direction, due to the tendency of these orientations to lead to greater energy consumption for cooling. East-facing DSFs led to excessive heat being generated in the mornings, whereas west-facing façades produced this effect after midday. These findings may be explained by the significant challenge involved in

50

addressing low-angle transmission of solar radiation, leading to increased cooling burden.

Furthermore, Kim et al. (2009) report that in buildings using natural ventilation, the benefits associated with DSFs were not gained when the DSF faced east, but that DSFs oriented towards the west gained sufficient solar radiation to naturally ventilate the user spaces of the building. Meanwhile, for buildings using mechanical ventilation, Haase et al. (2009) advise use of DSFs that face south west, south east or south.

The implementation of east or west oriented DSFs leads to greater gain of solar radiation within the cavity, and generally faster airflows, enhancing thermal performance when the surrounding environment is warm/hot. It must be considered, however, that where adequate shading is not put in place to manage shortwave radiation being transmitted into occupant spaces, thermal comfort inside these spaces could be reduced. Therefore, considering total solar incidence throughout the day, orientation towards the equator (north for the southern hemisphere and south for the northern hemisphere) is the most appropriate choice when implementing a DSF. Another consideration is that, where a building is placed in a high-density urban environment, the façade may be shaded by the buildings around it, which may reduce the cavity's stack effect to a level which is not sufficient to naturally ventilate the building.

2.7.2 Wind speed and direction

Along with radiation from the sun, wind has a significant influence on the way in which air flows through DSFs, with the face, lower end and top end of the façade experiencing variations in wind pressure. When it is windy, this pressure is a predominant factor in the flows within the cavity, and therefore impacts ventilation and temperature functions (Pasquay, 2004; Stec and Paassen, 2005; Lou et al., 2012).

Gratia and De Herde's (2007a) investigation of wind as a factor in air temperature in the cavity led to the conclusion that, for an average day with clear, sunny conditions, a wind speed of 4 metres per second can reduce the cavity/external temperature differential by as much as 10.2°C in comparison with windless conditions. Moreover, the direction of the wind can significantly alter directions and scale of airflows in the cavity and through different apertures in the building. A number of studies (Lou et al., 2012; Stec and Paassen, 2005; Nasrollahi and Salehi, 2015) have found that strong pressure coefficients are observed for DSFs positioned leeward of the building, with low cavity airflows when wind runs parallel to the DSF and higher flows when the wind blows at 90° to the façade.

Gratia and De Herde's (2004a) in-depth study demonstrate that, with a wind blowing at 90° outward from the DSF, the different storeys of the building showed comparable airflows, and external air was drawn through the occupied space and out into the DSF cavity, with stack effects being secondary to the impact of the wind at higher levels. Due to the variability of wind direction and

speed, however, high airflows cannot be guaranteed by the impact of wind on a continuous basis, and it is important to investigate which conditions will promote and negate stack effects.

2.7.3 External humidity and air temperature

Warmer external air temperatures also significantly affect the thermal performance of a building. For buildings that use natural ventilation, external air passes into occupant spaces. Consequently, the temperature of this air affects the required rate of ventilation for the comfort of those in the building.

Darkwa et al. (2014) assessed a building using a DSF and natural ventilation in Ningbo, subtropical China, investigating thermal performance across the warm period with a maximum temperature of 39°C, and the cool season with temperatures of -5°C. The average temperature differential between air in the cavity and external air in the cool season was 8°C, while in the hot season, it was 3°C. This seasonal variation depends on the angle of the sun, with smaller angles in the winter season. The authors report an average increase of 8.4°C in air temperature within the rooms of the building compared to outside air temperature, while in summer, internal air temperature was 0.5°C lower than external.

The results of the review suggest that, when solar incidence angles on the DSF of a building are lower during the winter months, the effectiveness of DSFs in ventilating buildings is improved. As for the hot season, the requirement of a

greater ventilation rate can be addressed by applying a combination of parameters of the building and façade.

2.7.4 Variations in Climatic Conditions and Weather

Gratia and Herde (2007) investigated offices using DSF designs and natural ventilation within conditions of sunshine and relative heat, considering the effects of façade orientation in relation to wind direction and speed. However, their results cannot be generalised for different types and parameters of DSF. Moreover, the study design did not produce satisfactory findings.

Wong et al. (2008) investigated the use of DSFs for an 18-storey office building using natural ventilation in a hot, humid climate. The authors linked natural ventilation closely to DSF function by considering stack effects and solar chimneys. Furthermore, they identified the possibility of applying this design type to produce a notable reduction in the amount of energy consumed by multi-storey tower blocks by naturally ventilating such structures.

Haase et al. (2009) produced a system for ventilating buildings with DSFs in hot and humid climates based on simulation work which considered airflow and thermal flow (COMIS, TRNSYS and TRNFLOW). The results of simulation were compared with site-based data and both these datasets reported temperature reductions based on implementing various ventilated façade designs. Real-life data did not match simulated data in terms of maximum values for radiation incidence, but the values did not depend on this parameter and they

demonstrated reduced sensitivity regarding the effects of incident radiation on the temperature of the surface of the glazing material for internal and external skins. Zhou and Chen (2010) considered this parameter when studying the possibilities of use for ventilated DSFs in areas of China that experience hot summers and in cold winter areas. In discussing research methodology in this area, the requirement for effective operation of the façades constituted an issue in terms of their performance in practice, dependent upon the dimensions and form of the cavity, the positioning of shading devices and ventilation rate chosen.

A large body of studies exist that investigate the ventilation of cavities in hot and humid climatic conditions. Among such studies, Hensen et al. (2002) suggest network approaches for airflow during design processes, as well as CFD. The results demonstrate that, as the height of the floor increased, the cooling load also increased based on temperature increases in the DSF cavity. Therefore, a segmented spatial design approach was suggested, in which openings for inflows and outflows were located based on height in order to address issues.

Several studies demonstrated parameters which constrained DSF use due to the severe variability of airflow and temperatures such that airflows may at times be reversed in comparison to the determined airflows.

2.8 Ventilation of Buildings with DSFs
A number of naturally ventilated towers exist, including the Commerz Bank in Frankfurt and the Deutsche post Office tower in Bonn. Each has one or more atria,

as well as a double-skin façade. Use of an atrium allows an airflow channel within the building, while the DSF is employed to provide heat and sound insulation in internal-external and external-internal directions. The use of both atria and DSFs creates high-complexity patterns and actions of flows for such buildings.

Among studies of DSFs in relation to natural ventilation, Irwin et al. (2008) state that DSFs offer a protective advantage which allows windows to be opened on the upper floors of towers regardless of wind strength. The Commerz Bank in Frankfurt was an early pioneer of DSFs and consists of a double façade with operable windows set into the internal skin. Separation of the building into different, individually functioning sections was undertaken to avoid stack effect problems. The sections included several atria as well as a garden which extended up four storeys.

DSFs are a popular design choice for climates which are not extreme, and in these conditions, can increase the effectiveness of natural ventilation. The effectiveness of the design in these conditions is related to thermal buoyancy within the cavity of the DSF. The Deutsche Post Office tower in Bonn is naturally ventilated and utilises sky garden and façade ventilation as shafts to exhaust air, producing forces to drive ventilation and respond to ventilation requirements changing over the course of the day and the seasons (Blaser, 2004). The space between the façades is continuous as it travels upwards. Thus, stack effects are employed to remove heat at high levels in the tower, reducing the risk of excessive heating.

However, this only forms a part of the overall approach to ventilating the building, with cross-ventilation of the external air drawn into the DSF, which flows through offices and into corridor spaces, and outflows via the building's central atrium via windows and vents positioned on floor 9 and on the top level of the atrium. However, in a hot and humid climate this strategy might pose problems due to the potential for excessive heating of the façade, raising the cooling load for rooms adjacent to the DSF (Ford and Schiano-Phan, 2005).

Megri and Al-Dawoud's (2007) study of atrium design considered various strategies in terms of their impact on the energy that a building consumes, including integrated HVAC systems within the covered atrium, as well as atria which were open above the courtyard. Multiple-zone simulation software was used, and the researchers investigated window designs, proportion of glazing to total area and number of levels, in warm and humid climates. The researchers explored designs applied within existing buildings, Argonne National Laboratories and the Foxconn Building. They examined the extent of the connections between the architectural plans and the systems of natural ventilation. Each of the buildings was a mixed-modality project; nonetheless, they demonstrate the possibilities of natural ventilation in warm and humid climates, utilising hollow floor and wall designs and atria which are uncovered.

A study by Acred and Hunt (2014) examined stack ventilation for multi-storey buildings containing atria using dimensionless designs and considered a sample

multiple storey office building. They investigated characteristics designed vertically to enhance natural ventilation systems, in which DSFs and solar chimneys were included. Their results demonstrate a reduction in the enhancing effect of atria on the upper floors because of decreased stack pressures. Thus, a larger area is needed for each vent in order to achieve the specified performance on the upper floors. A theoretical method was applied for the study, based on using the same method for numerous studies of ventilation within simpler buildings. However, it has not yet been demonstrated whether this can be applied to multi-storey constructions via numeric and experimental studies.

2.9 Conclusions

This chapter has presented a literature review of important factors for determining thermal activity in DSF buildings. This involved classifying and examining existing studies which related to factors arising in façade design, buildings and location. A summary of the key factors and conclusions drawn is given below:

1) Higher cavities produce stronger buoyancy effects, generally leading to greater rates of airflow within a building. The literature also showed, however, that even with solar incidence of up to 500 W/m2, in-cavity airflows based on buoyancy do not reach 1m/s. This could potentially be addressed to create a larger distance from the inflow to the outflow openings by extending the cavity to higher than roof level in order to move the NPL upwards and strengthen stack effects, or by closing the windows on higher levels and mechanically ventilating these areas.

2) Continuous height of the cavity is essential both for creating buoyancy forces and for the overall performance of the DSF. Therefore, the most appropriate types of DSF in buildings with natural ventilation are shaft-box and multi-storey designs.

3) Narrower cavities are favourable for use in buildings which use mechanical ventilation, because they strengthen stack effects and improve in-cavity rate of ventilation. In cases of natural ventilation, however, having the outer and inner layers close together could increase airflow resistance for flows drawn in from occupant spaces. Moreover, space may be required for maintenance access to cavities, with 40 cm being the smallest feasible gap.

4) As large openings lead to higher airflow rates within the cavity due to the reduced resistance to airflow, the top of the cavity is likely to be kept as large as possible to promote higher airflow rates through the building.

5) A greater WWR generally enhances thermal conditions in buildings by improving ventilation throughout, although when WWR reaches 90% the thermal gains from solar radiation could negatively affect the thermal comfort of occupants.

6) Buildings using natural ventilation, and which are in the northern hemisphere can maximise the effectiveness of solar gain to naturally ventilate the building by orienting the DSF towards the south, or up to 45° south. In designing the façade,

it is important to consider the height and density of neighbouring structures that could shade the façade.

7) Wind speeds can negate the impact of thermal buoyancy forces inside the cavity. In buildings using natural ventilation, improved performance is generally seen for DSFs where the wind is blowing outward from the façade at 90°, and performance should also be assessed from different potential wind directions at the building's location.

8) In summer, the angle of solar incidence is higher, and this works against the in-cavity air temperature rising. However, approaches to increasing the rate of ventilation must be considered to create effective designs. In terms of humidity, the literature suggests that a broad spectrum of humidity levels can be tolerated when occupant activities are sedentary, as is applicable for office blocks.

Research on natural ventilation and DSFs is in its infancy, with the majority of studies on DSFs using mechanically ventilated modelling. Furthermore, much of the research considers the DSF in isolation or as a localised thermal design feature, ignoring its impact on the building's occupied rooms. While there are many gaps in the research into implementation of DSF designs for buildings using natural ventilation, a number of broad principles from literature on other models are applicable to natural ventilation designs and are used here to guide the generation of a model for reference, along with identifying factors central to the thermal performance of buildings with DSFs.

CHAPTER 3. Mathematical and Turbulence Models

3.1 Introduction

The conservative laws of mass, momentum and energy are the base of mathematical models. By applying these laws, one can derive a set of partial differential equations that are called basic equations, i.e., the Navier-Stokes equations. The basic equations are equivalently mathematical expressions of the conservation laws. Therefore, the solution for the problems raised in Chapter 1 can be found through solving the basic equations under relevant and specific conditions. These conditions are involved in geometric configurations of double-skin façades and buildings, boundary and initial conditions, and are of quite complex forms.

Another complex aspect of solving the basic equations is turbulence. As is known, when a fluid flows fast, i.e., the Reynolds number is large, the flow will be turbulent. Turbulence makes it very difficult to obtain the solution of the basic equations.

Because of such complex conditions and factors, it is impossible to solve the equations analytically. Thus, numerical solutions for the equations are produced using the approach of Computational Fluid Dynamics (CFD).

The numerical solution of partial differential equations has a long history of over a hundred years. It was not particularly emphasised until the electronic computer was invented. After the computer appeared, it became possible to numerically

solve complex problems or partial differential equations. Computational fluid dynamics, i.e., numerically solving the Navier–Stokes equations, developed quickly.

In particular, as computers have become increasingly powerful over the last three decades, CFD has seen a marked advance and various computational fluid dynamics codes have been developed for use in conjunction with a variety of engineering applications. CFD offers an option for the simulation of actual fluid flows, thereby supporting both theoretical and experimental research on fluid dynamics. The increasingly powerful computers currently available mean that CFD models can be created with greater ease and fewer man hours, which results in increased affordability. Consequently, computational fluid dynamics is now used extensively in the field of engineering as a time efficient tool for bettering processes.

This chapter will address the basic equations, and turbulence modelling.

3.2 Basic Equations

Consider a Newtonian fluid flowing within a three-dimensional domain. Following the laws of mass, momentum and energy, the basic equations can be written with Cartesian coordinates.

3.2.1 Mass conservation

$$\frac{\partial \rho}{\partial t} + div(\rho U_i) = 0 \tag{3.1}$$

where U_i is the mean air velocity component in i direction. ρ is the air density.

3.2.2 Momentum conservation

According to Newton's second law, the rate of change in momentum is equal to

the sum of the forces acting on the fluid control volume considered, expressed as

follows:

$$\frac{\partial \rho U_i}{\partial t} + div(\rho U_i U_j) = -\frac{\partial P}{\partial x_i} + div(\mu grad U_i) + B_i \tag{3.2}$$

Above are the most compact forms of the general governing equations for fluid

flow, where Ui refers to the velocity components, P refers to the pressure, μ the

fluid viscosity and Bi the body force.

3.2.3 Energy conservation

Applying the first law of thermodynamics, i.e., conservative law of energy, the

energy equation can be derived that is expressed as:

$$\frac{\partial \rho He}{\partial t} + div(\rho U_i He) = -\frac{\partial P}{\partial t} + div(\lambda grad T) + S_T \tag{3.3}$$

where *He* refers to the enthalpy, λ refers to the thermal conductivity, S_T refers to

the source term and T to the temperature.

3.2.4 Transport equations

Using a general variable Φ to express a scalar quantity, we have the basic equation

for transport processes of this quantity:

$$\partial(\rho\Phi)/\partial t + div(\rho\Phi U_i) = div(\Gamma grad\Phi) + S_\Phi \tag{3.4}$$

In this equation, Γ represents the diffusion coefficient, and the four terms used in the equations are the rate of change, convective, diffusive and source terms respectively.

3.2.5 Equation of state

The independent unknown variables in the Navier-Stokes equations are U, V, W, P, ρ and T, thus, six unknown variables in five equations, and the system is not closed. The system for airflows can be closed by adding Eq 3.5, the equation of state, and Eq 3.6, the thermodynamic relationship between state variables.

$$P = P(\rho, T) \tag{3.5}$$

$$He = He(\rho, T) \tag{3.6}$$

This system of coupled nonlinear partial differential equations is exceptionally problematic to solve using analytical methods, particularly for turbulent flows and other complicated applications. This is due partly to the velocity components' rapid variation in time and space and partly because of problems in solving any heat transfer involved.

Fluid flows are divided into one of two main categories in terms of a Reynolds number, namely laminar and turbulent. Reynolds number is defined as Eq (3.7):

$$Re = UL/v \tag{3.7}$$

In this equation, U represents the characteristic velocity, L represents the length scale and v represents fluid kinematic viscosity. Meanwhile, the Reynolds number is a relative measure of the fluid's inertia and viscous forces. Typically,

in situations where inertia force is significantly greater than viscous force (high velocity), the fluid will be turbulent. Figure 3.1 shows the effect of the Reynolds number in the flows over a cylinder. In the case of a simple laminar flow not accompanied by heat transfer, Eqs (3.1) to (3.6) above can be solved analytically, e.g. as per Schlichting (1979). These equations must, nevertheless, be solved numerically in the case of complicated turbulent flows. This can be done using techniques like CFD.
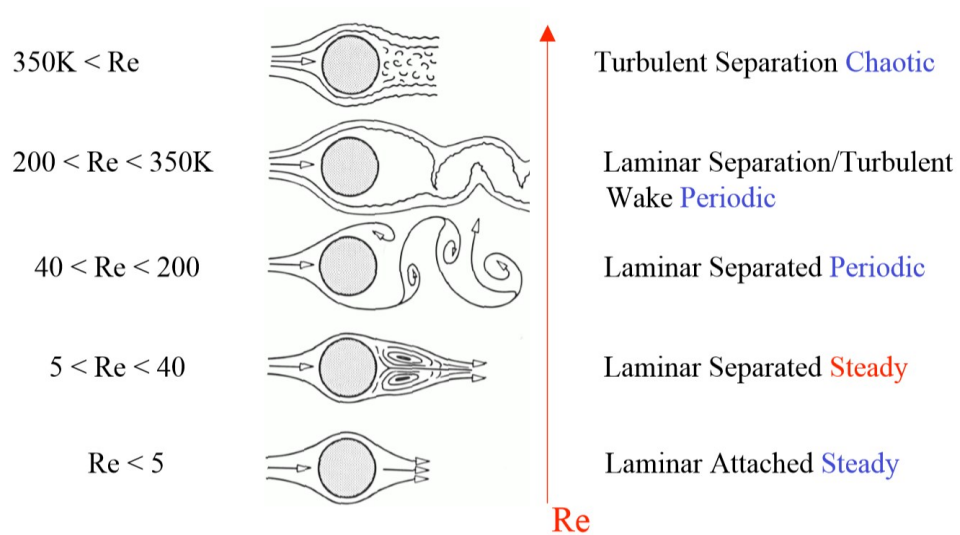
Figure 3.1: Reynolds number effect (Lienhard,1966).

3.3 Initial and Boundary Conditions

Boundary conditions define the nature of a physical problem and are necessary to begin the calculations for the aforementioned equations. CFD performs calculations to produce numerical solutions based on a process of iteration once the variables have had initial conditions assigned to them. According to Awbi (2003) and Nielsen (2007), in order for a closed system of flow transport equations to be defined, these physical parameters have to be given on the boundary of the

flow field, i.e., boundary conditions, as well as within it at the initial time, i.e., initial conditions. The present study, as detailed in the following sections, involves inlet and outlet boundary conditions, opening boundary conditions, wall boundary conditions and pressure boundary conditions.

3.3.1 Inlet and outlet boundary conditions

For inlet boundary conditions, the measure of the inlet velocity is specified, and the direction constraint requires that parallel to the boundary surface normal, is the flow direction.

Outflow boundary conditions are less troublesome. The zero gradient boundary condition is often used for the mean flow, and the fluctuating properties are extrapolated by means of a so-called convective boundary condition (Versteeg and Malalasekera, 1995):

$$\frac{\partial \phi}{\partial t} + \overline{u_n} = 0 \tag{3.8}$$

where $\overline{u_n}$ represents the velocity.

3.3.2 Opening boundary conditions

The state of the opening boundary of the air flow allows to cross the boundary surface in either direction. So, the air may flow fully to the area at the opening, or the air may flow fully outside the area, or a mixture of the two may occur. The opening boundary condition can be used where air is known to flow in both directions across the boundary.

3.3.3 Wall boundary conditions

Among the most widely used types of boundary in computational fluid dynamics is the solid wall boundary. It is particularly popular for use with applications wherein the fluid flow is enclosed, such as building ventilation. The velocity components on the boundary are zero, i.e., no-slip condition, because the fluid cannot flow across the wall boundary surface.

For adiabatic wall boundary conditions, the wall's heat flux is set as zero. Nevertheless, either setting a temperature or setting a heat flux to be applied to the energy conservation equation is possible and depends upon the concrete issues.

A situation may arise where the viscous layer of the wall cannot be resolved because the grid system in proximity to one of the boundary walls is not sufficiently fine. Here, provided that the wall temperature or its heat flux is specified, the wall shear stress and its heat flux or temperature can be calculated using a wall function. Fig (3.2).
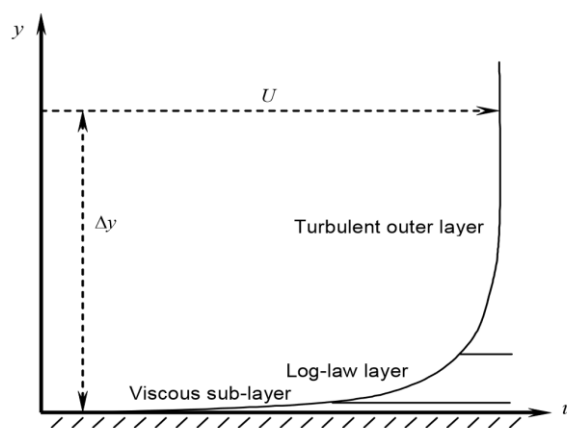
Figure 3.2 Fluid flow layers along a solid wall.

The wall-function approach produces near wall conditions for both the mean flow and the turbulence transport equations. This is achieved using empirical formulae. The most significant strength of this is that it does not factor viscous effects into the turbulence models, which of course reduces computational costs significantly.

3.3.4 Pressure boundary

When the detailed velocity distribution is not known, computational fluid dynamics calculates the mass flow across a boundary by using pressure boundaries. Each part of the fluid domain boundary can be specified as a surface of known pressure.

➢ Outflow through a pressure boundary

In cases where there is an outflow in a given pressure boundary, a number of processes occur: one is that pressure is given a user-specified value. Moreover, velocity and other transported variables, have zero normal gradients imposed on them.

➢ Inflow through a pressure boundary

In cases where there is an outflow in a given pressure boundary, a number of processes occur: one is that pressure is given a user-specified value. Moreover, some transported variables have user-specified values imposed on them. These transported variables include user scalars, mass fractions for multi-component flow and temperature for a non-isothermal flow. In addition, turbulence

quantities, Reynold's stress and velocity all have zero normal gradients imposed

on them. This procedure is identical to that applied to outflow.

Either the code or the user must specify the reference pressure, if pressure

boundaries are being employed. These pressures that are defined at the

boundaries will be relative to the aforementioned reference pressure. Meanwhile,

in inflow situations as well as in outflow situations, a fully developed flow will

be produced by the zero-gradient condition of velocity at the pressure

boundaries. This will be the result of discharge or expansion, for example.

3.4 Low Mach Number Flows

The basic equations in the above section are for fully compressible flows. Solving

the compressible Navier–Stokes equations numerically is very time-consuming,

given the acoustic modes involved. The acoustic modes are necessary for high

Mach number flows. When flows are in the low Mach number regime, they are

so little influenced by the acoustic modes as to be negligible. After removal of the

acoustic modes from the basic equations, the computational costs will be

dramatically reduced. In this section, the simplification with low Mach number

flow assumption is derived.

$$\text{Mach number} = \frac{V}{C} \tag{3.9}$$

Where V is flow velocity and C is sonic speed.

For compressible flows:

$$\frac{\partial \rho}{\partial t} + div(\overrightarrow{\rho v}) = 0 \tag{3.10}$$

$$\frac{\partial \rho}{\partial t} + \frac{\partial (\rho u_x)}{\partial x} + \frac{\partial (\rho u_y)}{\partial y} + \frac{\partial (\rho u_z)}{\partial z} = 0 \qquad\qquad (3.11)$$

3.5 Turbulence

Fluid flow in general is turbulent, e.g., the flows around cars, planes and buildings, the flows in combustions, the air movements in a room near the walls. In general, turbulent flow does not have a distinct definition due to the large fluctuations in its behaviour. However, there are some main characteristics that together help in identifying flows as turbulent or laminar. Although turbulence is often observed as random, the velocity field conserves mass, momentum and energy.

The main characteristics of turbulent flows are as follows:

➢ Irregularity: The flow is chaotic, random and irregular. This is also seen in the irregular fluctuations observed in dependent variables like temperature, pressure, velocity, etc., even when steady boundary conditions are implemented.

➢ Nonlinearity: Turbulence occurs when a nonlinear parameter like the Reynolds number exceeds a critical value and unpredictable behaviour in the flow is observed.

➢ Vorticity: Eddies, swirling structures in a flow, which occur in all sizes depending on the Reynolds number, are what characterise a turbulent flow.

> Dissipation: Dissipation of energy by means of the nonlinear transfer of energy between eddies, from larger eddies to the smaller ones, is observed in turbulent flow, and the smaller eddies' energy is then converted into internal energy.

> Diffusivity: Turbulent flows increase diffusivity—increase is seen in, for example, exchange of momentum in boundary layers, etc.—as compared to laminar flow.

Turbulence is governed by the continuity and Navier–Stokes equations. There are approaches for turbulence computations:

1) Reynolds-averaged Navier-Stokes approach: Averaging the equations gives the RANS, Reynolds-Averaged Navier–Stokes equations, although even here the fluctuating terms do not completely disappear and are accounted for in the nonlinear Reynolds stress term. A closure problem, i.e., having a larger number of unknowns than the number of equations, is observed while solving for the dependent variables. This leads to different approximation models, so-called turbulence models. The turbulence models can be divided into four classes: Algebraic models, One-equation models, Two-equation models and Reynold's stress models.

2) Large eddy simulation: This is an intermediate form of turbulence calculation which tracks the behaviour of the larger eddies. The method involves space filtering of the unsteady Navier–Stokes equations prior to

the computations, which passes the larger eddies and rejects the smaller eddies. The effects on the resolved flow (mean flow plus large eddies) due to the smallest, unresolved eddies are included by means of a so-called sub-grid scale model. Unsteady flow equations must be solved, so the demands on computing resources in terms of storage and volume of calculations are large, but (at the time of writing) this technique is starting to address CFD problems with complex geometry.

3) Direct numerical simulation (DNS): These simulations compute the mean flow and all turbulent velocity fluctuations. The unsteady Navier–Stokes equations are solved on spatial grids that are sufficiently fine to be able to resolve the Kolmogorov length scales at which energy dissipation takes place and with time steps sufficiently small to resolve the period of the fastest fluctuations. These calculations are very costly in terms of computing resources, so the method is not used for industrial flow computations. In the next section, we discuss the main features and achievements of each of these methods.

3.5.1 Reynolds-averaged Navier – Stokes equations

The Reynolds averaged Navier-Stokes equations are written as:

$$\frac{\partial(\rho u_i)}{\partial t} + \frac{\partial(\rho u_j u_i)}{\partial x_i} = -\frac{\partial p}{\partial x_i} + \frac{\partial}{\partial x_j}\left(\mu\left(\frac{\partial u_i}{\partial x_j} + \frac{\partial u_j}{\partial x_i}\right) - \rho\overline{u_i' u_j'}\right) + B_i \qquad (3.12)$$

$$\frac{\partial(\rho\phi)}{\partial t} + \frac{\partial(\rho\phi u_i)}{\partial x_i} = \frac{\partial}{\partial x_i}\left(\Gamma\left(\frac{\partial\phi}{\partial x_i}\right) - \rho\overline{u_i'\phi'}\right) + S_\phi \qquad (3.13)$$

It has a similar form as Eq (3.2), except for the presence of the Reynolds stress:

$\rho \overline{u_i' u_j'}$ similarly, Eq (3.12) and Eq (3.3) differ by the presence of the Reynolds

flux: $\rho \overline{u_i' \phi'}$. In Eq (3.13), ϕ is treated as an arbitrary scalar variable.

Turbulence models aim to obtain the Reynolds stresses in the Reynolds-averaged

Navier–Stokes (RANS) equations. Their attention is focused on the mean flow

and the effects of turbulence on mean flow properties. Prior to the application of

numerical methods, the Navier–Stokes equations are time averaged (or ensemble

averaged in flows with time-dependent boundary conditions). Extra terms

appear in the time-averaged (or Reynolds averaged) flow equations due to the

interactions between various turbulent fluctuations. These extra terms are

modelled with classical turbulence models; among the best-known ones are the

k– ε model and the Reynolds stress model. The computing resources required for

reasonably accurate flow computations are modest, so this approach has been the

mainstay of engineering flow calculations over the last three decades.

3.5.2 Eddy viscosity assumption

The eddy viscosity assumption is the basis for traditional turbulence modules

such as mixing-length and two-equations models, where it is assumed that the

turbulent or eddy viscosity is isotropic. One can consider Reynolds stresses as

proportional to the deformation rate of fluid mean quantities, equivalent to the

momentum equation's viscous stresses. The viscous stresses of an incompressible

fluid can be expressed as:

$$\tau_{ij} = \mu e_{ij} = \mu \left(\frac{\partial u_i}{\partial x_j} + \frac{\partial u_j}{\partial x_i} \right) \tag{3.14}$$

In this equation, τ_{ij} and e_{ij} constitute the suffix notations for the purpose of simplifying the equation form. Eq (3.14) defines the form Boussinesq proposed in 1877 for the Reynolds stresses, as:

$$\tau_{ij} = -\rho \overline{u_i' u_j'} = \mu_t \left(\frac{\partial u_i}{\partial x_j} + \frac{\partial u_j}{\partial x_i} \right) \tag{3.15}$$

There exists just one difference between Eq (3.14) and Eq (3.15), namely the presence or absence of turbulent or eddy viscosity μ_t. In the same way, one can assume turbulent transport of a scalar as being proportional to the gradient of the mean value of the quantity being transported. This is defined as:

$$-\rho \overline{u_i' \phi'} = \Gamma \frac{\partial \phi}{\partial x_i} \tag{3.16}$$

What turbulence models seek to do is to determine the eddy viscosity μ_t, which forms the basis for many classical turbulence models.

3.5.3 Two-equation model

The two-equation turbulence model is one of the most widely used models due to its ability to provide a good compromise between accuracy and numerical effort. The two-equation turbulence model aims to obtain the viscosity through solving two transport equations; usually the two variables are turbulent kinetic energy and turbulent length scale (Acharya, 2016).

3.5.3.1 Standard k-ε model

According to Acharya (2016), k- ε is a common and widely used two-equation model. The two transport variables solved for in this model are k, the turbulent kinetic energy and ε, turbulent dissipation. This model was implemented to improve the mixing-length model and proposing turbulent length scales in moderate to complex flows. This model has proven useful for free-shear layer flow, although only when the pressure gradient is relatively small.

It is assumed for this model that the turbulence viscosity is associated to the turbulence kinetic energy and turbulence dissipation by the expression (3.17);

$$\mu_t = C_\mu \, \rho \, \frac{k^2}{\varepsilon} \qquad\qquad (3.17)$$

The transport equations used for solving the transport variables k and ε are as follows:

For turbulence kinetic energy k,

$$\frac{\partial(\rho k)}{\partial t} + \frac{\partial}{\partial x_j}\left(\rho U_j k\right) = \frac{\partial}{\partial x_j}\left[\left(\mu + \frac{\mu_t}{\sigma_k}\right)\frac{\partial k}{\partial x_j}\right] + P - \rho\varepsilon + P_{kb} \qquad (3.18)$$

For turbulence dissipation ε,

$$\frac{\partial(\rho\varepsilon)}{\partial t} + \frac{\partial}{\partial x_j}\left(\rho U_j \varepsilon\right) = \frac{\partial}{\partial x_j}\left[\left(\mu + \frac{\mu_t}{\sigma_\varepsilon}\right)\frac{\partial\varepsilon}{\partial x_j}\right] + \frac{\varepsilon}{k}(C_{\varepsilon 1}P_k - C_{\varepsilon 2}\rho\varepsilon) \qquad (3.19)$$

In (3.18) and (3.19), P is the turbulence production due to the viscous forces and is presented by $P = \tau i \frac{\partial U_i}{\partial x_j}$. $C\varepsilon 1 = 1.44$, $C\varepsilon 2 = 1.92$, $C\mu = 0.09$, $\sigma\varepsilon = 1.3$ and $\sigma k = 1.0$ are the closure coefficients (Celik, 1999).

3.5.3.2 Standard k-ω model

This model solves for the transport variables k, turbulence kinetic energy and ω, the turbulence dissipation rate. This model is a more accurate version of the standard k-ε model that provides near-wall treatment for low-Reynolds number without involving complex nonlinear damping functions.

It is assumed for this model that the turbulence viscosity is associated with the turbulence kinetic energy and turbulence dissipation rate by the expression (3.20).

$$\mu_t = \rho \frac{k}{\omega} \tag{3.20}$$

The transport equations used for solving the transport variables k and ω are as follows:

For turbulence kinetic energy k,

$$\frac{\partial(\rho k)}{\partial t} + \frac{\partial}{\partial x_j}\left(\rho U_j k\right) = \frac{\partial}{\partial x_j}\left[\left(\mu + \frac{\mu_t}{\sigma_k}\right)\frac{\partial k}{\partial x_j}\right] + P_k - \beta' \rho k \omega \tag{3.21}$$

For turbulence dissipation rate ω,

$$\frac{\partial(\rho \omega)}{\partial t} + \frac{\partial}{\partial x_j}\left(\rho U_j \omega\right) = \frac{\partial}{\partial x_j}\left[\left(\mu + \frac{\mu_t}{\sigma_\omega}\right)\frac{\partial \omega}{\partial x_j}\right] + \alpha \frac{\omega}{k} P - \beta \rho \omega^2 \tag{3.22}$$

In (3.21) and (3.22), P is the turbulence production due to the viscous forces and is presented by $P = \tau i \frac{\partial U i}{\partial x j}$. $\alpha = 5\,9$, $\beta = 0.075$, $\beta' = 0.09$, $\sigma \omega = 0.5$ and $\sigma k = 0.5$ are the closure coefficients (Celik, 1999).

3.5.3.3 k- ω Shear Stress Transport (SST) model

The SST model tries to capture the best from two worlds, i.e. from the two earlier mentioned two-equation models, in order to be able to better predict the onset and amount of flow separation under adverse pressure gradients. This model, although very similar to the standard Wilcox k-ω model, is different in the following ways (Acharya, 2016):

- ➢ The standard k-ε and k-ω models are added together after being multiplied with a blending function designed in such a way that near the walls it is equal to one and activates the k-ω model, and zero when away from walls, activating the k-ε model.

- ➢ The blending between the models is achieved by introducing a cross-diffusion derivative term in the ω equation.

- ➢ The turbulent viscosity takes into account the transport of turbulent shear stress.

- ➢ Modelling constants are different.

The transport equation achieved now for k has been shown in equation (3.21) in the above section (3.5.3.2) while transport equation for ω:

$$\frac{\partial(\rho\omega)}{\partial t} + \frac{\partial}{\partial x_j}\left(\rho U_j \omega\right) = \frac{\partial}{\partial x_j}\left[\left(\mu + \frac{\mu_t}{\sigma_\omega}\right)\frac{\partial\omega}{\partial x_j}\right] + \alpha\frac{\omega}{k}P - \beta\rho\omega^2 + 2(1 - F_1)\frac{\rho\sigma_{\omega2}}{\omega}\frac{\partial k}{\partial x_j}\frac{\partial\omega}{\partial x_j} \qquad (3.23)$$

Where $2(1 - F1)\frac{\rho\sigma_{\omega2}}{\omega}\frac{\partial k}{\partial x_j}\frac{\partial\omega}{\partial x_j}$ is the cross-diffusion derivative term and $F1$ is a blending function.

3.5.4 Large Eddy Simulation (LES)

Deardorff (1970) explains that the Large Eddy Simulations Model (LES) involves filtering small eddies from instantaneous motions and remodelling them by way of simple models. Three-dimensional evolution of the large-scale turbulent flow field can be resolved using this model. The flow at any time can also be monitored using the LES models. An adequately long timescale must be used to calculate the mean flow quantities where necessary. Despite the fact, as Murkani (1997) states, that the LES model has lower computational costs than direct numerical stimulations, it does involve a prohibitively large amount of computing for the majority of engineering applications. At the same time, its usefulness cannot be denied, with Deardorff (1970) reporting its use to explore isothermal flows within channels.

3.5.5 Direct Numerical Simulation (DNS)

The objective of Direct Numerical Simulation is to solve the time-dependent N–S equations solving all the scales (eddies) for a sufficient time interval so that the fluid properties reach a statistical equilibrium. The most accurate means of modelling fluid flow numerically is direct numerical simulation (DNS), in which the mesh size of the domain needs to be small enough to model the full range of turbulent eddies within the domain (Murakami 1997). This is not practical, due to the wide range of length scales of turbulent eddies. In order to reduce the computing cost, the real fluid properties are modelled by time-averaged mean

quantities and the effects of their fluctuations. Considering the general variable Φ, its time-averaged form is given by:

$$\Phi\,(t) = \emptyset + \emptyset'(t) \tag{3.24}$$

The general time-averaged governing equation set therefore becomes:

$$\frac{\partial \rho}{\partial t} + \frac{\partial \rho_{ui}}{\partial x_i} = 0 \tag{3.25}$$

3.5.6 Wall treatment

Turbulence models are commonly used in CFD simulations nowadays. However, some mature turbulence models, such as k-ε, are only applicable in fully established turbulence and perform poorly near the wall. There are typically two approaches to dealing with the near-wall area. One where turbulence models are introduced to the wall. However, this is proven to be computationally intensive as it requires a huge mesh number (Wendt, J.F. ed., 2008). The other approach would be to utilise wall-functions.

Wall functions are used to empirically resolve the physics of the flow near the wall region, the log-law layer. Namely, the wall functions are categorised as standard, enhanced and scalable; generally, the variation in wall functions originates from the y+ value. Standard wall functions operate with y+ greater than 30 (turbulence sub-layer), whereas enhanced wall functions use a y+ value less than 5 (the log-law sub-layer). These wall functions show the boundaries of a tradeoff between computational intensity and results accuracy. The scalable wall functions (~y+>11.126) combine the features from these two, the reduced

computational intensity from the standard wall functions while producing more accurate results, which is suitable for the purposes of this research (Wendt, J.F. ed., 2008; Chmielewski and Gieras, 2013).

It should be noted that by using the wall functions method, the boundary layer does not need to be resolved, resulting in a substantial reduction in mesh size and computational domain. Despite the fact that wall functions are based on empirical relationships that are only applicable in certain cases, the result is reasonably reliable when used correctly (Davidson, L., 2003).

3.6 Modelling Natural and Forced Convection

Typically, it is thermal buoyancy that generates a building's natural convention flows. When they are influenced by forces such as wind effect, induced pressure difference or others, the convection flow will be natural convection and forced convection combined. In the case of engineering applications involving these types of flows where differences in temperature and compressibility effects are less, flow will be dealt with as incompressible and the Boussinesq(1903) approximation can be employed for the modelling.

The approximation treats fluid properties ρ, μ as well as the Prandtl number as constants, with the exception of density in the momentum. This is written as follows:

$$\rho = \rho_0[1 - \beta(T - T_0)] \qquad\qquad (3.26)$$

The Prandtl number is a relative measure of momentum diffusivity and thermal diffusivity. In this equation, ρ_0 is the density and β is the thermal expansion coefficient at T_0 (a reference temperature). Typically, T_0 can be either a natural convection boundary layer's ambient temperature or it can be the average temperature found within an enclosure, with $\beta \approx 1/ T_0$.

3.7 Summary

In the present study, the practical flows are turbulent, thus meaning that, if the equations given above can be solved directly, there will be involvement in the fluctuations on the part of the solutions and this will be with a wide range of frequency. Moreover, the resolution of the meshes ought to be particularly high, resulting in very high-cost computing. The Reynolds average is, therefore, applied to the equations given above with a view to making the process more cost effective. Ultimately, this gives a set of Reynolds-averaged N–S equations. The Reynolds average leads to the generation of a set of Reynolds stresses and the effects of turbulence. Moreover, the basic equations also become unclosed. Turbulence models must then be used if the equations are to be closed and the problems are to be made solvable. Of the many turbulence models that have been proposed in recent times, the model that will be applied in the present study is the highly popular kappa-epsilon turbulence model. For calculating Reynolds stresses, turbulence takes the form of turbulent viscosity in this model, thus rendering the Reynolds averages computable.

CHAPTER 4. Numerical Methods

4.1 Introduction

Numerical methods for solving the partial differential equations (PDEs) in chapter 3 are discussed in this chapter. Due to the fact that computers can only process binary data, they are unable to produce a direct solution for PDEs, although they are able to manipulate numbers of multiple times. As a result, every term in the partial differential equations is first converted via 'numerical discretisation' to entirely and numerically-computable equations. Discretisation can be performed by one of three processes: the finite volume method, the finite element method and the finite difference method. These methods are used at finite points within a particular domain to generate the equations for the variable's different values. In order to define the calculations, a group of initial conditions and the boundary conditions are needed so that every boundary's variables are established and/or calculated.

While the finite element method generates equations for elements on an independent element by element basis, numerical equations are produced at a specific point according to the values of neighbouring points in the finite volume and finite difference methods. In the finite element method, the interaction between elements only becomes a factor after the production of global matrices generated from a collection of finite element equations. This method involves obtaining a limited or 'finite' number of elements, by dividing the flow domain. Meanwhile, in the finite volume and finite difference methods, it is easy to insert

the values into the solution, thereby applying the fixed values boundary conditions, as dealt with in-depth by Zienkiewicz and Taylor (1989). Nevertheless, they must make modifications to the equations in order to allow for the occurrence of derivative boundary conditions.

Smith (1985) and Tamura (2003) explain that the finite difference method is based on using algebraic difference quotients to substitute the partial derivatives found in N–S equations. This produces a system of algebraic equations in line with Taylor-series expansion that are able to be solved for the flow variables at the flow's specific, discrete grid points.

The method used in the current research is an adaptation of the finite volume method, wherein the researcher splits the region of interest into 'control volumes' which are smaller sub-regions. An approximate value for every value at specific points in the domain can be performed by way of discretisation, and iterative solution of the equations for every control volume is conducted. This allows the user to obtain a complete picture of how the flow behaves, which involves the establishment of volume integrals and surface integrals by way of the integration of the flow equations over the fixed control volume. Surface integrals are made by integrating the source and accumulation terms' fluxes and volume integrals.

Use of the three methods mentioned above is standard in energy applications. All three have their foundations in Smith's (1985) methodology, with modifications made for specific PDE types. They have been dealt with in depth

in multiple pieces of literature (Hirsch, 1989; Versteeg and Malalasekera, 1995; Wesseling, 2001).

According to Patankar (1980), the initial development of the finite volume method was as a special finite difference formulation. Discretisation is conducted for the PDEs that represent the conservation principle relating to a flow variable over an extremely small control volume. This allows the expression of that principle over a finite control volume. Likewise, matching is done for control volume boundaries and physical volume boundaries.

The primary distinction between the finite volume technique and the finite difference technique is how the control volumes are integrated. This means that each finite cell's relevant properties have a discretised expression for their exact conservation, which is achieved by integrating the differential equations over each control volume.

Evaluation for the flow variables' properties and values is done at the nodes. Calculation of the fluxes and gradients present at the control volume faces is performed by approximating the distribution of properties between the nodes present. This means substitution of interpolated values at the source terms and fluxes as well as at the control volume faces, with these being substituted into the PDEs' integral form, which represents each volume's flow field. This procedure results in a series of algebraic equations. According to Versteege and

Malalasekera (1996), one can then establish the flow properties at every node location by iteratively solving said equations.

4.2 Computational procedures

CFX and Fluent are CFD codes, and they use the finite-volume method which discretises the spatial domain using a mesh. Variable values for quantities such as mass, energy and momentum are stored in these control volumes constructed with the help of the mesh.
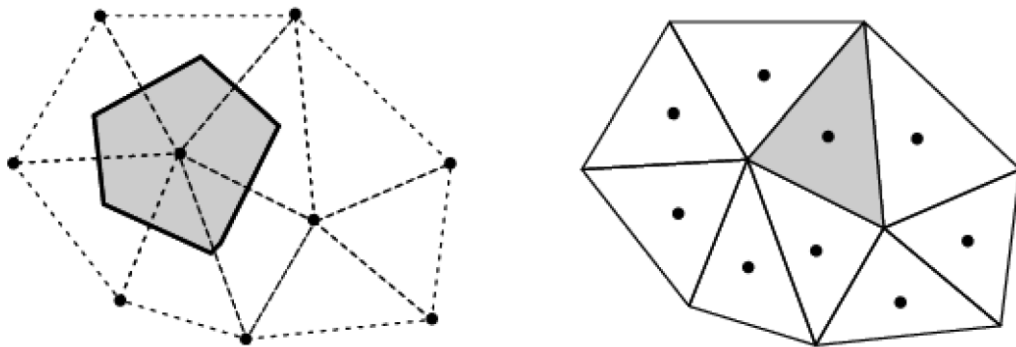
Figure 4.1: Left: Vertex-centred. Right: Cell-centred (CFX Solver Theory).

When it comes to the finite volume method used for discretisation in both solvers, CFX uses the vertex-centred method—more precisely dual-median method—while Fluent uses the cell-centred method. The basic difference between the two methods is the location of the unknowns that are to be solved for, as shown in Figure 4.1. In the cell-centred approach, the cells themselves serve as control volumes and the average variable value is stored in their centre. On the other hand, for the vertex-centred method, control volume is formed by combining smaller sub-control volumes surrounding the vertex, and the variable value is stored in the vertex.

4.2.1 Turbulence models in CFX

There are some basic differences in the formulation of the turbulence models between solvers, especially the values of model constants used. This section will present the equations used for the respective solver and the default value of the model constants implemented in CFX model.

- **Standard k-ε model**

CFX model

The transport equations used for turbulence kinetic energy k and its dissipation ε are given by equations (4.1) and (4.2) respectively.

For turbulence kinetic energy k,

$$\frac{\partial(\rho k)}{\partial t} + \frac{\partial}{\partial x_j}\left(\rho U_j k\right) = \frac{\partial}{\partial x_j}\left[\left(\mu + \frac{\mu_t}{\sigma_k}\right)\frac{\partial k}{\partial x_j}\right] + P - \rho\varepsilon + P_{kb} \tag{4.1}$$

For turbulence dissipation,

$$\frac{\partial(\rho\varepsilon)}{\partial t} + \frac{\partial}{\partial x_j}\left(\rho U_j \varepsilon\right) = \frac{\partial}{\partial x_j}\left[\left(\mu + \frac{\mu_t}{\sigma_\varepsilon}\right)\frac{\partial \varepsilon}{\partial x_j}\right] + \frac{\varepsilon}{k}\left(C_{\varepsilon 1}P_k - C_{\varepsilon 2}\rho\varepsilon + C_{\varepsilon 1}P_{\varepsilon b}\right) \tag{4.2}$$

Here, P_{kb} and $P_{\varepsilon b}$ represent the influence of buoyancy forces and P_k is the turbulence production due to viscous forces. The model constants possess the values $C\varepsilon 1$ = 1.44, $C\varepsilon 2$ = 1.92, $C\mu$ = 0.09, $\sigma\varepsilon$ = 1.3 and σk = 1.

- **Standard k-ω model**

CFX model

The transport equations used for solving the transport variables k and ω are as follows:

For turbulence kinetic energy k,

$$\frac{\partial(\rho k)}{\partial t} + \frac{\partial}{\partial x_j}\left(\rho U_j k\right) = \frac{\partial}{\partial x_j}\left[\left(\mu + \frac{\mu_t}{\sigma_{k,3}}\right)\frac{\partial k}{\partial x_j}\right] + P_k - \beta'\rho k\omega + P_{kb} \qquad (4.3)$$

For turbulence dissipation rate ω,

$$\frac{\partial(\rho\omega)}{\partial t} + \frac{\partial}{\partial x_j}\left(\rho U_j \omega\right) = \frac{\partial}{\partial x_j}\left[\left(\mu + \frac{\mu_t}{\sigma_\omega}\right)\frac{\partial \omega}{\partial x_j}\right] + \alpha\frac{\omega}{k}P_k - \beta\rho\omega^2 + P_{\omega b} \qquad (4.4)$$

Here P_{kb} and $P_{\omega b}$ represent the influence of buoyancy forces, P_k is the turbulence production due to viscous forces. The model constant's values are α = 5/9, β = 0.075, β' = 0.09, σk = 2 and $\sigma \omega$ = 2. For details on the development of the constants please refer to the Ansys Documentation on CFX Solver Theory.

CFX can run 3D simulations, which means the number of nodes is doubled. On the whole, the preference is for using CFX as long as it is necessary to use a 3D model, due to its powerful solver requiring a smaller number of iterations, the ease of monitoring magnitudes at different measurement points, modern user-interface and tolerance towards meshes.

4.2.2 Development of Computational procedures

Natural convection is of great importance in many applications, such as energy technology, atmospheric and environmental science, chemical engineering, fire safety management, etc., and is hence an active research subject of thermal fluid mechanics. This work employed a multiscale finite element method recently

proposed by Liu (2009) to large eddy simulation (LES) of the turbulent natural convection in an enclosed tall cavity.

Turbulence is a random motion of fluid generated by a deterministic flow system, i.e., Navier–Stokes equation system. This implies a maintained turbulence, that is most of the turbulence in practice originates in an unstable flow state that exceeds some critical conditions. Some random disturbances in the flow are amplified and evolve into turbulence. In the evolution, the nonlinear effect of the Navier–Stokes equation system plays a key role. If there were no nonlinear terms in the Navier–Stokes equations, there would not be any turbulence. The nonlinear effect not only creates new fluctuation modes when two random disturbance modes act upon each other in the nonlinear system, but also provides new energy to maintain turbulent fluctuations. Hence, initially finite disturbance modes will develop into infinite turbulent fluctuation modes after the transition from lamina to turbulence.

As a matter of fact, each turbulence represents very different structures and patterns from other turbulence. If we accurately produce information records of a turbulence in the characteristic space domain and the time interval, we can calculate various statistical quantities of the turbulence and these records can therefore be regarded as a solution of this turbulence. This is perhaps the best approach to solve turbulence problems. Direct numerical simulation (DNS) or its approximation, large eddy simulation (LES) of turbulence, is such an approach

to produce these records. Therefore, this work solves a vertical natural convection in an enclosed tall cavity using LES of multiscale finite element method.

4.2.2.1 Problems of turbulence

Experimental observations show the following:

Laminar flow = regular structures

Turbulent flow = regular structures + stochastic fluctuations

The stochastic fluctuate-ons result from flow instability and are controlled by the nonlinear interactions of flow quantities, which lead to a huge difficulty for the turbulence theory. The existence of the stochastic fluctuations implies that turbulence is a stochastic process and cannot be expressed by a set of determinate quantities.

- **Assumption**

Turbulence is theoretically a solution of the Navier–Stokes (N-S) problem:

Turbulence or solution of N–S problem = solved scale flow unsolved scale flow

- **Reformulation of basic equations**

$$\frac{d\rho}{dt} = F(p) + f(p,q) \qquad p \in S_m \qquad \dim(S_m) = m \qquad (4.9)$$

$$\frac{d\rho}{dt} = G(q) + g(p,q) \qquad q \in T_\infty \qquad \dim(T_\infty) = \infty \qquad (4.10)$$

p is the finite dimensional vector

q is the vector of infinite dimensions and is independent of p.

Approximate representation of turbulence

When energy of q is minor, that is $\| q \| \le \mathcal{E}$, p is defined as an approximate representation or solution of turbulence.

Direct numerical simulations (DNS)

Simply ignoring $f(p,q)$, an approximate solution of turbulence can be obtained from equation (4.9).

Large eddy simulations (LES)

A projection of $f(p,q)$ on is S_m essential so that equation (4.9) can produce the approximation of turbulence.

The approximate projection, $f(p,q) \approx f(p)$, is called _**turbulence model**_.

Measurement of the interactions of the flow quantities of unsolved scales and solved scales can precisely be obtained only through solving for the coupled system of (4.9) and (4.10). Therefore, they are always approximate in a practical sense.

The solved scale flow p is a component in the interpolation function space of computational meshes; it is obtained by any one of the standard numerical methods, for example: standard finite element method or finite volume method.

The unsolved scale flow $q/\ f(p,q)\approx f(p)$ is approximated in each element of the computational meshes.

Interactions between p and q: influence of q on p is through turbulence model. Effect of p on q is the force driving the unsolved scale flow.

Unsolved Scale Flow

Mathematical problem for unsolved scale flow:

$$\frac{d\rho}{dt} = G(q) + g(p,q) \qquad q \in T_\infty \qquad in \quad E \qquad\qquad (4.11)$$
$$q = 0 \qquad\qquad\qquad on \quad E$$

E is the element of computational meshes.

Decomposition of the computational meshes into four types of elements:

(a) Tetrahedral element   (b) Pyramidal element

(c) Prisms element   (d) Hexahedral element

All the above elements can be decomposed into one or several hexahedral elements; a hexahedral element can be mapped into a cubic element. Problem (4.11) needs to be approximately solved only on cubic domain.

4.3 Conclusion

An overview of the basic principle and concepts of numerical modelling in computational fluid dynamics has been presented in this chapter. The chapter contains details of a number of key concepts, including boundary conditions, Boussinesq approximations, fluid governing equations, natural ventilation modelling and turbulence modelling. Moreover, it deals with the turbulence modelling technique employed by computational fluid dynamics for modelling natural convection and forced convection in a building.

Etheridge and Sandberg (1996) recommend a fluid domain temperature variation ΔT not exceeding 30°C for the application of the Boussinesq approximation for the purpose of modelling buoyancy driven flows.

Air temperature variations and density variations are typically negligible in building simulations, meaning that the Boussinesq approximation can be said to be sufficient.

Overall, it can be surmised that computational fluid dynamics provide great detail regarding airflow internally and externally to buildings as a result of wind and stack effects. They are also more time effective and more cost effective than the alternatives, making them a particularly useful tool for those researching building ventilation. Moreover, they are extremely flexible and can be adapted to different designs and conditions. This versatility makes them particularly useful for parametrical studies.

CHAPTER 5. Validations of Numerical Methods

This section presents a detailed validation work for ANSYS CFX 5, as a proposed solution method, comparison an experiment similar in principles to the intended work.

5.1 Validation of Computing with Experimental Results

The case studied in this work corresponds to the configuration investigated experimentally by Betts and Bokhari (2000). Hence the computational results are compared with the measured data for the validation of the numerical model.

5.1.1 Computational details

The computational domain of the rectangular cavity is meshed by tetrahedral elements into two meshes, fine and coarse. The fine mesh is for computational results and the coarse mesh is for checking the mesh–independency of the numerical solution. The elements are non-uniformly distributed in the computational domain, and near walls they are denser than those in the core zone. The parameters of the simulation and dry air values used in the present work are summarised in tables 5.1 and 5.2, respectively.

The computing flow begins with a static state. A 128-processor job of 12 hours can carry out approximately 700-time step integrals. In general, 4 ~ 5 such jobs can produce fully developed turbulent convections. After the fully developed state was reached, the sample records could start. The checkpoint set was allocated on 5 lines across the cold and hot walls in the central section of the

cavity that corresponded to the measurement data. Each line had 40 points that recorded all the flow and temperature variations with the time. The statistical analysis of each physical quantity was performed using 1800 nods at each line, i.e., based on the turbulent information in 90 seconds.

Raleigh number based on the cavity thickness	1.43×10^6
Hot wall temperature ($^\circ C$)	55.5
Cold wall temperature ($^\circ C$)	15.6
Height of the cavity (m)	2.18
Width of the cavity (m)	0.52
Thickness of the cavity (m)	0.076
Number of tetrahedral elements for fine mesh	12,000,000
Number of tetrahedral elements for coarse mesh	1,500,000
Time step width (s)	0.05
Reference length (m)	0.076
Reference temperature ($^\circ C$)	39.9

Table 5.1: Summary of simulation parameters

Temperature ($^\circ C$)	15.1	34.7	54.7
Thermal conductivity ($W/mK \times 10^3$)	25.3	26.8	28.3
Thermal expansion coefficient ($K^{-1} \times 10^3$)	3.47	3.25	3.05
Kinematical viscosity ($m^2 s^{-1} \times 10^6$)	14.6	16.5	18.4
Prandtl number	0.704	0.700	0.697
Heat specific capacity (kJ/kgK)		1.005	

Table 5.2: Variations of air physical properties

5.1.2 Experiment setup

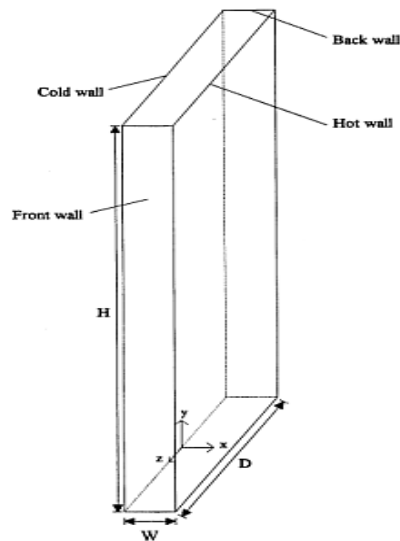Figure 5.1: Configuration of numerical simulations and experiments (Betts and Bokhari, 2000)

The natural convection of air in a rectangular tall cavity studied experimentally

has the same conditions as the computation (see Figure 5.1). The vertical cold and

hot walls are made of polished aluminium and are backed by temperature-

controlled water jackets and the water passes upwards along channels behind

each wall. Temperatures at entry were controlled to $\pm 0.5^{\circ}C$. Such a setup ensures that the temperatures on the entire vertical walls will be almost isothermal. Two side walls are built of 9.5 mm thick acrylic sheet, such that temperature gradients normal to these faces are minor (close to adiabatic condition). The top and bottom walls are constructed from 50 mm thick natural hard rubber. The outside of the rubber walls is covered with 100 mm thick polystyrene insulation and the inner side by a thin (0.01 mm) sheet of adhesive aluminium foil to reduce radiation absorption. Such construction would produce a linear variation from the low temperatures of the cold wall to the high temperature of the hot wall, on the top and bottom walls.

Temperatures are measured by K–type thermocouple. The diameter of the Chromel-Alumel wires is 75 mm and the response time is 0.065 s. Therefore, a temperature fluctuation under 13 Hz may be accurately measured. A single component LDA system with a 15m W He–Ne laser was used for velocity measurements. The measured volume has a diameter of 0.37 mm and a length of 4 mm. A more detailed description of the experiment may be seen in Betts and Bokhari (2000).

5.1.3 Comparisons between computational and experimental results

In order to compare with the experimental data in detail, we chose five representative heights with equal distance from the cold wall to the hot wall in the central section of the cavity: z/H=0.1, 0.3, 0.5, 0.7, 0.9. The experimental data

have been published in Betts and Bokhari's work and can also be downloaded from ERCOFTAC Database. All the statistical calculations were carried out in 1,800 sampled data for each spatial point. The statistic mean profiles of temperatures at the five heights are shown in Figure 5.2.

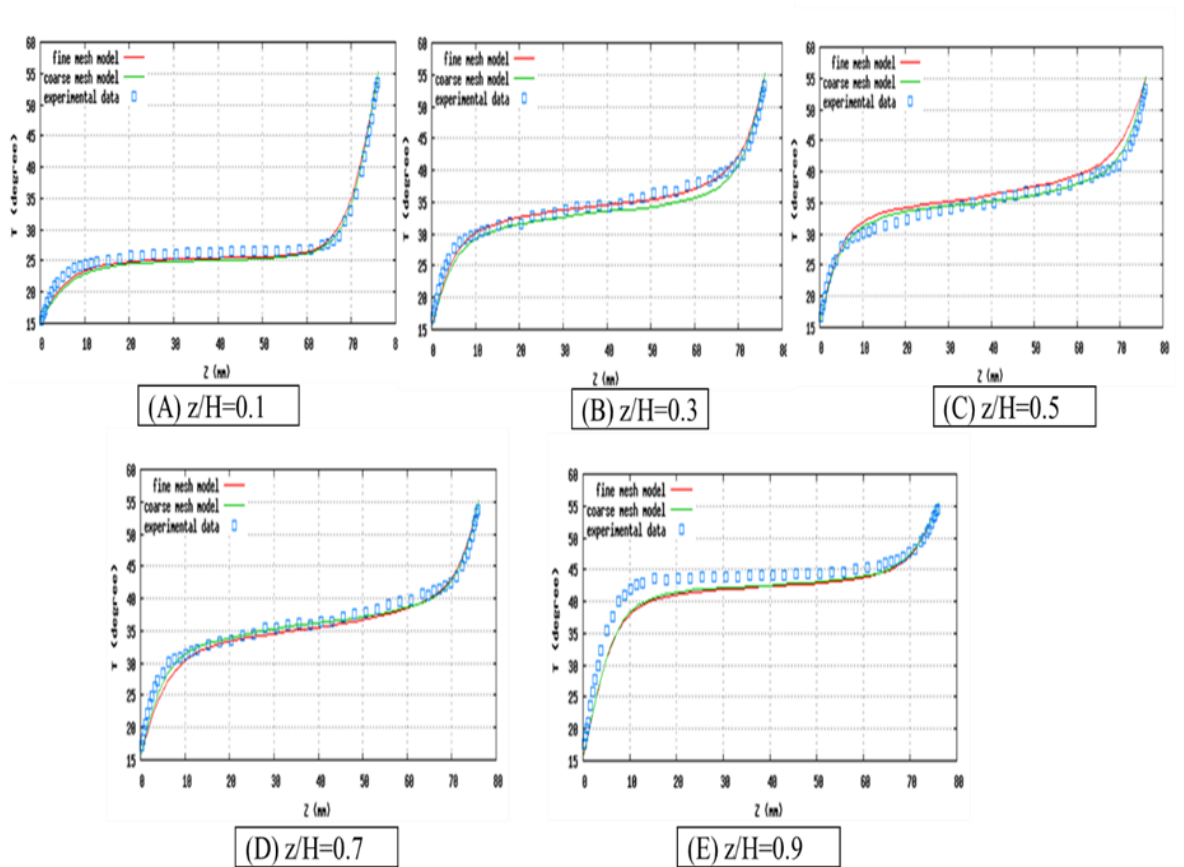(A) z/H=0.1   (B) z/H=0.3   (C) z/H=0.5

(D) z/H=0.7   (E) z/H=0.9

Figure 5.2: Statistical mean profiles of temperatures at the five heights.

It is evident that the computational results agree very well with the experimental results. Figure 5.3 illustrates the statistical mean profiles of vertical velocities. It shows the agreement between the computational and experimental results at two heights close to the top wall and bottom wall, z/H=0.1 and 0.9. However, a discrepancy between the experimental and computed results can be seen at the three inner heights. The numerical results under-predicted the peak velocities at the borders of the hot or cold boundary layers. The maximum discrepancy was observed at the border of the cold boundary layer at the height, z/H=0.7. Presumably, the major reason for this discrepancy is that the sampled data are insufficient, since the statistical mean in a less recorded set would lead to a larger discrepancy, as tested.
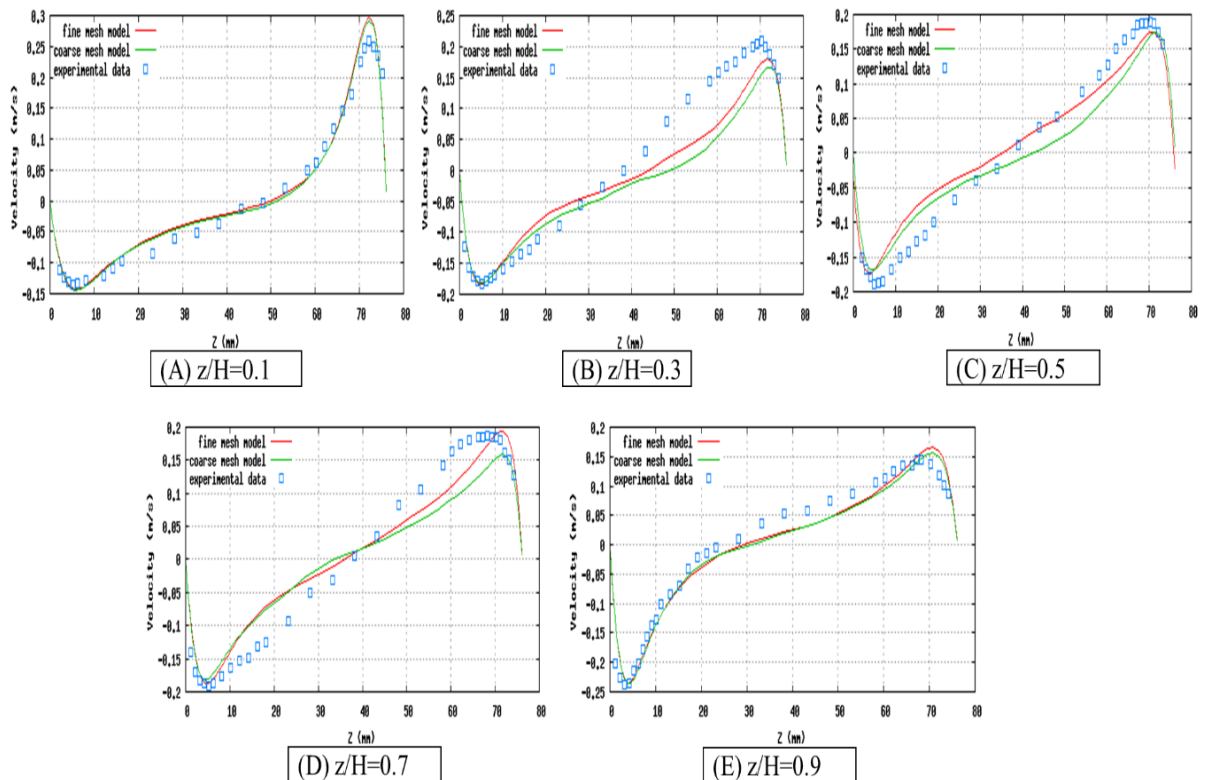

Figure 5.3: Statistical mean profiles of vertical velocity at the five heights.

Three temperature profiles produced by the experimental, computational and theoretical results are illustrated in Figure 5.4. As seen therein, the numerical solution in the buffer layer under–predicts, but in the outer layer over–predicts, the temperature. The experimental results slightly over–predict the temperature in the entire layers. This discrepancy is supposed to be caused because of sample and statistical errors.
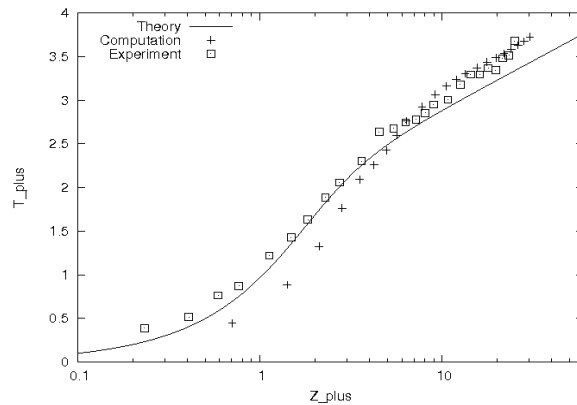

Figure 5.4: Statistical mean profiles of temperature at z/H = 0.5 that show the comparison of the experimental, computational and theoretical results

5.1.4 Mesh independency test

Two meshes, one fine and the other course, were used to test mesh independency of the numerical solutions. The fine mesh is 8 times as dense as the coarse mesh. Therefore, the cost of performing the computation for the fine mesh is about 8 times that for the coarse mesh. Figure 5.5 shows the typical comparisons of the fine mesh, coarse mesh and measured results at the height z/H=0.5. It is apparent that the two meshes produced consistent numerical solutions.
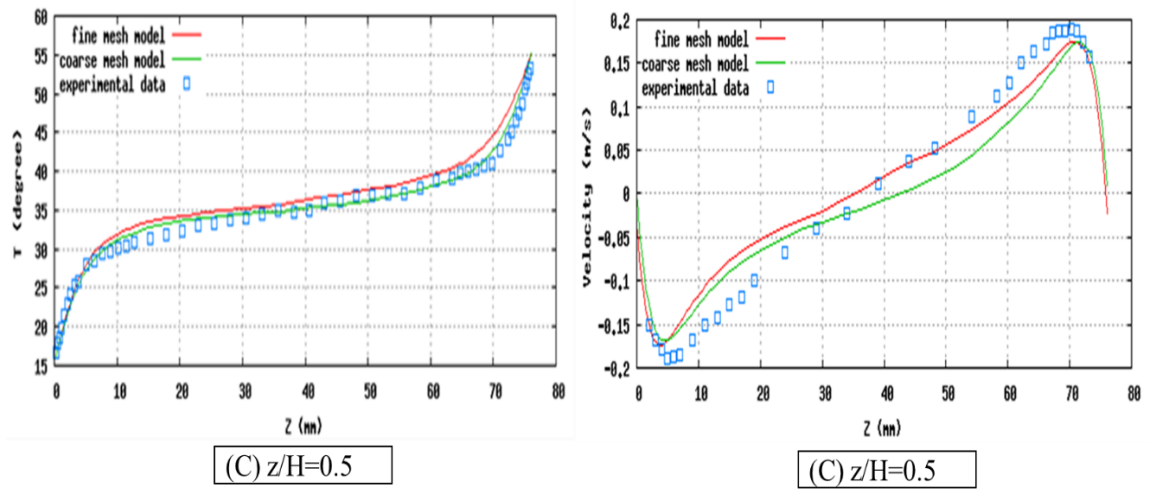
Figure 5.5: Comparisons of the results produced on fine and coarse meshes with the experimental data

5.1.5 Summary

Comparisons between the computational and experimental results show that the statistical means of the numerical solution agree well or are consistent with the measured data. The computed results are qualitatively consistent with the other experimental and computed results. The mesh–independency test shows that the applied fine mesh is adequate to produce a reasonable solution. The work on this aspect further verifies the capability of the new LES approach. This work was published at the International Conference on Model Integration across Disparate Scales in Complex Turbulent Flow Simulation (ICMIDS) held in the USA (Alharbi, 2015).

5.2 Validation of natural ventilation flow rate

5.2.1 The experimental model

Figure 5.6 is an eight-storey office building with an atrium space on the north side is considered. Staircase and utility space are contained in the atrium. The south façade of the building is a double-skin façade and a three-storey high thermal storage space called solar chimney is considered above the double-skin space. The double-skin space is connected with the chimney channel (Ding et al., 2005).
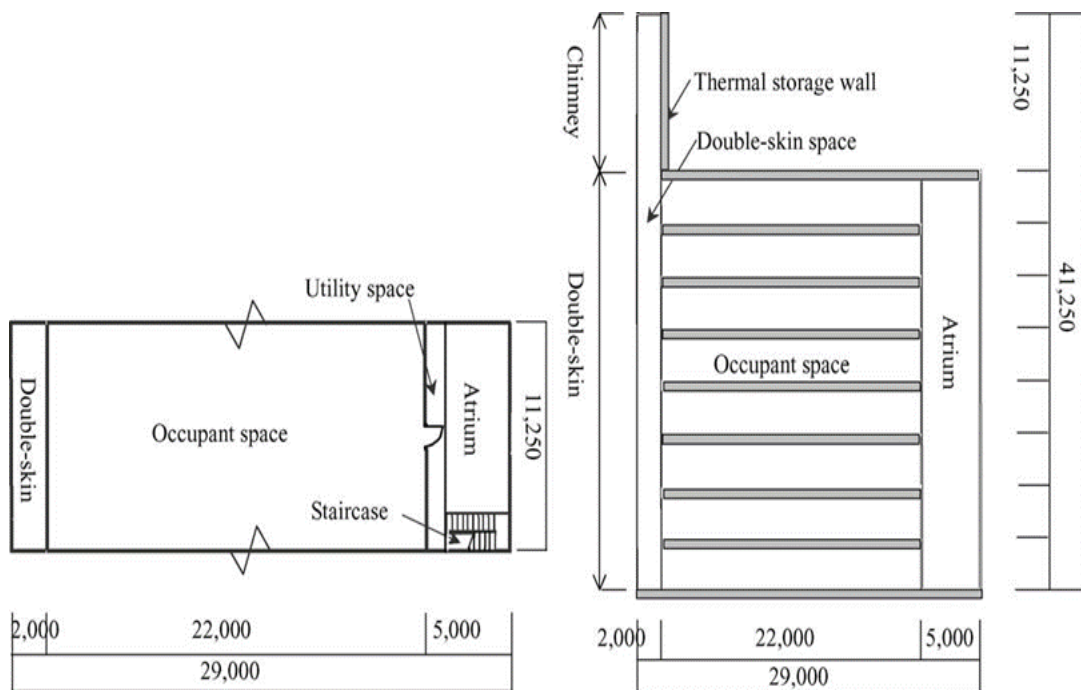

Figure 5.6: Outline of the prototype building (left: plan; right: section; units: mm). (Ding et al., 2005).

Considering manual operability of the experiments and the similarity of the basic characteristics of the flow in the reduced scale model and the full-scale prototype building, the experimental model is reproduced as 1/25 of the full-scale prototype building. Figure 5.7 shows outlines of the experimental model.

Figure 5.7: Picture of the experimental model (Ding et al., 2005).

Panel heaters are used to simulate the temperature rise of the double-skin façade and blinds due to the absorption of sunlight. Although temperature rise occurs on the surfaces of both glazing and blinds, the experiment temperature rise of the glazing is considered small and only temperature rise of the blinds is reproduced. Panel heaters are attached to the interior surface of the outer façade for easy operation. Temperature rise of the thermal storage wall is also reproduced by

panel heaters. Insulators are used as exterior surfaces to reduce heat loss from the

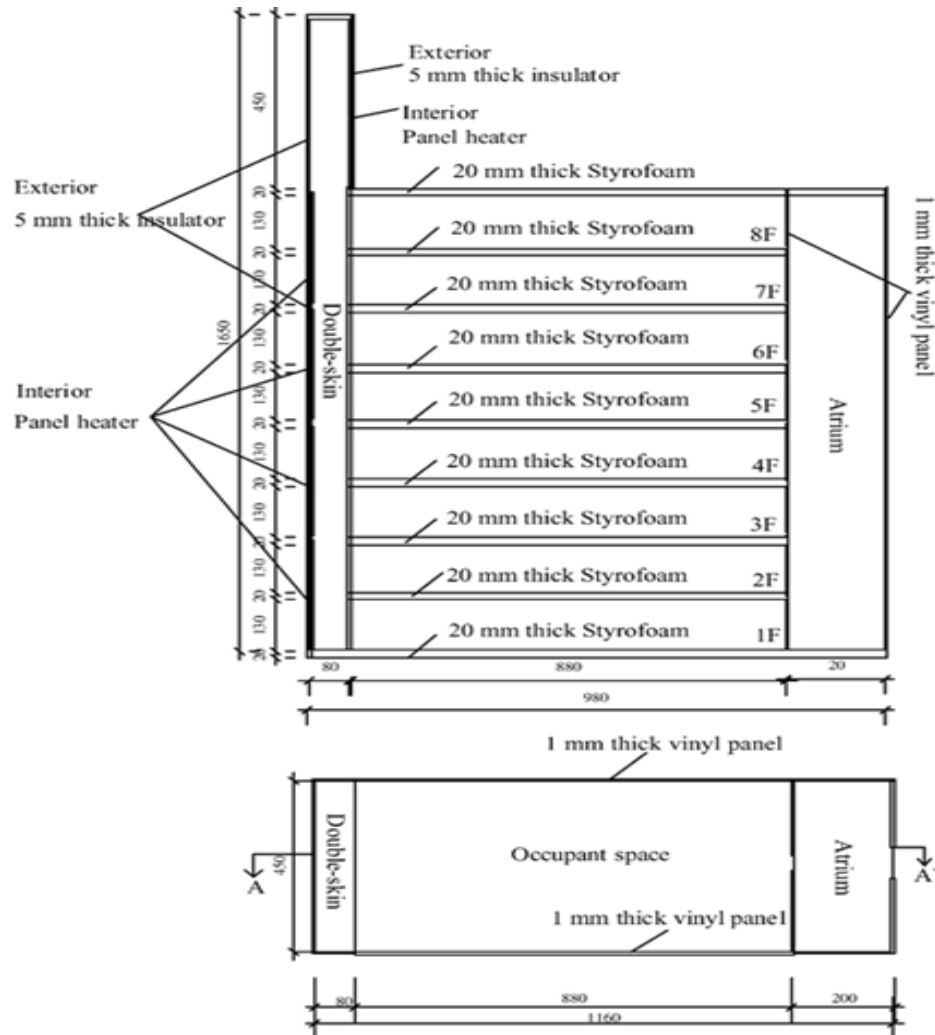double-skin space and chimney channel, figure 5.8.

Figure 5.8: Outline of the experimental model (Ding et al., 2005)

5.2.2 The simulation model of mesh-independent solution

Ding et al. (2005) state that a comparison is made between the numerical results

and the experimental measurement for the purpose of validating the numerical

models.
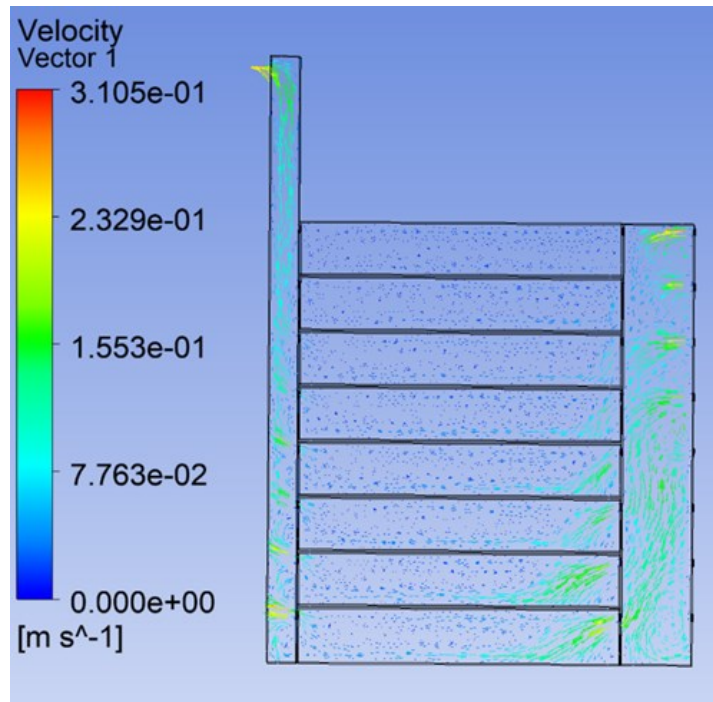
Figure 5.9 : The simulation model

Figure (5.9) shows the simulation design, while Figure (5.10) shows low airflow

in the upper floors as found in the results mentioned by Ding et al. (2005).

Figure 5.10: Airflow through the floors

The present study also involved studying the mesh independent solutions. In

order to do so, the computational domains were meshed by three of the six

elements, with the following dimensions: 0.010m × 0.010m × 0.010m, 0.012m ×

0.012m × 0.012m and 0.03m, 0.03m and 0.03m. The comparison of the numerical

104

results can be seen in Figure 5.11 below. It can be observed that accurate numerical results can be generated with a 0.010 m fine mesh and 0.012 m control volume. This is a viable option due to the fact that usin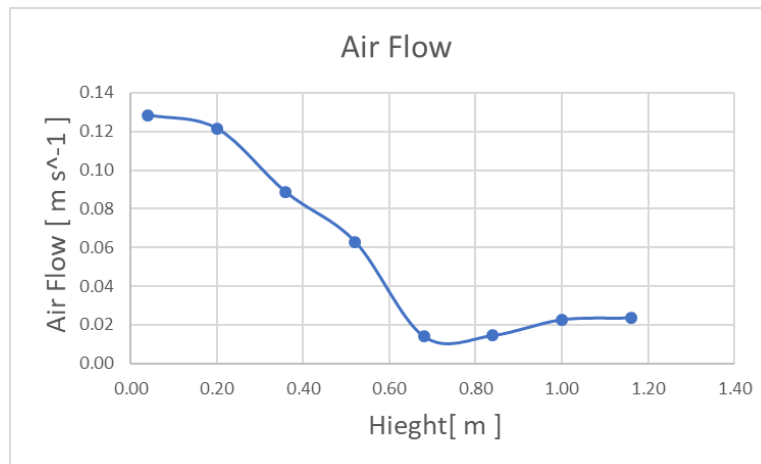g 0.012 m offers similar results to those produced by 0.010 but does it quicker and more affordably. The experimental results slightly over–predict the temperature in the entire layers. This discrepancy is supposed to be caused because of sample and statistical errors.

Table 5.1 Mesh Information for CFX

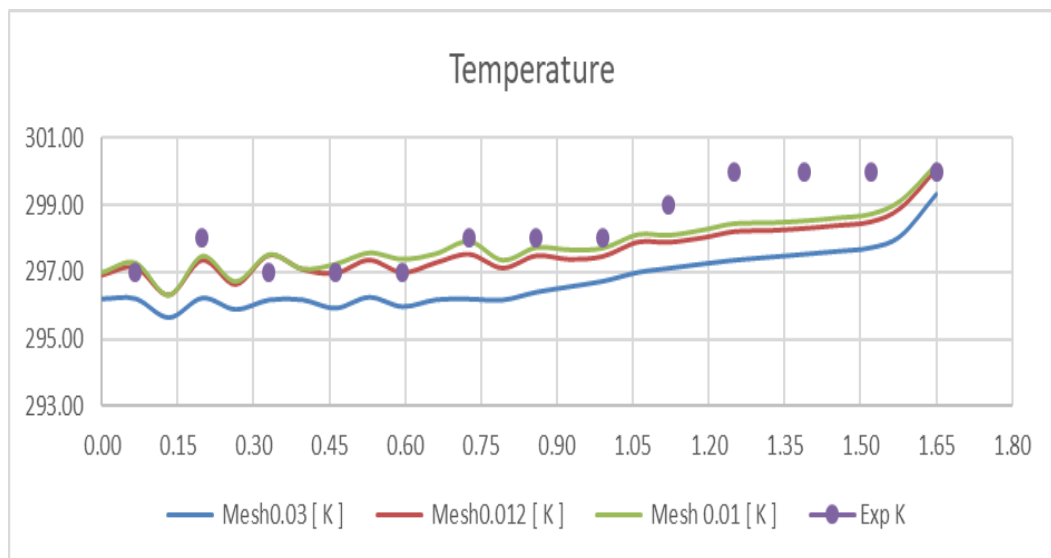| Domain	Nodes	Elements
Mesh 0.01	319487	1623260
Mesh 0.012	315446	1604358
Mesh 0.03	38604	181626

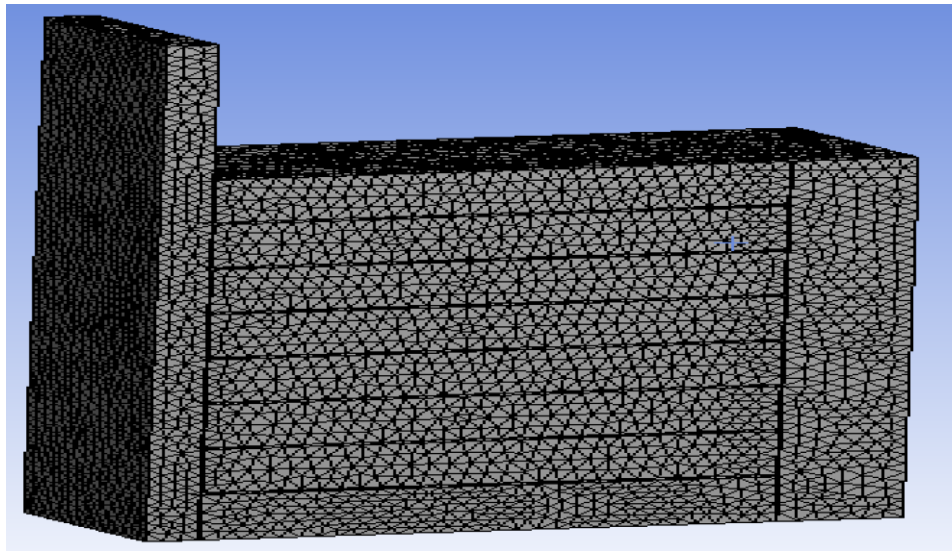Figure 5.11: Mesh-independent solution

Figure 5.12: Mesh-independent solution

Table 5.2 Mesh independence results

Domain	Mesh 0.01	Mesh 0.012	Mesh 0.03	EXPERIMENT	Predicted results	%Error from predicted	%Error from fine mesh
Nodes	319487	315446	38604	None			
Elements	1623260	1604358	181626	None			
T1 [K]	297.25	297	296.25	297	297.376	0.13%	0.08%
T2 [K]	297.5	297.5	296.25	297.75	297.66	0.03%	0.08%
T3 [K]	297.5	297.25	296.25	297.25	297.66	0.14%	0.08%
T4 [K]	297.25	297	296	297.25	297.41	0.05%	0.00%
T5 [K]	297.5	297	296	297.25	297.69	0.15%	0.08%
T6 [K]	298	297.5	296.25	297.75	298.22	0.16%	0.08%
T7 [K]	297.75	297.5	296.5	298	297.91	0.03%	0.08%
T8 [K]	297.75	297.5	296.75	298.25	297.88	0.12%	0.17%
T9 [K]	298	298	297	298.75	298.626	0.04%	0.25%
T10 [K]	298.5	298.25	297.5	299.75	298.63	0.37%	0.42%
T11 [K]	298.5	298.5	297.5	300	298.63	0.46%	0.50%
T12 [K]	298.75	298.5	297.75	300	298.88	0.37%	0.42%
T13 [K]	300	300	299.75	300	300.03	0.01%	0.00%

Based on the grid extrapolation method of mesh independent solution introduced in the reference (Almohammadi et al., 2013). As seen in Table 5.2, the method is successfully applied and the predicted results led to close agreement to the obtained results from the fine mesh compared to the experimental results which make the conclusion drawn from the analysis reliable.

5.3 Grid

An appropriate numerical approach is not all that is required to predict airflow; a suitable computational grid must also be generated. The use of an appropriate grid system in conjunction with a fine grid resolution is proposed (Nielsen, 2007; Awbi, 2008) to reduce dispersive errors as well as false diffusion. This is to maximise the accuracy of predictions, especially in those areas that feature large gradients. Poor grid quality can lead to degenerated cells yielding numerical errors. Therefore, in order to increase the likelihood of accurate, plausible results with good convergence, an independent grid study is advised before undertaking the main study.

A grid distance in the region of 100mm is recommended for a 5m room and a grid distance of about of 300mm for a 20m room. Nielsen (2007) also recommends finer cells in those areas where flow phenomena are of significance.

Schneider and Raw's (1987) finite element based finite volume method forms the discretisation scheme employed in CFX. The domain is divided into multiple unstructured elements. Nodes are found here at the vertices, the location where the properties are stored.

5.4 Computational Methods

The purpose of using finite volume methods is the discretisation of the Reynolds-averaged N-S equations in space. On the other hand, unstructured mesh containing either tetrahedral or hexahedral elements is applied to the

computational domain. While the elements' vertices are in the place where all the fluid properties and flow variables are located, every element surrounding the vertex (medial dual control volume) contributes to form the control volume related to a vertex. In order for the integrations over the control volume as well as on the surfaces to be made, second order accuracy numerical schemes must be applied.

The primary area of focus in the present study is the discretisation results as steady states produced from a set of ordinary differential equations integrated by way of the first order backward Euler scheme. Ultimately, a set of algebraic equations approximate to the Reynolds-averaged N–S equations are generated.

The strategies comprising the algebraic system, of which there are many, can in simple terms be split into the segregated approach and the coupled approach. The segregated approach involves solving the flow velocity and the pressure separately, whereas the coupled approach solves all the equations at once. According to Patankar (1980), the fact that there is a collocated arrangement in CFX, implying that the unknowns are all stored at the mesh's nodes, means the algebraic equations' matrices could be singular, generating a checkerboard pressure field if the surface integrations and volume integrations for spatial discretisation are calculated via the direct application of simple schemes. This pressure field is nonphysical and can be eliminated by using a body-force

redistribution term and a pressure redistribution term to correct the mass equation integration's velocity.

CFX5 works by constructing a single large matrix to accommodate the complete set of coupled equations. It then solves all the equations at once, rather than solving each equation individually in order. The fully implicit solver technique that it uses means that the equations are all advanced at once without time step size restrictions. During each time step, additional sweeps are performed by the solver on coarser grids as part of CFX5's multigrading system.

Once the CFX-Solve Manager has been set in motion, the initial adaption step will occur by the 100-iteration point. Information such as the dimensions of the new mesh and how many elements have been refined will be stored in the out file.

As a result of the interpolation of the old mesh into the new, a jump then occurs within the residual levels following the mesh being refined. Moreover, the W-Mom-Bulk equation will also now have a new residual plot. On the z axis, the mesh now becomes more than one element thick, meaning that it has become 3-dimensional rather than 2-dimensional. This is due to the orthogonal refinement of its hexahedral elements.

5.5 Conclusion

It is advisable to carry out validation for the accuracy and reliability of CFD models against dependable data generated by other experiments, whether large or small in scale.

Nonetheless, in order to minimise errors and uncertainties and to maximise accurate, cost effective results, care does need to be taken in certain respects, such as whether to select a steady state or unsteady state approach to simulation, selecting an appropriate turbulence model, accurately defining boundary conditions and ensuring that the computation grid is properly defined.

CHAPTER 6: Buoyancy-Driven (Stack) Ventilation

6.1 Introduction

The performance of DSFs is affected by a number of factors. The most important of these factors are radiation from the sun, wind pressure and the internal configuration of the building. Because natural ventilation is dependent on thermal buoyancy and wind, the problem faced by architects is a lack of knowledge regarding the airflow behaviours in the DSF cavity which directly affects the ventilation within buildings.

Wind is inherently variable. The wind pressure driving ventilating flows depends on numerous interacting factors such as wind speed and direction, positioning and orientation of vents and façades, and the surrounding terrain and buildings. De Wit and Augenbroe (2002) suggest wind pressure calculations as the most important source of uncertainty in natural ventilation design, with a probabilistic, rather than deterministic, design approach.

The main aim of this study is, therefore, to acquire more information about buoyancy and airflow, which result from wind pressure and solar radiation, and how they are affected by the presence of a double-skin façade. To this end, modelling was conducted on the abovementioned factors that affect airflow, to try to understand the relationship between these factors. Understanding the nature of the interactions between them fulfilled the first objective of this study.

On this basis, a model was proposed with the intention of improving control over airflow in the double-skin façade. The model was the result of development of the multi-storey double-skin façade pattern. Testing was conducted on this model for the effects of solar radiation and wind pressure. Both the testing and the double-skin façade model were based on previous studies that explain the advantages and disadvantages as mentioned in the literature review. The results obtained in the present study were compared to those of previous studies, to enable us to exploit DSF and to improve conditions inside occupational space.

The study was divided into two parts in accordance with the objectives:

1- Studying the performance of DSF in a single room as a part of buildings and conducting the necessary simulations to fulfil the first and second objectives of this study. This is the topic of the present chapter.

2- Applying the model to more complex configurations, i.e., high-rise buildings, that consume more energy in ventilation. This is in accordance with the third objective of the study. This topic also is discussed in the following paragraphs.

6.2 Configuration of Case Studies

A multi-storey façade pattern was developed, to enhance airflow inside the building by the way of creating a duct between the double-skin façade and the atrium. The development was then tested to check for effectiveness and performance in enhancing airflow. To this end, a three case studies were

conducted. The first one was an initial simulation for one DSF room only where the simulation was conducted without ducts, to establish the effects of buoyancy on airflow. The buoyancy can be as a force controlling the movement of air within any building.

The second case study was the simulation with five floors. On one side of the model was the atrium while on the other side was the double-skin façade. The two were connected with two parallel ducts at the top. A variety of parameters were tested to establish the depth and height of the double-skinned façade.

The final case study involved 15 floors that can be applied as a standalone building or as part of a high-rise building. In this case study, the first step was to test all 15 floors together without ducts but with a double-skin façade as one zone running from the bottom of the building to the top without interruption. The next step was to segment the double-skin façade every five floors. The third one, which is the model being proposed in this study, was not only to segment the double-skin façade every five floors, but also to introduce two parallel ducts above every five floors to link the atrium to the double-skin façade. Each duct was 1m wide and 0.5m in height. The purpose of these ducts was to balance the airflow within the building. Usually, with a double-skin façade on one side of the rooms and an atrium on the other side, the flow of air in the upper part of the building is higher in velocity than that in the lower part of the building. The presence of ducts every five floors was, therefore, intended to create a relatively balanced airflow throughout the floors. It was also intended to disperse excessive

heat generated in the façade that might otherwise make the occupation area overly hot, thereby maintaining IEQ. The final stage will be discussed in the next chapter.
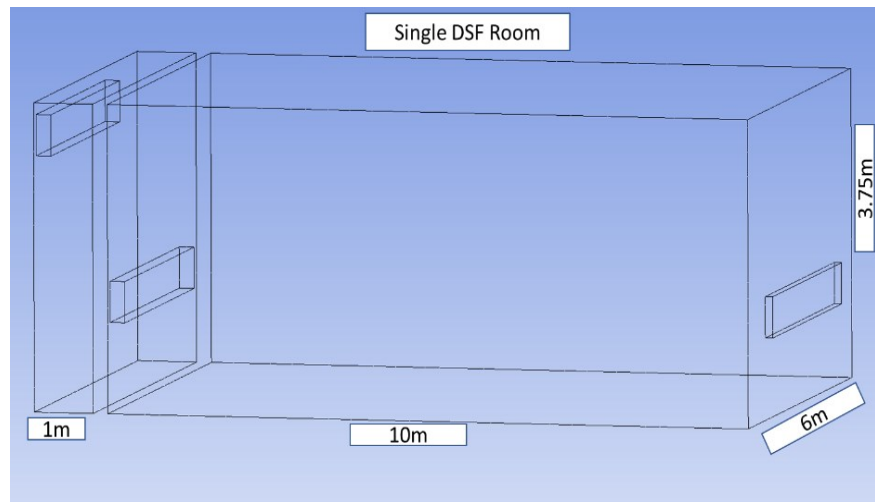
6.3 Case Study for Single Room

Figure 6.1: A single DSF room with 10 m width

In order to study the effects of double-skin façade on airflow within single rooms, simulation was conducted for a room with the dimensions of 6m depth, 10m width and 3.75m height, as can be seen in Figure 6.1. Several tests were conducted to establish the relation between height and depth and their effect on airflow within the room. Tests were also carried out to study the effects of vent position to establish the performance of the double-skin façade in regulating ventilation within the room.

6.3.1 Effects of room width on air flows

A single room with a double-skin façade was tested twice by different width (22m and 10m). To investigate the effects of room width on air flows, The results

in figure 6.2 show that using the double-skin façade when the width to height (W/h) ratio is more than 5 results in poorer ventilation, while when the ratio is less than 5, the ventilation is good (See figure 6.3). This result convenient with the general principle mentioned by Etheridge and Ford (2008), that spaces with a width to height (W/h) is more than 5 suffer from poorer ventilation than those with a ratio of less than 5.
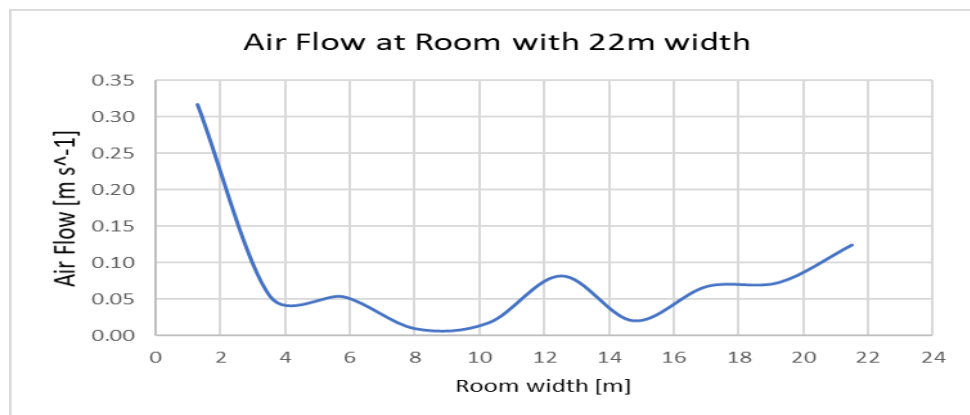

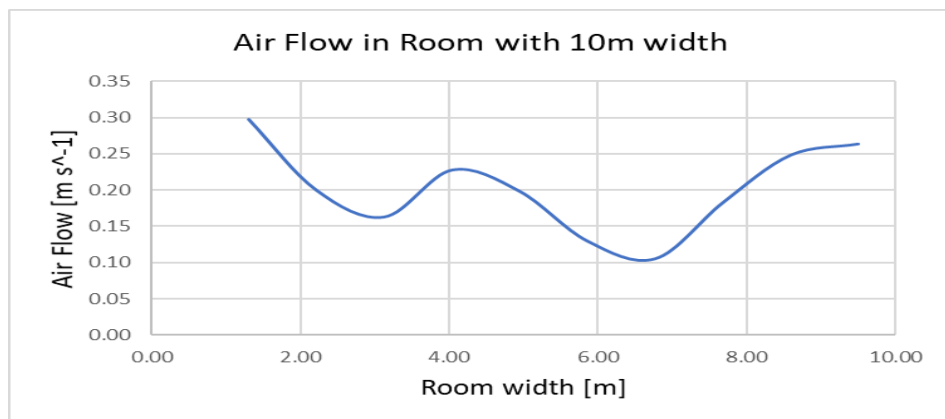Figure 6.2: Airflow in room with 22 m width

Figure 6.3: Airflow in room 10 m wide

6.3.2 Effects of vents position to air flow

A buoyancy can be produced through heating the air inside the cavity of the double-skin façade, which acts as a source to drive airflow. The results show that when the room has a temperature lower than that inside the cavity of the double-

skinned façade and the external openings are at the same height in both, the air flows from the room to the double-skin façade cavity due to the fact that the room has a lower temperature (Figure 6.4). The tests (Figure 6.5) also show that when the two external openings differ in one space, the air flows upwards from the lower opening toward the higher opening. This is due to the buoyancy force. These findings confirm the principle presented by Chenvidyakarn and Woods (2010), stating that air flows from lower openings upwards to higher openings and moves from less heated spaces into more heated spaces. This helps us control the direction of airflow by using different heights for openings and different temperatures in spaces.
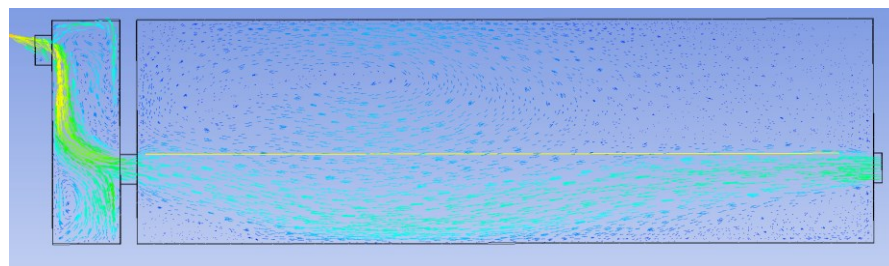

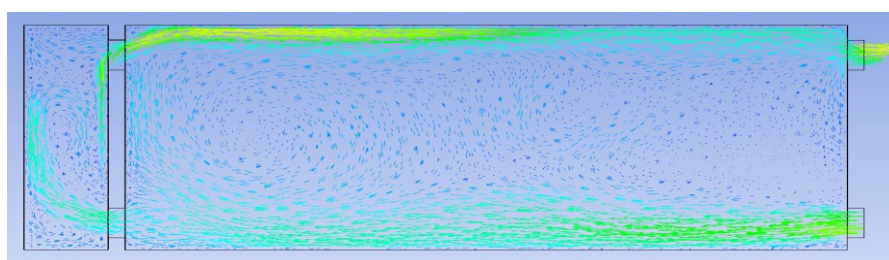Figure 6.4: Room with vents on same level

Figure 6.5: Room with vents on different levels

6.3.3 Summary

From the results of the two foregoing sections (6.3.1 & 6.3.2), it can be seen that DSF enhances ventilation in the room. This is by virtue of the sun heating the air in the cavity of the DSF, which causes buoyancy, which in turn acts as a force

causing the air to flow through the spaces. These results serve to strengthen the case for further tests of performance of DSF in part of a building, not just one room. This matter is dealt with in the following section.

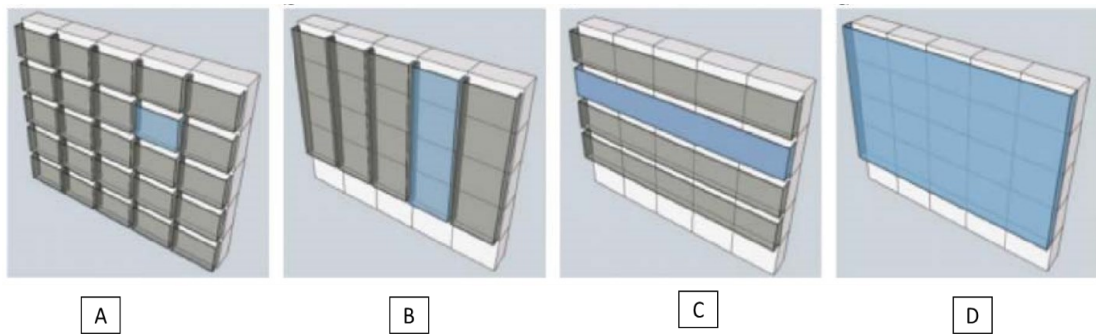## 6.4 Case Study for Multiple Floors

Figure 6.6: Patterns of DSFs: (A) Box window, (B) shaft-box, (C) corridor and (D) multi-storey double-skin façade

Double-skin façades are placed on multiple floors of a structure that itself has a number of skins and are typically divided into the categories of air-tight and ventilated (Chan and Chow, 2009), (Barbosa and Ip, 2014). Ventilation strategies employed within the cavity are also used in order to classify typologies for DSFs (Shameri et al., 2011). This effectively means that thermal insulation is improved and increased by airtight double-skin façades during winter, and that in summer, heat gain is reduced by way of ventilated double-skin façades that gain heat energy by way of sunlight (Chan and Chow, 2009). Double-skin façades are categorised by researchers into window, shaft-box, corridor and multi-storey façades (Kim and Song, 2007; Wong, 2008) (see Figure 6.6). Airflow is crucial to DSF design, and different DSF patterns in the varying seasons and climates determine airflow.

Furthermore, DSFs are developed in diverse configurations. This research represents a new development of multi-storey façade pattern (as shown in Figure 6.7). This design allows the air to pass from the cavity of the double-skin façade to the atrium on the other side of the building through a duct at the top. This mode allows excessive heat to dissipate in the cavity away from the rooms and also reduces wind pressure on the windows of the rooms.
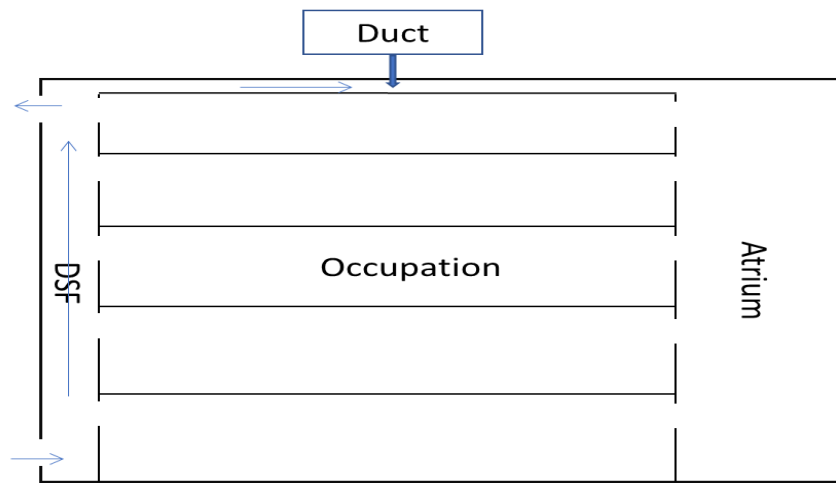

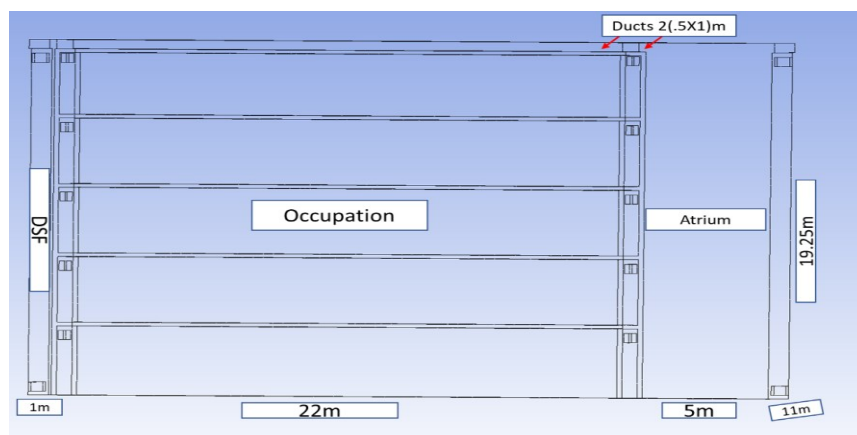Figure 6.7: The development of a multi-storey façade pattern

6.4.1 Setting up the model

Figure 6.8: Setting up the model

Table 6.1 Mesh Information for CFX

Domain	Nodes	Elements
Default domain	471327	2431801
Option	Steady state	

Figure 6.8 shows the model tested to establish the performance of DSF in part of a building consisting of five floors. This test was intended to discover how air flows, and the nature of ventilation plus its effect on temperature in occupied spaces. The part of the building tested was 28m in depth, 11m in width and 19.25m in height. The two parallel ducts at the top were 0.5m in height and 1m in width. Table 6.1 provides more information about the CFX.

The significance of these results in determining the appropriate cavity depth and height of the double-skin façade is discussed below.

Testing was conducted for DSF cavities 1m and 2m deep. Once it had been established that 1m depth was the more effective, testing was conducted for a part of a building containing four floors, followed by a test for five floors. This was in order to establish the best way of segmenting taller buildings. It was established that five floors would be used.

Thereafter, another test was conducted for ambient temperature and wind to see how the proposed model would perform.

6.4.2 Advantages and Disadvantages of DSF

DSFs have been recommended by a number of researchers (Chou, Chun and Ho, 2004; Weir, 1998) as an energy efficient means of lowering heat gains for low

energy buildings, with Shameri et al. (2011) being arguably the greatest supporters of the approach. The basis of the idea is an air gap/cavity containing nothing (Gratia and De Herde, 2008). According to Gratia (2007), DSFs were developed from entirely glass façades. Mingotti et al. (2011) stress that a DSF's internal layers must feature versatile openings to enable ventilation in both the cavity and the spaces adjacent thereto. Thus, there is a relationship between ventilation and temperature on one hand and cavity size on the other (see section 6.3.1 & 6.3.2). According to Balocco (2002) and Balocco and Colombari (2006), a decrease in cavity width increases the chances of overheating within the façade layer, especially in hotter weather. However, DSFs can typically have an extra glaze skin added to the building, improving energy performance, natural lighting and visual comfort. Functional capabilities of façade are represented by Figure 6.9 below:
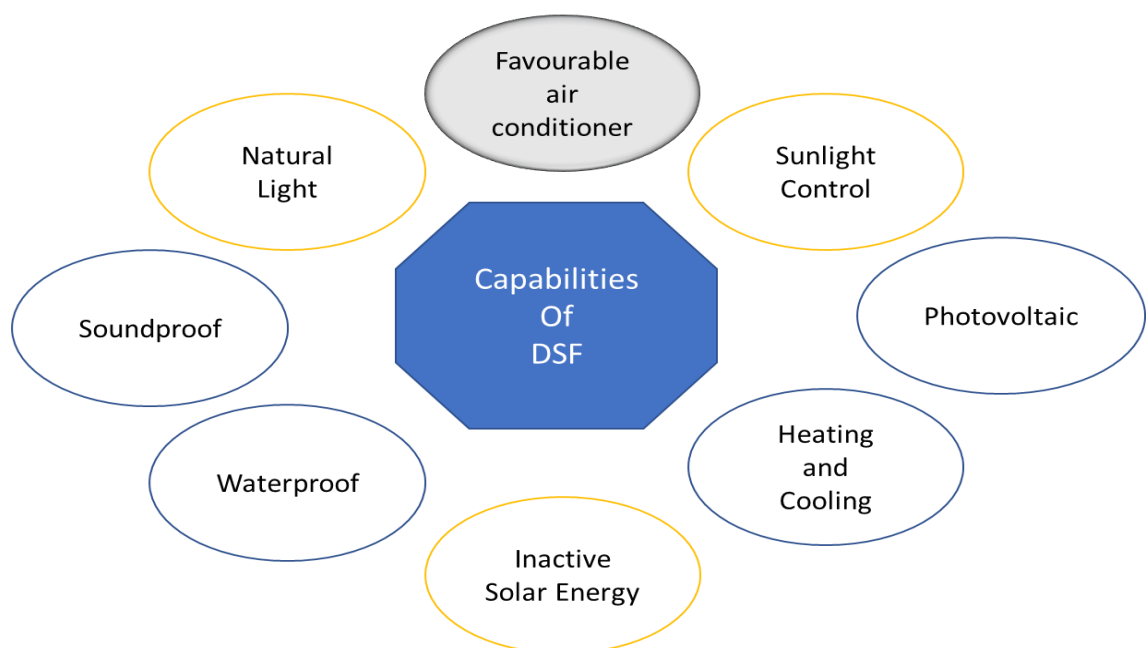

Figure 6.9: Functional capabilities of façade. (Ghasemi and Ghasemi, 2017)

The results in this study corroborate the results of previous studies, where it is clear from the comparison between the temperature in a building with double-skin façade and single façade building that the temperatures are lower at the occupation spaces in buildings with double-skin façade in the summer when the temperature is 35°C (Figure 6.10), while being slightly higher in the winter season when temperature is 10°C (Figure 6.11). Therefore, double-skin façades act as insulators in the hot seasons and provide warm the air inside in the cold season as they move warmth into the occupation spaces, while buildings with unilateral façades are directly affected by external weather and wind.
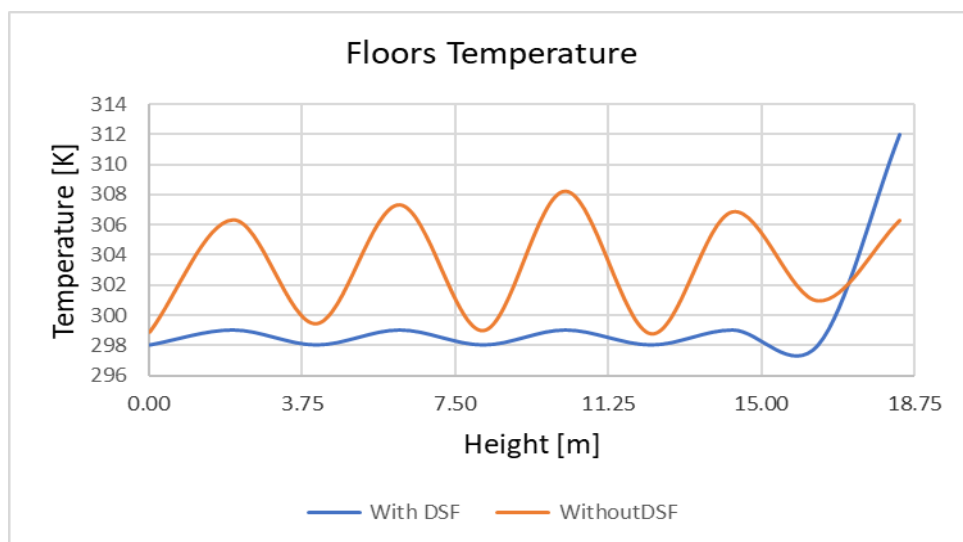

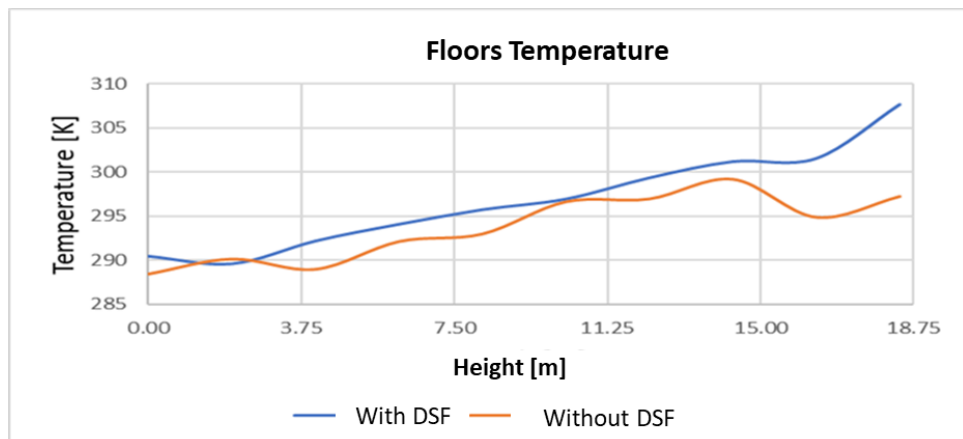Figure 6.10: Occupation spaces temperature with and without DSF at 35°C

Figure 6.11: Occupation spaces temperature with and without DSF at 10°C

Oesterle et al. (2001) stress that DSFs must enable window ventilation or significantly increase the time that natural ventilation can be used, for meaningful energy savings to be made. Thus, DSFs can be highly beneficial in modern developments, with the caveat that they are more expensive than single glass façades. This initial cost is cancelled out in the long term due to DSFs' superior durability. DSFs have other advantages over their single-skin equivalents, including being environmentally friendlier and therefore cutting costs. This study therefore seeks to develop DSF systems.

6.4.3 Cavity size DSF

The depth of the cavity affects how much solar radiation transfers across the layers of the DSF, affecting air temperature and airflow rate, as reported in various studies (Gratia and De Herde, 2007a; Torres et al., 2007; Rahmani et al., 2012; Radhi et al., 2013) using various models. However, they all found that temperatures were higher, airflow faster and stack effects were stronger where smaller depths were used. Therefore, narrow DSF cavities allow for more warm air to be extracted, with lower thermal transfer inwards to the occupied space of the building, which in turn allows lower energy use during hot weather.
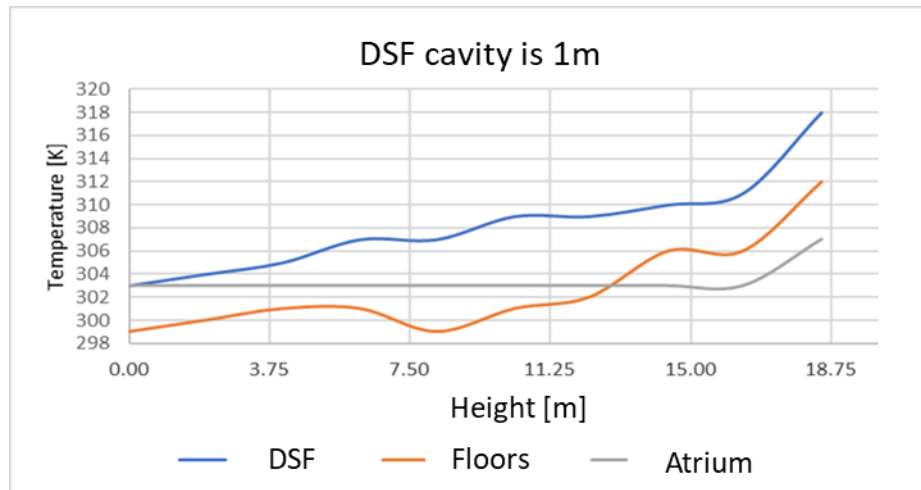
Figure 6.12: Variance of temperature with height.

The results of this study demonstrate a significant correlation with what was mentioned in the previous studies. Figure 6.12 shows that the temperature in the cavity of the double façades was higher than that in the occupation space, especially for lesser depths, whereas the temperature of the cavity was higher at a depth of 1m. It increased by more than four degrees at a depth of 2 m. Meanwhile, the temperature inside the building was equal to or higher than that in the cavity of DSF when the depth was 2 m (see Figure 6.13).
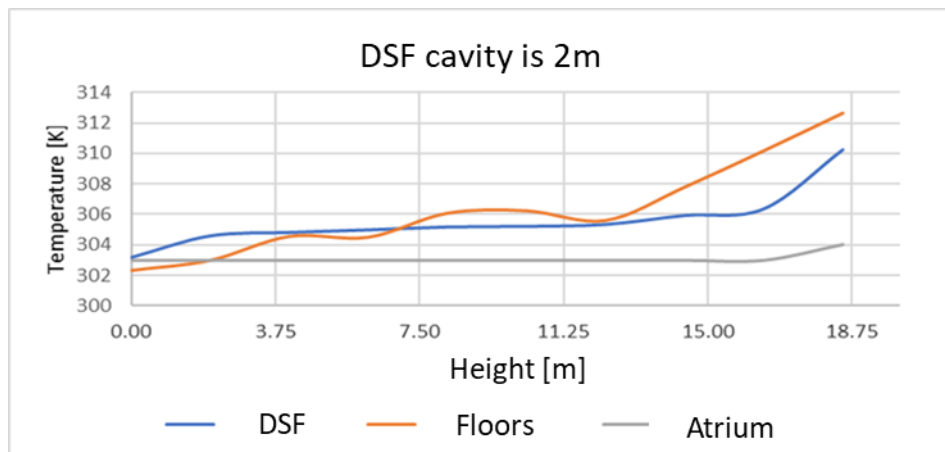

Figure 6.13: Variance of temperature with height.

According to Joe et al. (2014), energy consumption decreases when the cavity depth of the DSF decreases. This indicates that greater depths are not efficient, because lesser depths are hotter (See Figure 6.14).
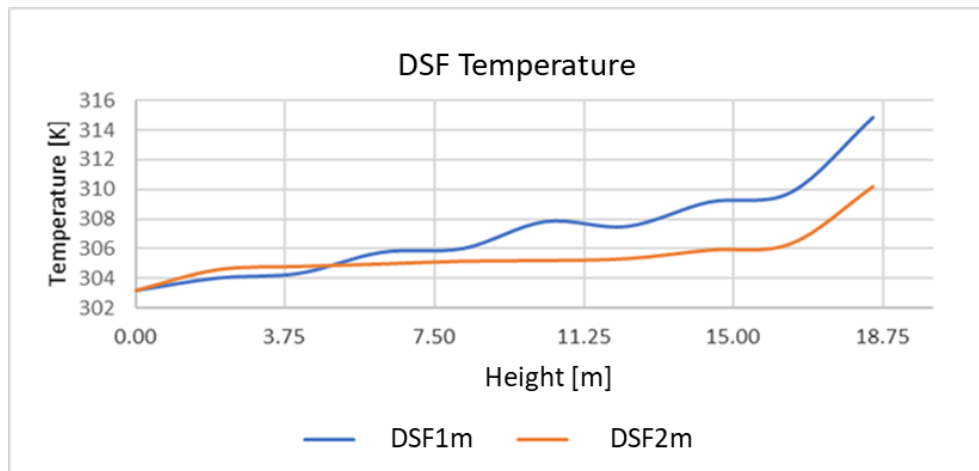

Figure 6.14: Variance of temperature with height for two cavity sizes.

This is, therefore, a reflection of the fundamental relationship between cavity size on one side and temperature and ventilation on the other. Balocco (2002) and Balocco and Colombari (2002) assert that reduced cavity width means an increased risk of the façade overheating in hot weather. However, the results of this study do not fully support this. They show an acceptable difference in temperature rise in the cavity of DSF at 35°C, compared to the temperature reached when the external temperature is 25°C (see fig. 6.15). It can be observed that there are suitable solutions that reduce the temperature inside the cavity when the temperature is very high, such as increasing the number of vents on the external side. This requires further research.
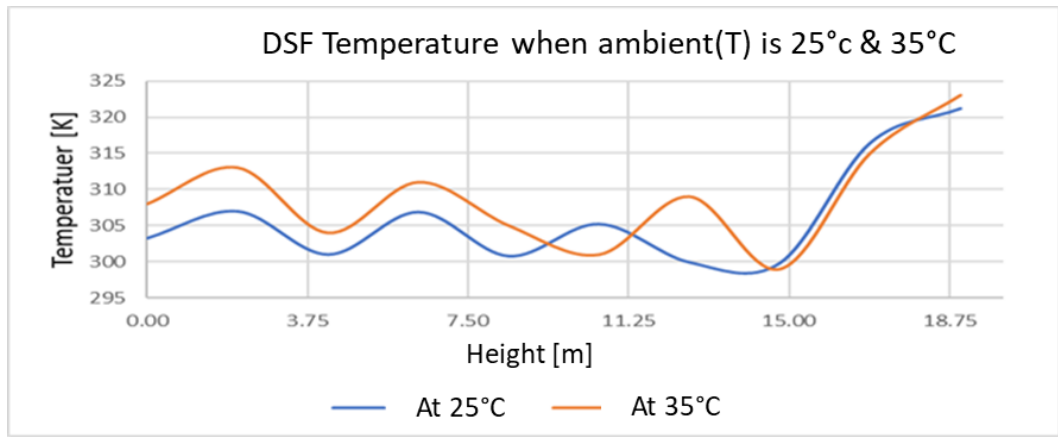
Figure 6.15: Variance of temperature with height at different ambient temperatures.

6.4.4 Performance of 5 Floors DSFD and 5 Floors DSF

Table 6.2: Impact of various air speeds on occupant comfort levels in a building (Auliciems and Szokolay, 1997, p. 14)

Air speed	<0.25 m/s	0.25–0.5 m/s	0.5–1.0 m/s	1.0–1.5 m/s	>1.5 m/s
Impact on Building Occupants	Unnoticed	Pleasant	Awareness of Air Movement	Drafty	Annoyingly Drafty
Note	Higher velocities are acceptable in hotter and humid climates				

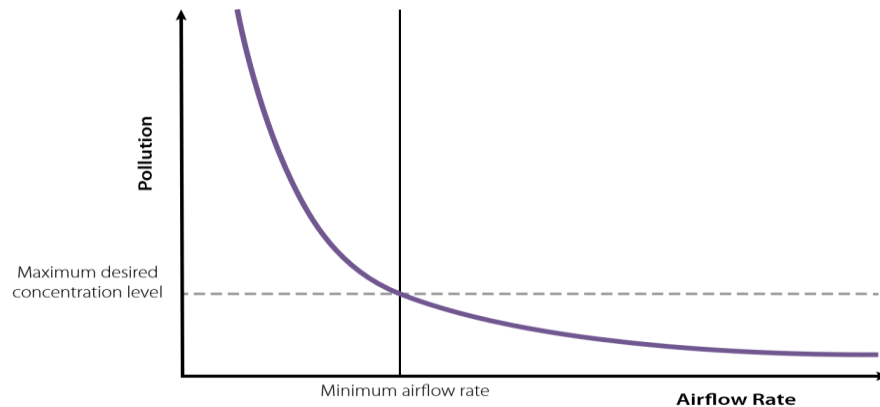Figure 6.16: Natural ventilation for indoor air quality showing the relation of pollution level to the airflow rate (Allard and Santamouris, 1998, p. 3)

Figure 6.16 illustrates that, as the airflow resulting from natural ventilation becomes greater, there is a massive decrease in indoor pollution levels. Moreover, in order to maintain internal pollution at acceptably low figures, there is a need

for a minimum airflow rate. However, excessively high air velocity in offices may result in compromised thermal comfort for occupants, apart from the fact that it can lead to papers being displaced from their appropriate locations (see Table 6.2). According to Yeang (2006), conditions featuring a temperature of between 18° and 24° Celsius combined with 30% to 60% relative humidity are typically considered to be comfortable. However, culture and a variety of other elements can have a considerable effect on what is accepted as thermal comfort.

There are six factors that contribute to occupant comfort: air velocity, relative humidity, air velocity, temperature, the activity level of the occupant and their clothing insulation. Considering the aims of this research, this simulation only sought to test air velocity and temperature. This was to test the performance of the model under development, i.e., the double-skin façade with duct (DSFD), against the model containing a DSF but without a duct. The proposed model features five floors. The two models in figure 6.17 were tested using simulation.
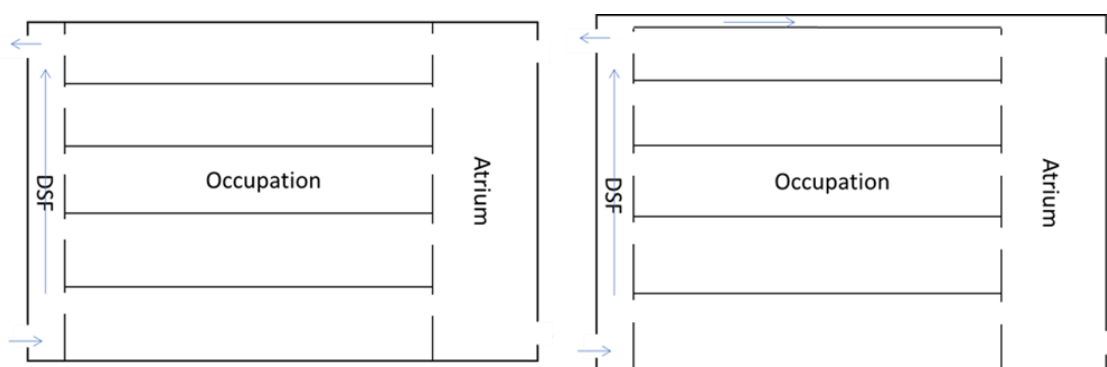

Figure 6.17: DSF building without duct (left) and DSFD with duct (right)

6.4.4.1 Ambient temperature

Tests were conducted for a number of different ambient temperatures to compare the two models and to see whether the differences in temperature affected

airflow and temperature in the occupational space. The temperatures tested were 10°C, 25°C and 35°C.

- **Temperature and Airflow at 10°C**

At 10°C ambient temperature, there was negligible difference between the two models in terms of the temperatures in the occupational spaces (see Figure 6.18). However, it was observed that there was greater airflow through the fourth and fifth floors of the model without the duct than there was in the DFSD. This can be explained by the fact that, when the temperature increases in the DSF cavity, this causes the air to flow within the cavity and move upward. In the model with the duct, the undesired air that is pushed up is dispersed by way of the duct, whereas in the model without the duct, the air travels across the occupational spaces. This simulation, therefore, demonstrated the benefits of the use of ducts to keep airflow at an acceptable level (see Figure 6.19).
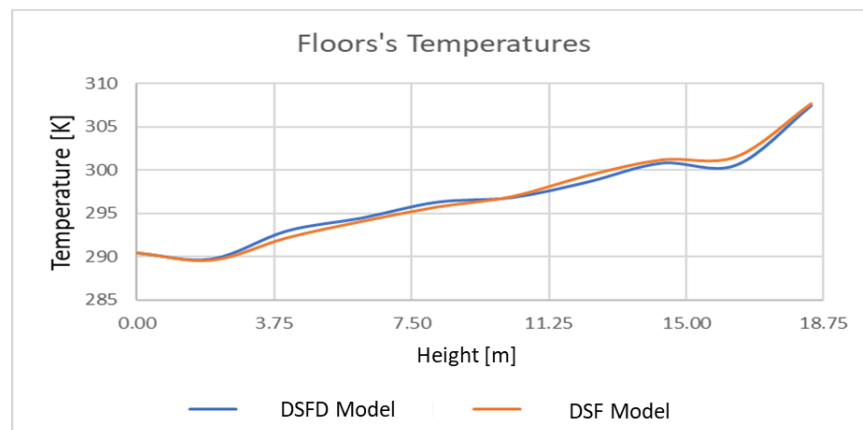

Figure 6.18: DSFD and DSF occupation space temperature at 10°C

Figure 6.19: DSFD and DSF occupation space airflow at 10°C

- **Temperature and Airflow at 25°C**

At 25°C ambient temperature, there was negligible difference between the two models in terms of the temperatures in the occupational spaces (see Figure 6.20), except on the fifth floor where the temperature was more than two degrees higher in the model without the duct than it was in the DSFD.
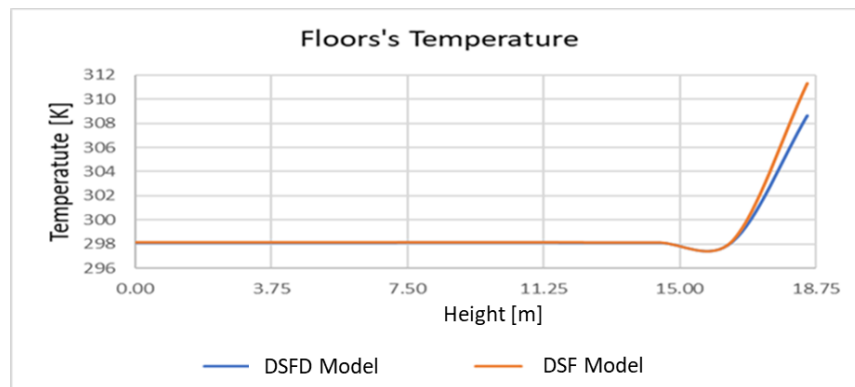
Figure 6.20: DSFD and DSF occupation space temperature at 25°C

It was observed that there was a significantly greater airflow on the fifth floor of the model without the duct than there was in the DFSD, at almost 0.8 compared to 0.35 in the latter. This can be explained by the fact that, when the temperature increases in the DSF cavity, this causes the air to flow within the cavity and move upward. In the model with the duct, the undesired air that is pushed up is

dispersed by way of the duct, whereas in the model without the duct the air travels across the occupational spaces. This simulation, therefore, demonstrated the benefits of the use of ducts to keep airflow at the acceptable level (Figure 6.21).

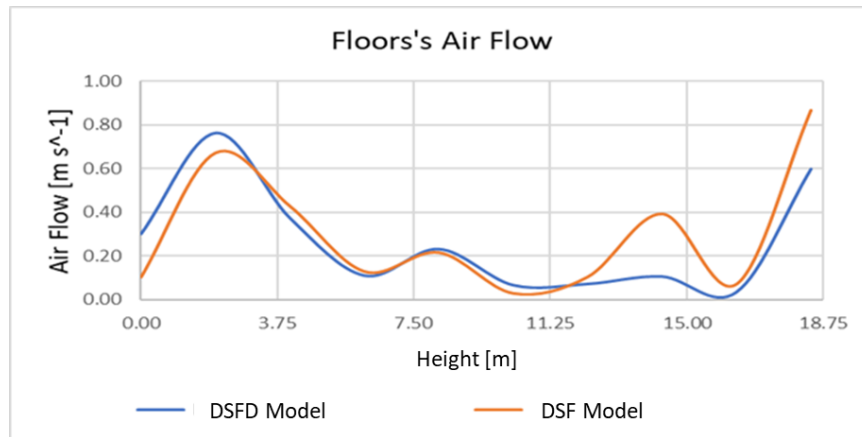
Figure 6.21: DSFD and DSF occupation space airflow at 25°C

Figure 6.22 shows that the model featuring the duct has lower airflow than the model without the duct. This is because the duct allows the air to disperse through it rather than through the occupational spaces.
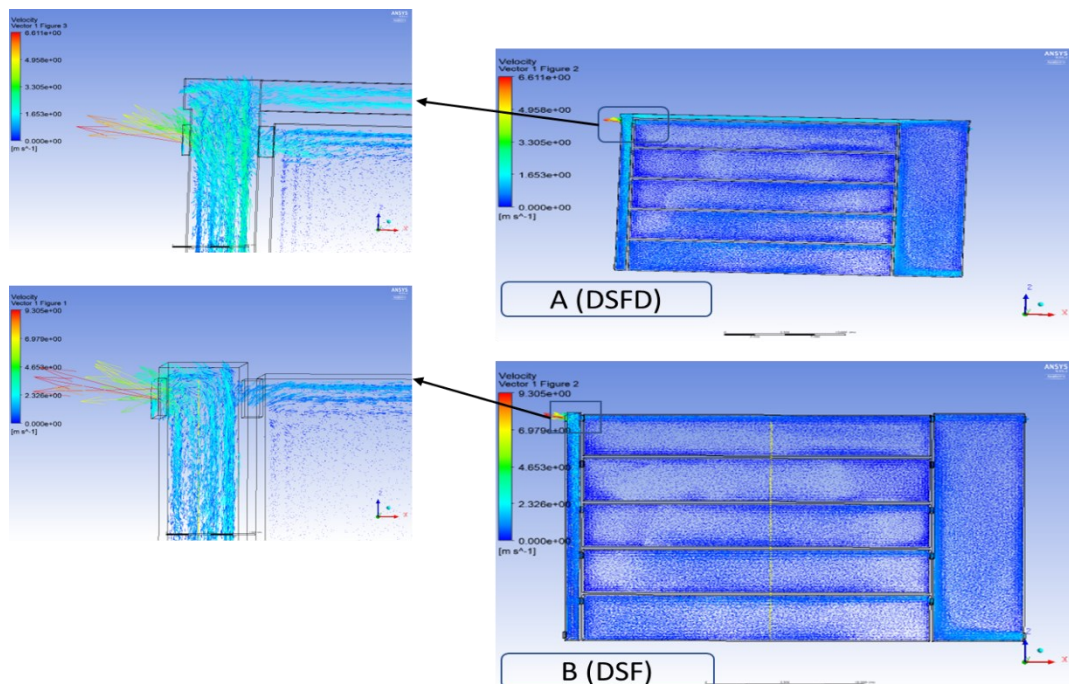
Figure 6.22: Airflow with DSFD and DSF

- **Temperature and Airflow at 35°C:**

At 35°C ambient temperature, the difference between the two models was negligible in terms of the temperatures in the occupational spaces (Figure 6.23), except for a two-degree difference at the top of the fifth floor, with the model without the duct being hotter.
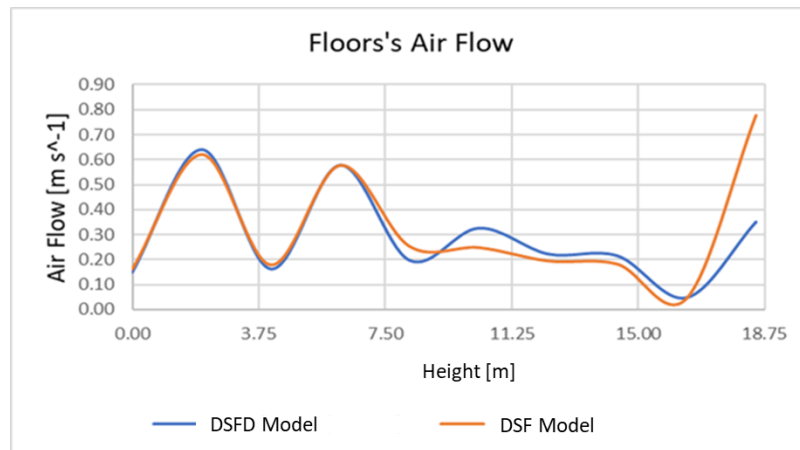
 It was observed that there was a significantly greater airflow on the fifth floor of the model without the duct than there was in the DFSD, at 0.46m/s compared to 0.28m/s for the latter. This can be explained by the fact that, when the temperature increases in the DSF cavity, this causes the air to flow within the cavity and move upward. In the model with the duct, the undesired air that is pushed up is dispersed by way of the duct, whereas in the model without the duct, the air travels across the occupational spaces. This simulation, therefore, demonstrated the benefits of the use of ducts to keep airflow at the acceptable level (see Figure 6.24).
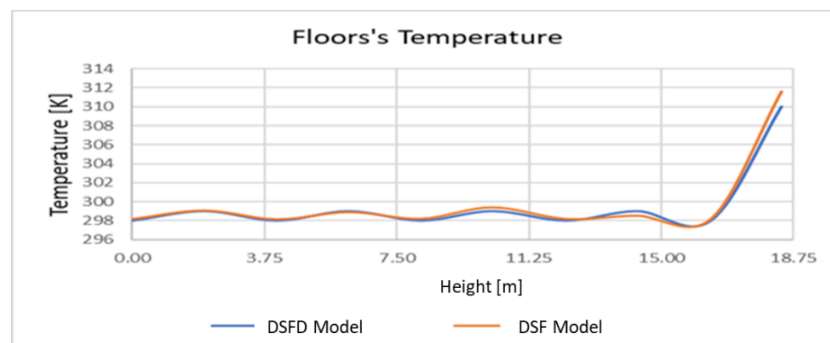
Figure 6.23: DSFD and DSF occupation space temperature at 35°C
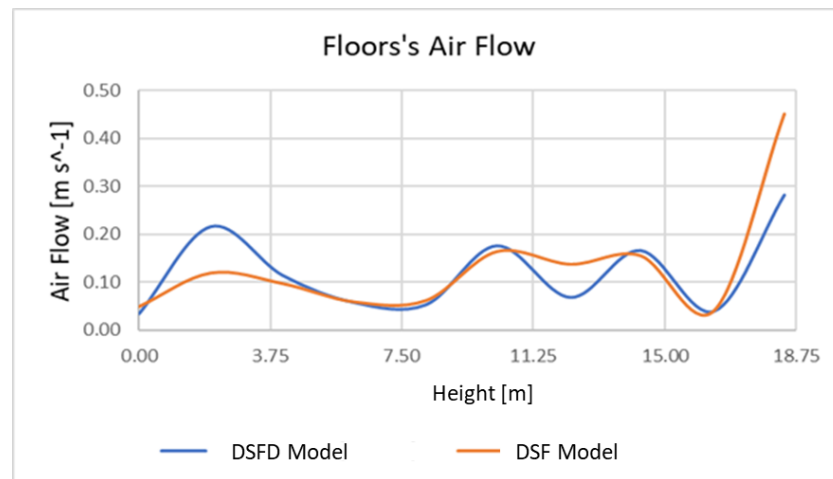
Figure 6.24: DSFD and DSF occupation space airflow at 35°C

- **Wind**

Testing was conducted with a wind speed of 2m/s to establish the effect of wind speed on airflow and temperature within the models. The direction of wind was assumed perpendicular to the facades, however, this was not extensively tested as the focus was on the comfort inside the occupation space. Occupation space comfort will be primarily influenced by the air pressure inside the DSF cavity, where this will be influenced by how much air is moving into the cavity from outside, as opposed to how it is flowing inside (i.e., the direction the wind as it entered through the opening). This is because the wind is entering the DSF cavity through openings in the DSF, instead of hitting the occupation space directly.

It was observed that the temperature was higher on the third and fourth floors of the model without the duct when compared with the DSFD, (Figure 6.25). This can be explained by the fact that there is no duct wind pressure that causes the warm air to be pushed through the third and fourth floors.
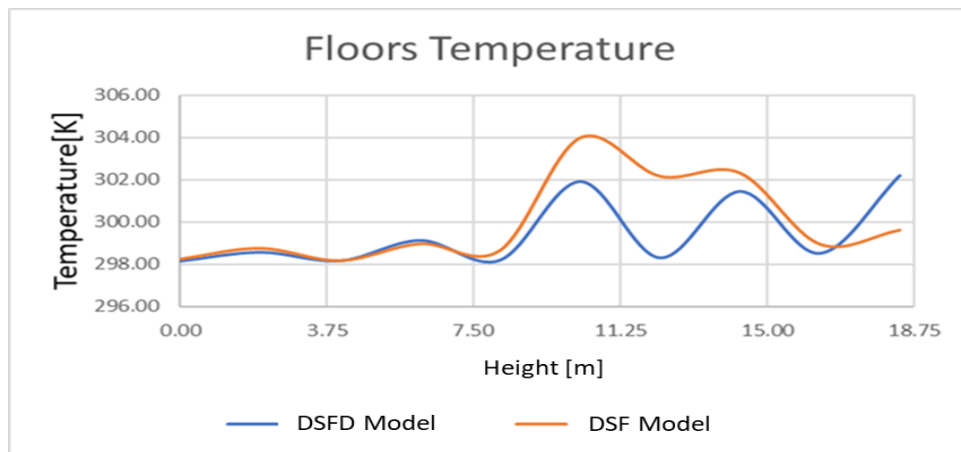
Figure 6.25: DSFD and DSF occupation space temperature with wind

It was observed that the airflow was greater on the fourth and fifth floors of the model without the ducts when compared with the DSFD. However, at the very top of the fifth floor, levels were almost identical (Figure 6.26). This shows that the duct helped disperse the pressure inside the DSF cavity without sacrificing occupation room comfort.
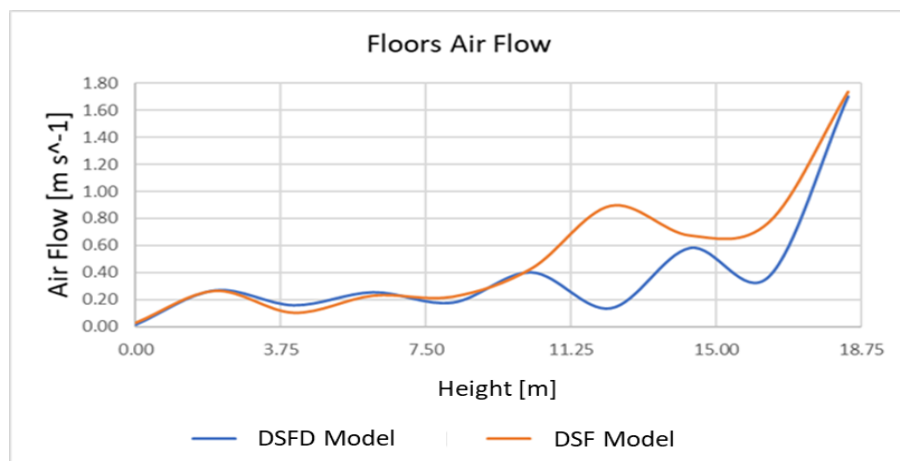
Figure 6.26: DSFD and DSF occupation space airflow with wind

6.5 Performance of 5 Floors DSFD and 4 Floors DSFD

The height variance between the cavity's air outlets and inlets is a key factor for thermal buoyancy magnitude within the DSF, as this sets the pressure differential of the openings, in which the higher the cavity the greater the stack effect, with a

higher level of airflow (Oesterle et al., 2001; Mingotti et al., 2011). Airflow level inside the cavity is a key concern, particularly for climates with high temperatures and humidity levels, as there must be sufficient buoyancy to draw out excess thermal energy by cross-ventilating user occupied spaces.

In principle, the higher the cavity the greater the pressure variation between the openings, with greater differences promoting greater airflow. Based on the literature, however, patterns of stratified heat within the cavity in practice vary based on the type of building and the solar radiation pattern. Thus, each building requires an individual analysis of ventilation based on its geometric design and climatic considerations.

There is a way around the problem, and that is the use of segmentation, i.e. the building is divided into several segments that are isolated from one another by open spaces. The design problem now is to achieve the required flow directions and magnitudes for each segment. Ventilated façades on tall buildings can provide the driving force for a segmented natural ventilation strategy and help to control varying diurnal and seasonal ventilation requirements.

The model developed in this study is aimed at use in the segmentation of high buildings and the discharge of the high flow of air through the openings of the upper channels and not through the occupation spaces. In this section, the results of the study carried out on the performance of the four-floor and five-floor buildings are compared to arrive at the most effective pattern for the performance

of natural ventilation through the double-skin façade with ducts connected to the other side of the building.

6.5.1 Temperature in cavity and occupation spaces

The results in Figure 6.27 compare the air temperature in the cavity of the DSF in the four-storey zone and the five-storey zone. They show that there is no significant difference between the two. This indicates that the temperature distribution is almost identical, whether the zone consists of four or five floors.

Figure 6.27: Air temperature in the cavity of the DSF

The results in Figure 6.28 compare the temperature in the occupational space in the four-storey zone and the five-storey zone. They show that there is no significant difference between the two. This indicates that the temperature distribution is almost identical whether the zone consists of four or five floors.

Figure 6.28: Temperature in the occupational space

134

6.5.2 Airflow in The Cavity and Occupation Spaces

The results in Figure 6.29 compare the airflow in the cavity of the DSF in the four-storey zone and the five-storey zone. They show that there is some difference between the two, with the four-floor zone having an airflow of 1.45 m/s at the top of the zone compared to 0.95 at the top of the five-floor zone. This difference in airflow does not affect comfort within the occupational zone.

Figure 6.29: Airflow in the cavity of the DSF.

The results in Figure 6.30 compare the airflow in the occupational space in the four-storey zone and the five-storey zone. They show that there is no significant difference between the two. This indicates that the airflow is almost identical whether the zone consists of four or five floors.

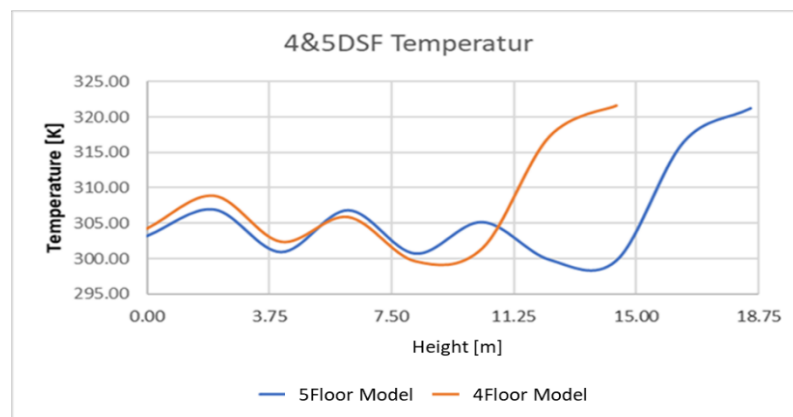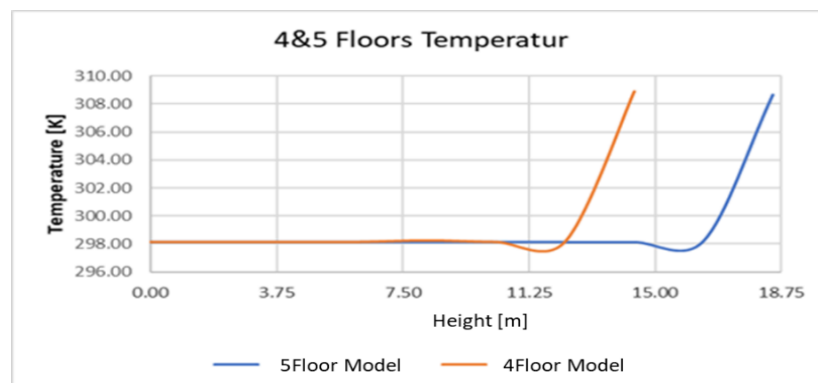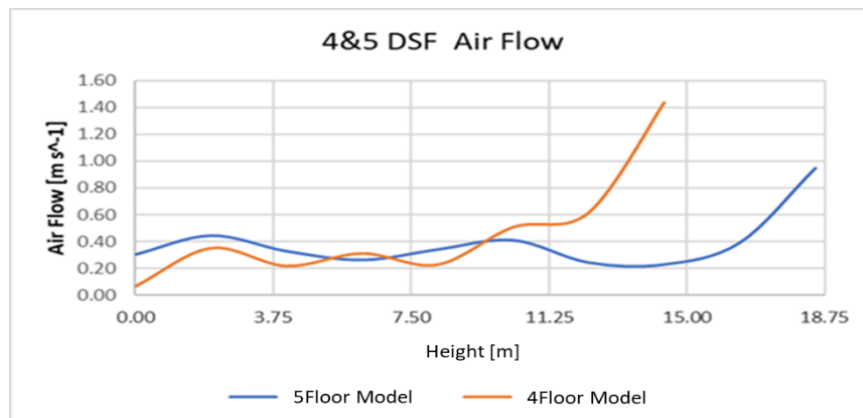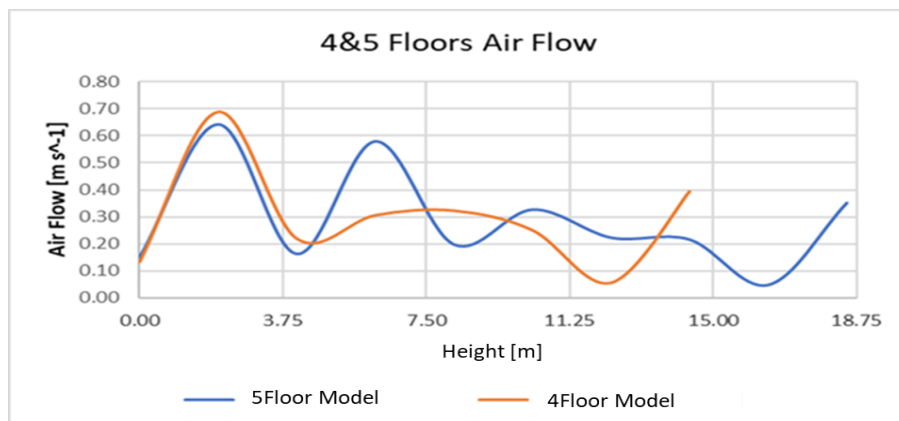Figure 6.30: Airflow in the occupational space

6.6 Summary

The results in this study corroborate the results of previous studies, where it is clear from the comparison between the temperature in a building with double façades and a single façade building that the temperatures are lower in the occupation spaces in buildings with double façades in the summer when the temperature is 35°C (Figure 6.10), while they are slightly higher in the winter season when the temperature is 10°C (Figure 6.11). Therefore, double-skin façades act as insulators in the hot season and warm the air inside in the cold season as they move warmth into the occupation spaces, while buildings with unilateral façades are directly affected by external weather and wind.

It has been shown that DSF plays an important role in the development of modern buildings, with the only drawback appearing to be the fact that it is costlier than the single glass façade that has been used for so long, which in fact is not a real drawback as initial losses are recouped over time due to DSF's greater durability. It should also be mentioned that it has other unique benefits, including its creation of greater comfort in the office environment besides being more eco-friendly. DSFs act as insulators in hot weather and move warm air up to occupational spaces in cold weather, maintaining acceptable airflow within these spaces (as mentioned in section 6.4.2). This makes for lower expenditure on maintenance due to the fact that it helps preserve the energy resources of the building. Double-skin façades can also potentially reduce the use of energy in multiple research areas.

The results of this section correspond with those of a number of studies mentioned in the literature review, in that the depth of the cavity has a significant effect on the performance of the DSF. The results of the current study suggest that the optimal depth for the cavity is between 0.7m and 1m for buildings in regions where the external temperature does not exceed 35°C. This fulfils the first objective of the study.

This study is based on a development of the multi-storey pattern of double-skin façade. In this pattern, the DSF cavity is divided into zones. At the top of each zone is a duct connecting the cavity to the atrium. The aim of this design is to disperse the high load thermal buoyancy at the top of each zone and reduce air speed, thereby avoiding the negative effects of high load thermal buoyancy and air speed on the occupational spaces. This also helps to reduce wind pressure, which in turn reduces airflow within the occupational spaces. This fulfils the second objective of the study.

The following chapter will feature testing on buildings consisting of 15 storeys, which could be used for an independent building or for a part of a taller building.

CHAPTER 7: Ventilation into the Segmentation of Tall Buildings

7.1 Introduction

Today it is common to find non-domestic buildings employing natural ventilation only. It is of particular success in 'green field' sites and city centres. Nevertheless, design difficulties have meant that it is less common to find entirely naturally ventilated high-rise buildings, despite the fact that they have equal or greater potential than smaller non-domestic buildings in terms of savings and the other advantages.

There are a number of well-known high-rise buildings that use natural ventilation, but as part of hybrid systems using mechanical ventilation as well due to the risks of an entirely natural system. The results of this study are intended to support the case for using natural ventilation in tall buildings, whether that be as part of a hybrid system or an entirely naturally ventilated system.

In this chapter, it is proposed that part-segmentation (segmentation at DSF cavity only) might offer the least risky approach for the envelope design of non-domestic tall buildings. The effect of segmentation on the consequent flow rates of associated office spaces is of interest in this study. For this study, a double-skin façade envelope flow is adopted for evaluating the off-design conditions of three types of building configuration: non-segmented, segmented DSF cavity and segmented DSF cavity with duct for tall buildings (Figure 7.1).

The steady-state airflows through openings are evaluated under a specified design condition. Although the non-segmented case may not be allowed in some jurisdictions in terms of fire safety issues, the detailed investigation of flow rates and flow patterns with and without segmentation is of interest. Consequently, the effect of segmentation is evaluated by comparing the overall ventilation performance under three different building configurations. The designs are all based on the strategic options and core principles pertaining to natural ventilation in high-rise buildings.

The purpose of all of this is to increase the potential for controlling airflow in part of high-rise buildings to minimise the effect of wind pressure and to disperse undesirable hot air, taking it far from occupational spaces. This is to fulfil objectives 3 and 4 of the current study.

7.2 Mechanisms for natural ventilation

There is little need to state that there is no difference between the physical mechanisms for naturally ventilating high-rise buildings and those for low-rise buildings; ventilation is produced by way of pressure differences, which are created by gravity and wind acting on temperature/density differences, within openings found in the envelope of the building. The difference in wind pressure is expressed as follows:

$$\Delta p = 0.5 \rho U 2 \Delta C p \qquad \text{Eq (7.1)}$$

Here, U denotes wind speed as measured at the building's height, ρ denotes air

density. Meanwhile, ΔCp is a pressure coefficient determined by factors such as the direction of the wind and the shape of the building. A higher value of U can make for high wind pressure. Moreover, the fact that the building is particularly exposed means a high Cp. The significance of this for designing natural ventilation systems is that the system will be required to function throughout a greater range of wind pressures, which can make for even greater difficulties in terms of control.

Overall buoyancy pressure is measured as follows:

$$\Delta p = \Delta T \rho g h \qquad\qquad \text{Eq (7.2)}$$

Here, ΔT denotes temperature difference, g denotes gravitational constant and h denotes the height the temperature difference acts over. When the temperature difference acts on the entire building height, H, there can be significant buoyancy pressures.

Daniels et al. (1993) present examples of the pressures that these mechanisms can generate. Their design exercise for high-rise buildings is arguably one of the first and most comprehensive published, as well as indicating how important a building's aerodynamics are in these designs.

For any type of building, including conventional, it is very difficult to make the design entirely ventilated. There are even greater challenges when it comes to envelope design and designing the openings of the envelope, which is in part due

to the pressures resulting from wind and buoyancy increasing and the wider range over which their relative magnitudes can vary.

Aerodynamics are especially important for high-rise buildings because of their high exposure. Moreover, the fact that there are so many openings makes for numerous combinations of envelope configurations.

When high-rise buildings have ventilated façades, this can be the driving force in segmented natural ventilation, besides playing a role in controlling for varying seasonal requirements for ventilation. The outstanding benefit of a DSF is that it creates both a thermal and acoustic buffer between the inside and the outside, as has been used in numerous office buildings in Germany to engender natural ventilation by way of thermal buoyancy produced in the glazed cavity.

To ensure minimum risk in envelope design for non-residential buildings, segmentation is the best option as long as designers can reliably account for aerodynamic effects. It may finally be time for natural ventilation in high-rise buildings if sufficiently robust strategies to cater to the wide variety of conditions can be developed.

7.3 Building of Fifteen Floors (3X5 Floors DSFD)
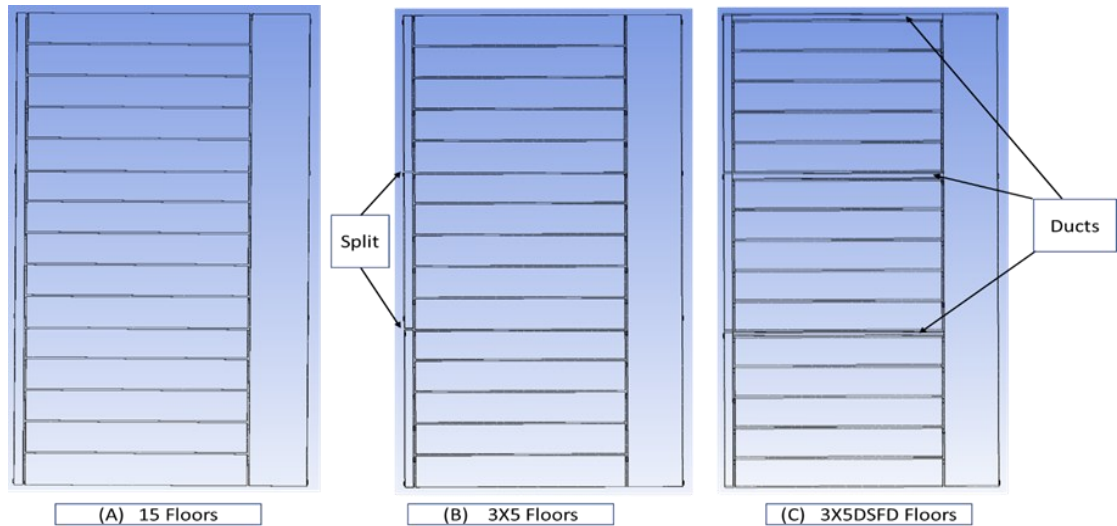
Figure 7.1: Three design models of fifteen-floor buildings

Table 7.1 Mesh Information for CFX (Fig 7.1 B)

Domain	Nodes	Elements
Default domain	380492	1909486
Option	Steady state	

Figure 7.1(A) shows the model tested to establish the performance of DSF in part of a tall building consisting of fifteen floors. This test was intended to discover how air flows and the nature of ventilation, plus its effect on temperature in occupied spaces. The part of the building tested was 28m in depth, 11m in width and 56.25m in height (3.75m per floor). The external envelope of the building is a ventilated double-skin façade (DSF) with three openings (8 m²), and the atrium-vents of the same size are in the wall opposite to the DSF-vent side, while vents connected to individual office space are (2m²).

Figure 7.1(B) shows the same model, with the DSF cavity divided into three parts with a height of five floors per part with Table 7.1 showing an example of the number of nodes and elements of 7.1 (B) domain. All simulations were carried out under steady state. Figure 7.1(C) shows the same model, with the two parallel ducts at the top, 0.5m in height and 1m in width.

The significance of these tests of the performance of DSF in segmenting the taller parts of a tall building consisting of fifteen floors is discussed below. The tests were conducted for ambient temperature and wind to see how the proposed model would perform.

7.3.1 Ambient Temperature

This section presents the results of the three designs of high-rise buildings as mentioned in Figure 7.1 in terms of the effect of ambient temperature on each design. Accordingly, the model internal temperature was set to 25°C.

7.3.1.1 Temperature and Airflow at 10°C

This subsection discusses the effect of an ambient temperature of 10°C on temperature and airflow within the occupational space and the atrium.

7.3.1.1.1 Temperature and Airflow in Occupation area at 10°C

Figure 7.2 shows the temperature in occupational spaces. The performance of the DSF in the three designs can be seen here. The DSF increases the internal temperature in all three designs. In the non-segmented design, it can be observed

that the temperature increases significantly in the upper five floors, whereas in the segmented design the temperature increases floor by floor within each five-storey segment and then drops on the first floor of the segment above. It can also be observed that the temperature on the top floor of each segment is less in the segmented model that features ducts. These results support one of the hypotheses of this study, that segmentation with ducts will increase the ability to manage the airflow within the building or part of it.
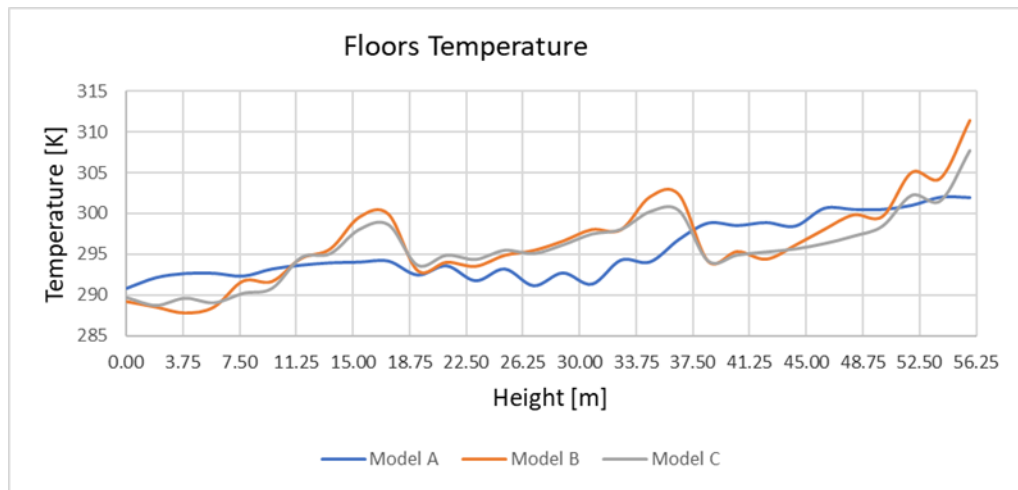

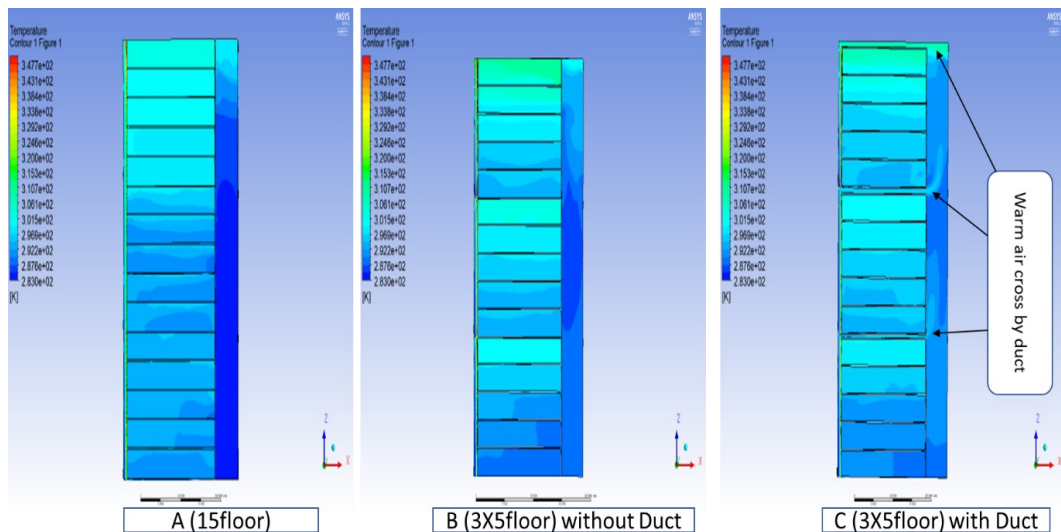Figure 7.2: Floor temperature against floor height with 10℃ ambient temperature

Figure 7.3: Simulated temperature of the three design models with 10℃ ambient temperature

Figure 7.3 clearly shows the differences in temperature distribution between the three models. In model A, which is non-segmented, there is a significant difference in temperature within the first ten floors compared to that in the upper five. Moreover, it can be observed that the temperature within the atrium is noticeably lower below the top two floors. In addition, there is clearly a dramatic difference between the temperatures in the atrium and those in the adjacent occupational spaces, with the exception of the top floor. Thus, the atrium is considerably cooler than the occupational space. The reason for this difference is that the relatively warm air from the DSF does not enter the atrium sufficiently to warm it, except at the top. The atrium air temperature, therefore, remains similar to the ambient temperature. In model B, there is a clear, remarkable difference within the occupational space between the temperature of the lower three floors and that in the floors above them. The same can be said for the temperature in the occupational space compared to that in the atrium, with the atrium being significantly cooler.

Model C, which is segmented with ducts, stands out from the other two models in that there is significantly less variation in temperature throughout the building, with the exception of the area through which the cold air enters from outside. The atrium is relatively warmer than that of the other two models. This is because, in Models A and B, the warming effect of the DSF is only felt in the occupational space, whereas the ducts in Model C allow the warm air to pass into

the atrium, thus increasing the temperature therein and making the temperature throughout the building more uniform.
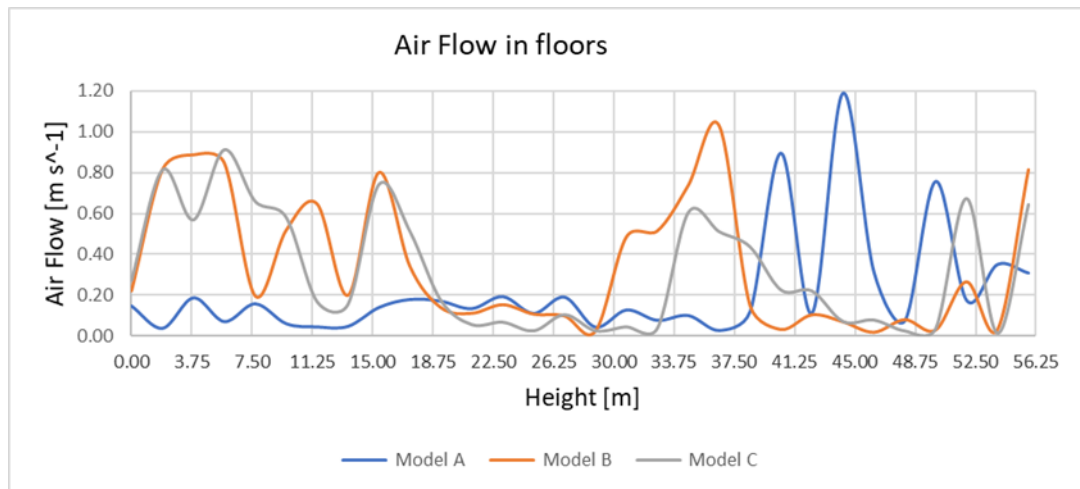
Figure 7.4: Floor airflow against floor height with 10°C ambient temperature

Figure 7.4 shows airflow through all three models' occupational spaces. It can be observed in Model A that the airflow is relatively uniform, under and around 0.2m/s throughout the first ten floors. In the top five floors, there is a dramatic increase in airflow, reaching as high as 1.20 m/s on the 12th floor. This contrast in airflow is a result of the fact that there is a higher temperature on the five upper floors. Meanwhile, in Model B, the airflow in the first five floors fluctuates between 0.2 m/s and 0.9 m/s. In the middle segment of Model B, there is a significantly lower airflow on floors 6, 7 and 8 than there is on floors 9 and 10, wherein the airflow increases dramatically to 1.1 m/s. This drop in airflow is due to the fact that the middle section has similar air pressure to that found externally, i.e., it is at the natural pressure level (NPL). There is then a significant drop in airflow on floors 11, 12 and 13 before it increases in the top two floors within the top segment. Model C is largely similar to Model B, with the exception that the

airflow does not reach the same levels as with B; Model C's airflow does not

exceed 0.9 m/s. This means that the airflow rate remains within acceptable limits

throughout the occupational spaces. This is due to the ventilation caused by the

ducts, which creates greater equilibrium throughout the model (see Figure 7.5)
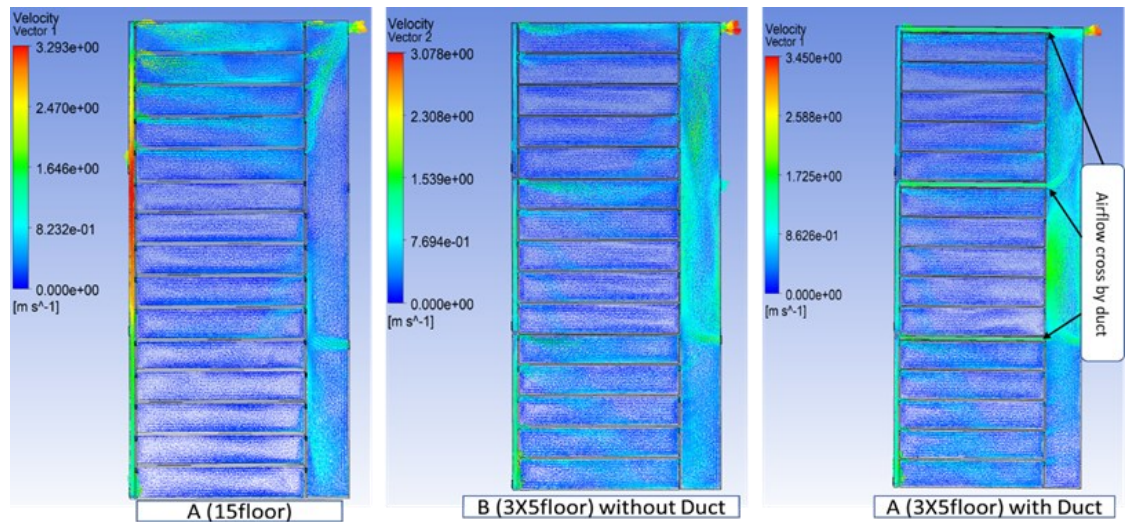
Figure 7.5: Simulated airflow of the three design models with 10℃ ambient temperature

7.3.1.1.2 Temperature and Airflow in Atrium at 10°C

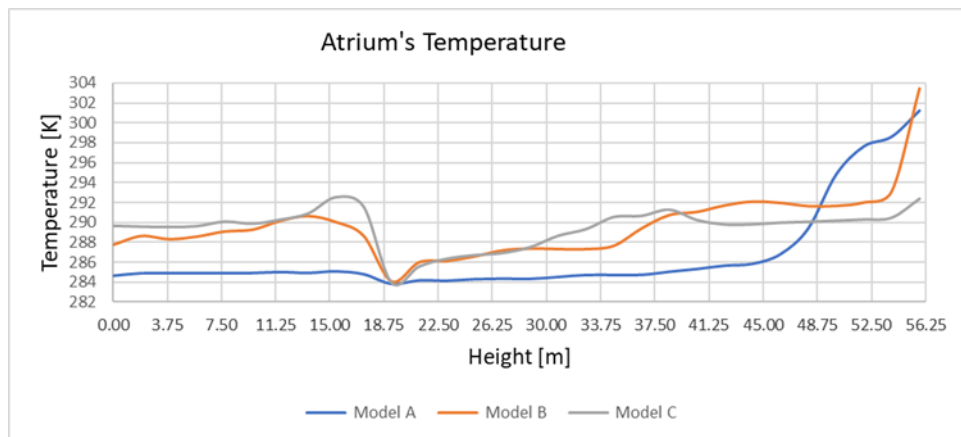Figure 7.6: Atrium temperature against height with 10℃ ambient temperature

Figure 7.6 shows temperature in the atriums of the three models when the

external temperature is 10°C. Here, it can be observed that, in Model A, the

temperature remains relatively stable and low over the first ten floors. It then

increases slightly on the 11th and 12th floors, before increasing dramatically on the 13th, 14th and 15th floors. In Models B and C, the temperature is generally higher than that in Model A, although it does drop on the 6th floor due to the presence of the vent which introduces cold air from the outside. However, Model B, which does not feature ducts, experiences a dramatic increase in temperature on the top floor. It can thus be seen how the duct allows the temperature by and large to be maintained at similar levels throughout the atrium.
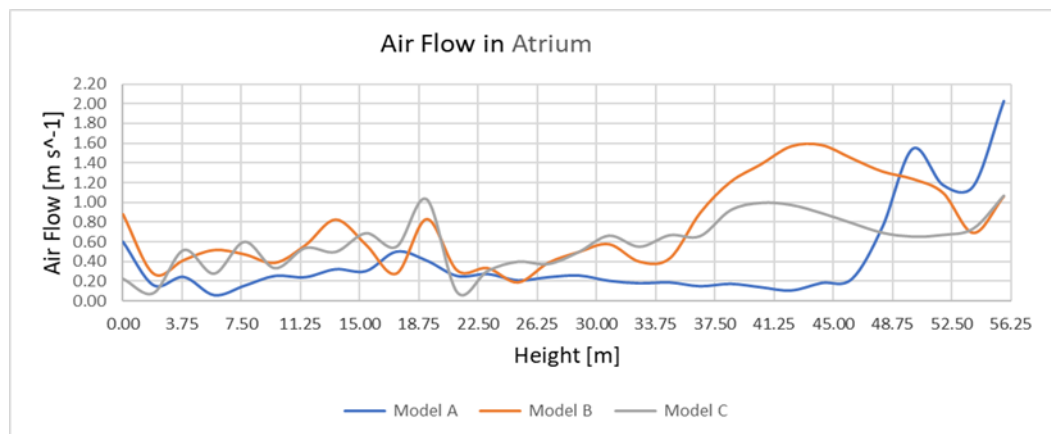
Figure 7.7: Atrium airflow against height with 10℃ ambient temperature

Figure 7.7 shows airflow in the atriums of the three models when the external temperature is 10°C. In Model A, it can be seen that airflow is generally low from floors 1 to 12, typically between 0.2 and 0.4 m/s, before increasing dramatically on the 13th, 14th and 15th floors, reaching 2.0 m/s on the top floor. In Models B and C, the airflow is within desirable limits in the atrium for all the floors, with the exception of the 11th to 14th floors in Model B, where airflows are significantly higher than those in Model C. This shows that Model C, which contains ducts, is better able to control airflow and does not experience the same fluctuations as Models A and B.

7.3.1.2 Temperature and Airflow at 25°C

This subsection shows the effect of an ambient temperature of 25°C on temperature and airflow within the occupational space and the atrium.

7.3.1.2.1 Temperature and Airflow in Occupation area at 25°C
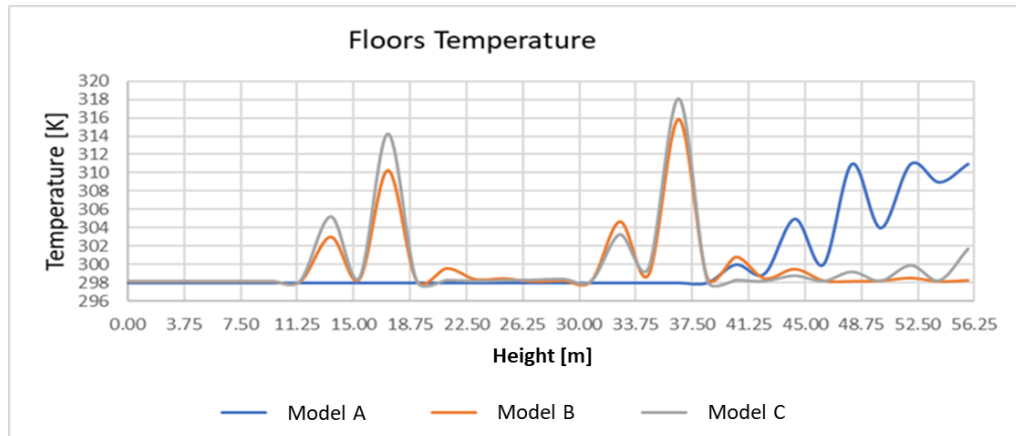
Figure 7.8: Floor temperature against floor height with 25℃ ambient temperature

Figure 7.8 shows the temperature within the occupational space of the three models when the external temperature is 25°C.

In Model A, it can be seen that the temperature across the ten lower floors is consistent at around 28°C. Then, there is a dramatic increase through the top five floors, with the temperature exceeding 30°C in the top four floors. This is because the temperature in the DSF functions as a chimney, heating and pushing up the air which then enters the rest of the building from the top floors. In Models B and C, the temperature remains around 28°C throughout the building, with a slight increase on the top floor of Model C. However, floors 4 and 5 as well as floors 9 and 10 experience increased temperatures, reaching about 40°C. Nonetheless, these higher temperatures are only recorded in the part of the floors closer to the

ceiling of that floor. This means that the lower space in each of these floors remains relatively comfortable in terms of temperature, at below 30°C.
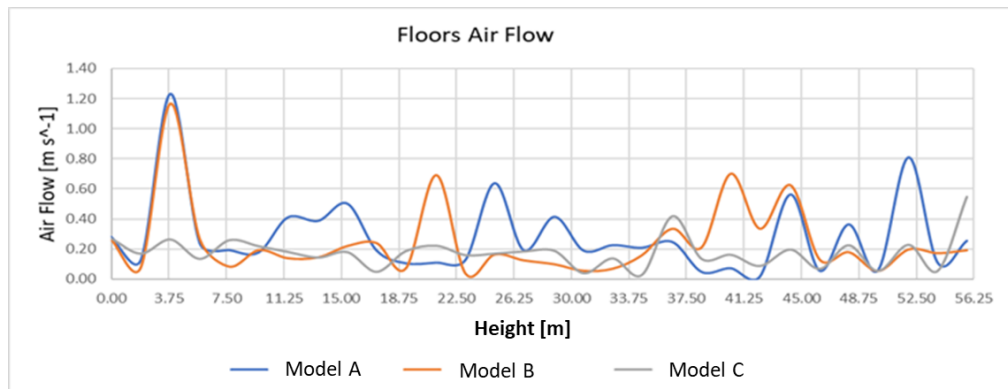
Figure 7.9: Floor airflow against floor height with 25℃ ambient temperature

Figure 7.9 shows the airflow in the occupational space when there is an ambient air temperature of 25°C. In Models A and B, there is fluctuation in airflow throughout the floors of the building, reaching unacceptable heights on the first and second floors. Thereafter, it fluctuates between 0.1 and 0.8 m/s. Model C performs remarkably well, maintaining a largely constant airflow of around 0.2 m/s throughout all floors. This demonstrates the benefit of the duct in the configuration. This can also be seen in Figure 7.10.
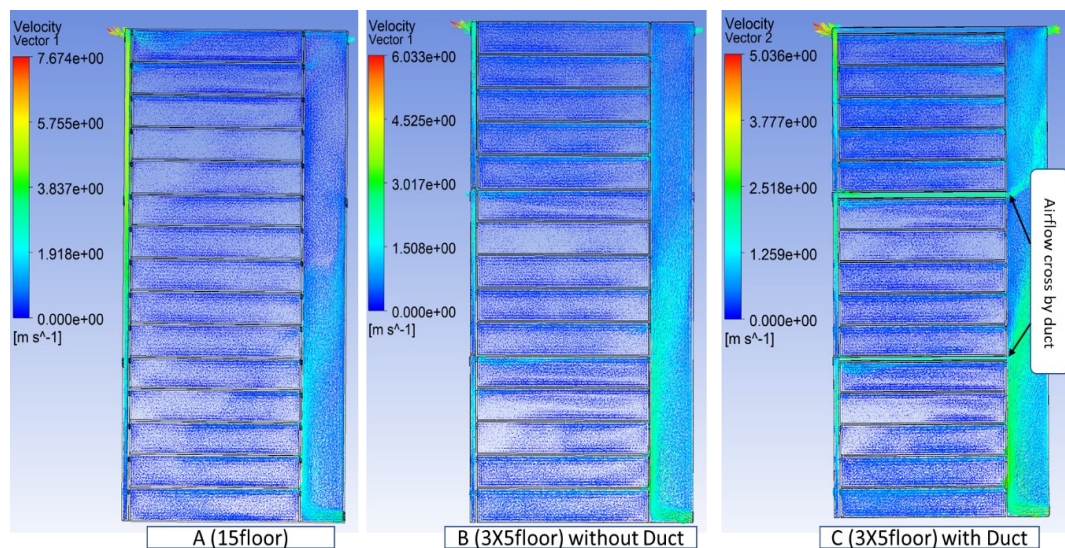
Figure 7.10: Simulated airflow of the three design models with 25℃ ambient temperature

7.3.1.2.2 Temperature and airflow in atrium at 25°C
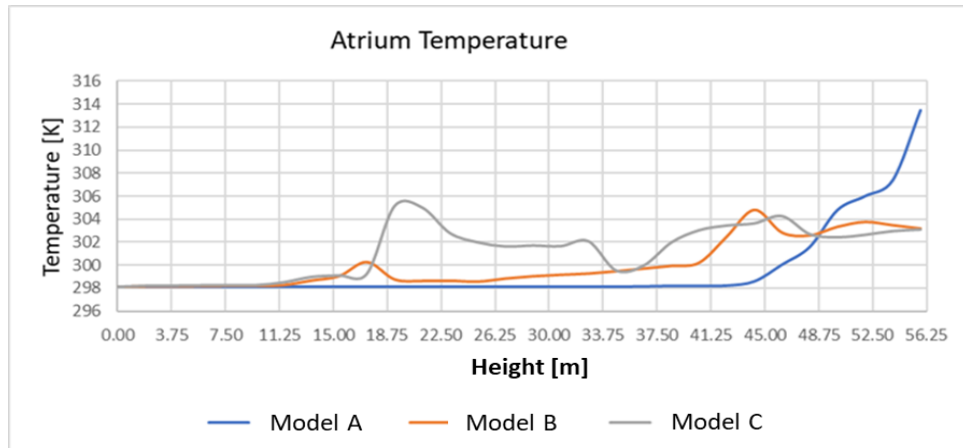
Figure 7.11: Atrium temperature against height with 25℃ ambient temperature

Figure 7.11 shows air temperature within the atrium when there is an external temperature of 25°C. In Model A, it can be seen that the temperature remains uniform over the lower twelve floors at around 28°C before increasing sharply over the top three floors, reaching as high as 40°C. In Model B, the temperature begins to increase from the 4th floor. There is also a slight increase in the 12th floor, with the temperature remaining slightly higher up to the top floor. This model performs significantly better than A, with a 10°C difference in the highest temperatures recorded. Model C is similar to B, except that the biggest temperature increase is between the 6th and 12th floors before falling again in the upper floors, but not exceeding 30°C at any point.
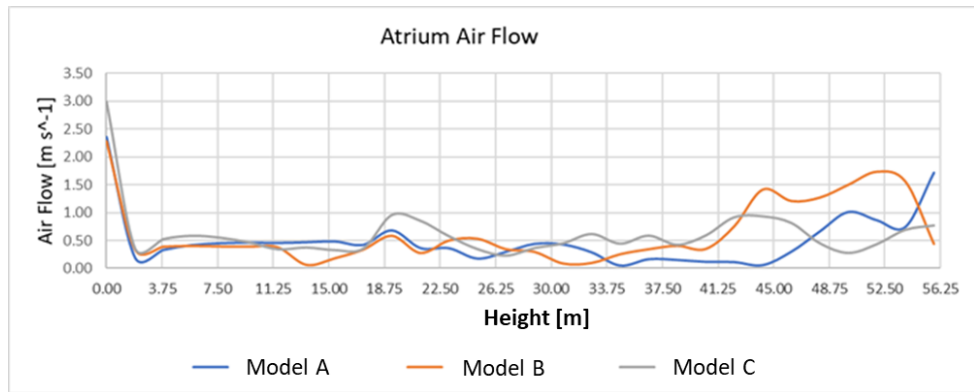
Figure 7.12: Atrium airflow against height with 25℃ ambient temperature

Figure 7.12 shows atrium airflow when the ambient temperature is 25°C. It can be seen that there is minimal difference between the three models. The airflow in all three is typically around 0.5 m/s in the first eleven floors, before increasing through the top floors to varying degrees but not exceeding 1.7 m/s. This similarity in airflow is the result of the atrium temperature being comparable to the outside temperature.

7.3.1.3 Temperature and Airflow at 35°C

This subsection shows the effect of an ambient temperature of 35°C on temperature and airflow within the occupational space and the atrium.

7.3.1.3.1 Temperature and airflow in occupation area at 35°C

Figure 7.13: Floor temperature against floor height with 35℃ ambient temperature

Figure 7.13 shows the temperature across the floors in the occupational spaces when the external temperature is 35°C. In Model A, the temperature is around 28°C until the 13th floor. Then it increases, reaching approximately 35°C. The results for Models B and C are similar to one another, with temperature increases on the 5th and 10th floors, where the temperature increase is significant; in Model B it reaches approximately 45°C on the 10th floor. While this increase is undesirable, it is only experienced on two floors of the building. The reason for this increase is that the segmentation of the DSF cavity forces the hot air to enter the highest point of each segment. On the other hand, in Model A, which is non-segmented, the hot air rises through the DSF cavity all the way up to the top floors and is not interrupted by segmentation.

Figure 7.14: Floor airflow against floor height with 35°C ambient temperature

Figure 7.14 shows the airflow across the floors in the occupational spaces when the external temperature is 35°C. Models A and B have similar results. It can be seen that the bottom of the 2nd floor experiences an increase in airflow. From the 3rd floor until the top floor, Model B begins to fluctuate between 0.2 and 0.5 m/s after the 11th floor until the top. Meanwhile, the airflow in Model C is maintained

at below 0.2 m/s except on the 10th and 15th floors, where it reaches 0.6 m/s. This is acceptable as the external temperature is higher than is desirable for the residents; thus, a slight decrease in temperature when air enters the building is desirable.

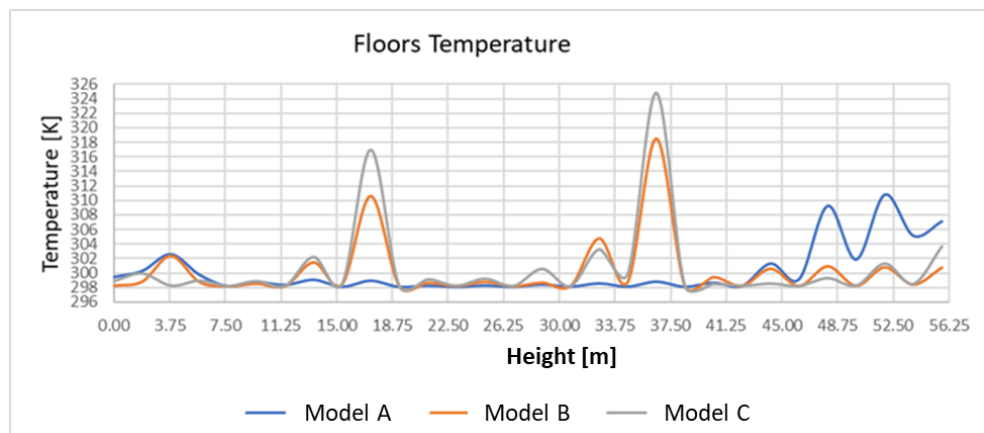### 7.3.1.3.2 Temperature and airflow in atrium at 35°C
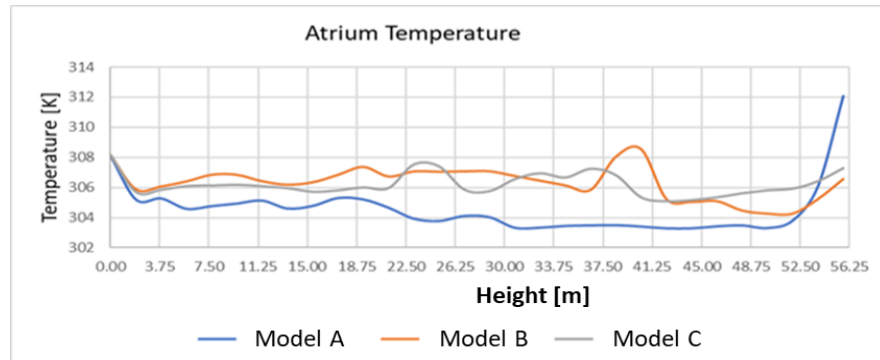
Figure 7.15: Atrium temperature against floor height with 35°C ambient temperature

Figure 7.15 shows the temperature across the floors in the atrium when the external temperature is 35°C. In all three models, the temperature is relatively consistent. It is around 33°C in Models B and C and around 2°C lower in Model A. There is also no unexpected increase in temperature.
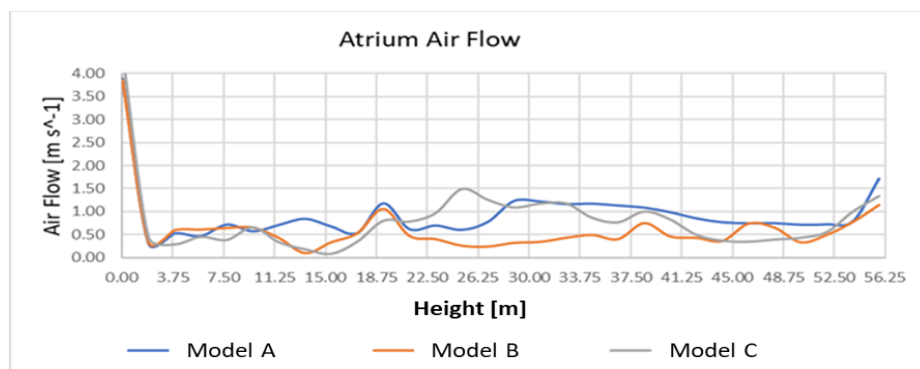
Figure 7.16: Atrium airflow against floor height with 35°C ambient temperature

Figure 7.16 shows the airflow across the floors in the atrium when the external temperature is 35°C. There are no significant differences between the results for the three models.

7.3.2 Wind

7.3.2.1 Temperature and airflow in occupation area

Figure 7.17: Floor temperature against floor height with 2 ms^{-1} ambient wind speed

Figure 7.17 shows the temperature across the floors in the occupational spaces when the external wind speed is 2 m/s. It can be seen that wind speed increases the temperature in all three models by causing the hot air in the DSF cavity to enter the occupational space. In Model A, the temperature starts increasing slightly from the 4th floor until the 9th floor where it drops significantly and then begins to increase again from the 10th floor until it peaks on the 13th floor at 37°C, before dropping to below 30°C across the upper two floors. In Models B and C, the temperatures, including their rises and falls, are largely similar to one another. The pattern across the segments is repeated, showing the effect of segmentation. The temperature increases in the lower portion of each segment, increasing overall segment by segment as the floor numbers increase. It reaches 35°C on the 7th floor and 37°C on the 12th floor. However, on the rest of the floors, it remains below 30°C.
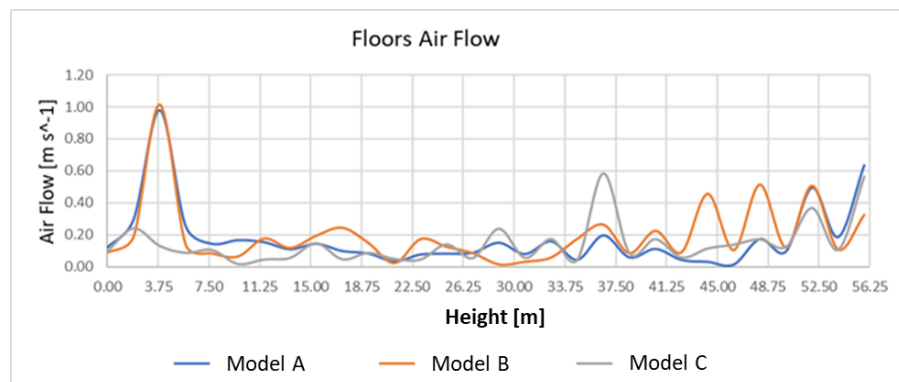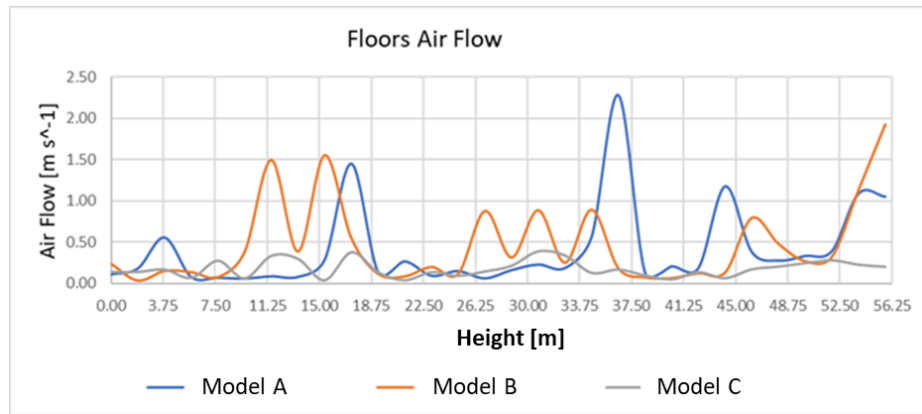
Figure 7.18: Floor airflow against floor height with 2 ms⁻¹ ambient wind speed

Figure 7.18 shows the airflow across the floors in the occupational spaces when the external wind speed is 2 m/s. It can be seen that there is a high level of airflow in Model A, reaching 1.5 m/s on the 5th floor and exceeding 2 m/s on the 10th floor. In Model B, it reaches 1.5 m/s on the 4th and 5th floors and nearly 2 m/s at the top of the 15th floor. Meanwhile, in Model C, airflow remains below 0.4 m/s on every floor of the building. This is because the ducts disperse the effects of the high wind pressure throughout the building, as can be seen clearly in Figure 7.19.
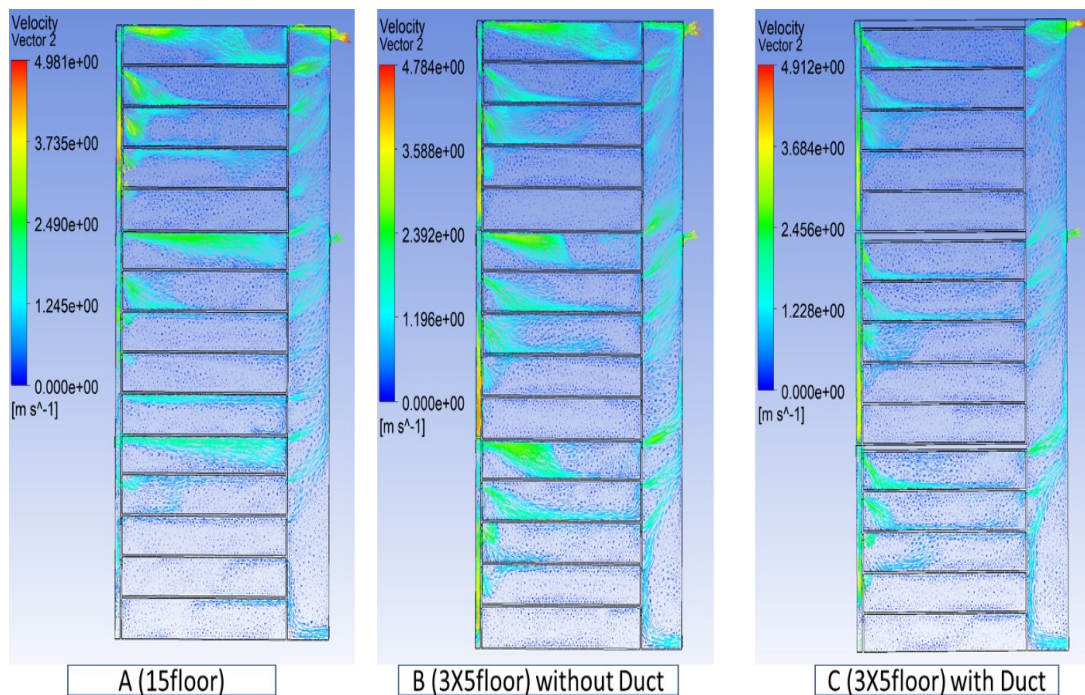
Figure 7.19: Simulated airflow of the three design models with 2 ms⁻¹ ambient wind speed
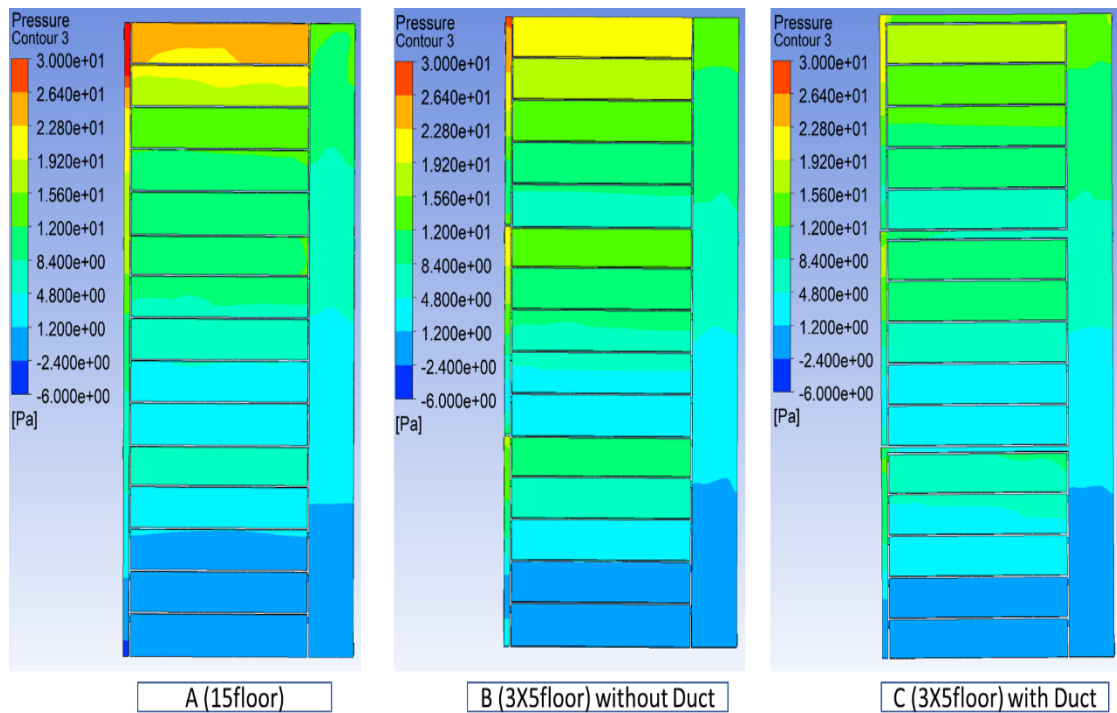
Figure 7.20: Simulated pressure of the three design models at 2 ms^{-1} ambient wind speed

Figure 7.20 shows the air pressure throughout the building in each of the three models when the ambient temperature is 25°C and the wind is blowing at the DSF side of the building at 2 m/s. It can be seen in Model A that there is a stark contrast between the air pressure at the bottom of the building and that at the top. In Model B, the difference is slightly less pronounced, whereas in Model C the contrast is even less and there is greater uniformity across the building.

7.3.2.2 Temperature and Airflow in atrium

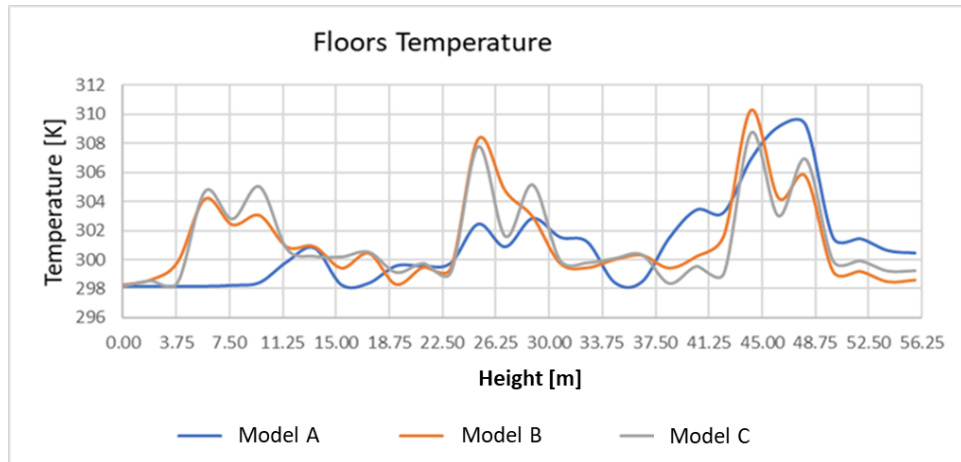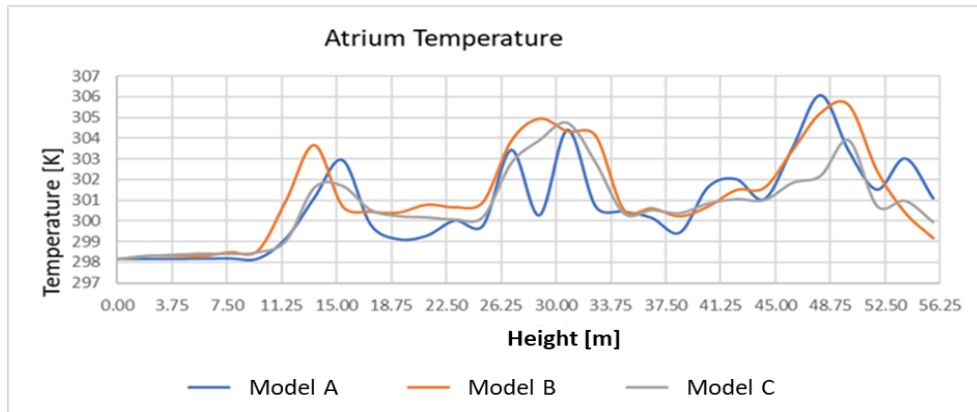Figure 7.21: Atrium temperature against height with 2 ms^{-1} ambient wind speed

Figure 7.21 shows the temperature across the floors in the atriums when the external wind speed is 2 m/s. It can be seen that the temperature does not exceed 33°C at any point in any of the models. This implies an acceptable temperature within the atrium at all times.
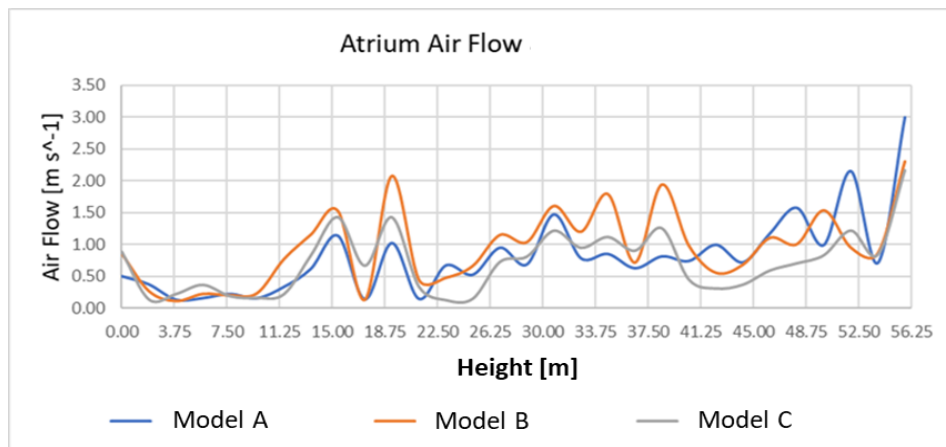
Figure 7.22: Atrium airflow against height with 2 ms^{-1} ambient wind speed

Figure 7.22 shows airflow across the floors in the atriums when the external wind speed is 2 m/s. It can be seen that airflow is generally below 1.5 m/s. There is an exception in Model B, which exceeds 2 m/s on the 6th and 11th floors. Model A exceeds 2 m/s on the top two floors. These exceptions have no significant effect, as they are in the atrium.

7.4 Conclusion

This chapter has shown the performance of double-skin façade in three different configurations: Model A without segmentation, Model B with segmentation of the DSF cavity but without ducts and Model C with both segmentation and ducts. The cavity was segmented in order to reduce the effect of elevation on airflow, because unsegmented cavities can generate a high level of airflow as the cavity functions as a solar chimney. The purpose of introducing the ducts was to disperse the hot air produced by the solar heat within the cavity to other parts of the building far from the occupational spaces.

It can therefore be seen that ambient factors play an important role in the performance of these three models. One of the most significant findings in this chapter is the effectiveness of the ducts linking the DSF cavity to the atrium, which has a pronounced effect on airflow in the occupational spaces and in dispersing unwanted airflow. The ducts also contribute to warming the whole building in cold weather. With ducts, there is not the same pronounced difference in temperature in various parts of the building that is observed in the other two models. This chapter has shown the effectiveness of ducts in controlling the airflow resulting from external wind pressure and preventing it from having a negative effect on the comfort of residents.

Segmentation is effective in creating relative uniformity of air pressure, airflow and temperature between the top and bottom of the building. However, the

model developed in this study, which combines segmentation of the DSF cavity and ducts, benefits from the advantages of segmentation and those of using ducts.

The following chapter will feature the application of the study model to a real building in the city of Al Khobar in Saudi Arabia to measure its effectiveness in ventilating more complex buildings.

This research focussed on whether there are benefits to be had from implementing ducts alongside the DSF deployment. The implementation presented is far from optimal and this could be an area of further research in the future. This includes further investigating the affect of duct size and position.

CHAPTER 8: Ventilation in A Real High-Rise Building - Bdaia Tower in Khobar of Saudi Arabia

8.1 Introduction

Due to climate modification and the nature of internal load dominated office buildings in hot areas, even reduction of cooling loads cries out for further research. Double-skin façades are emerging in the Middle East as an architectural concept to deal with direct solar radiation as a shading system, as an acoustic barrier and an aesthetic option for refurbishment without interrupting activities in the building.

Thermal comfort is defined as the state of being that expresses satisfaction with the thermal environment (Zhang et al., 1992). In other words, it reflects the state of mind of occupants on how they feel from a thermal perspective (e.g., hot, cold, etc.). Generally, indoor thermal comfort is affected by several parameters, which include ambient climate, urban context, building design (configuration) and construction materials. Most importantly, people may respond differently to typical environmental conditions due to differences in their adaptation levels. Commonly, it is recommended that indoor thermal conditions satisfy at least 80% of the occupants in order to be considered as thermally comfortable (ASHRAE,1992).

However, while air temperature could be the most critical indicator of thermal comfort or thermal stress, other factors are also important and vital. For example,

increasing air velocity (or enhancing air distribution) allows relatively higher air temperature values to be accepted within the thermal comfort range.

This chapter looks at the impact of segmentation of double-skin façade cavities with ducting on aspects such as cavity temperatures and occupational space temperatures, and its impact on airflow and temperature throughout the building for reducing reliance on HVAC systems to provide indoor comfort. The simulation model was constructed based on a real building, the Bdaia Tower in Khobar city in Saudi Arabia. The results have been taken at three different ambient temperatures, 25°C, 35°C and 45°C.

8.2 Location and Climate of Al Khobar City

The climate of the Kingdom of Saudi Arabia (KSA), a developing country located in the Middle East, is mainly classified as hot and dry. Khobar City is located in the Eastern Province (26.28°N 50.21°E 8m asl.). It experiences hot summers with relatively cool winters.
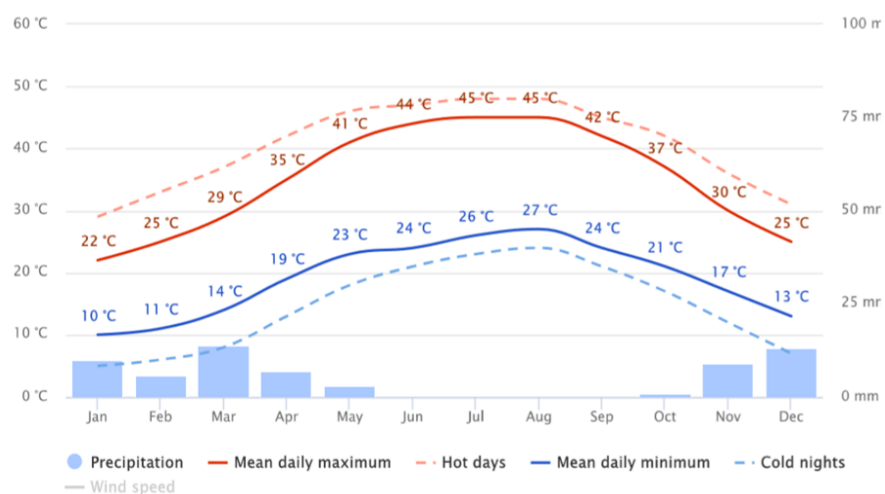
Figure 8.1: Average temperature and precipitation

In figure 8.1, the solid red line shows the mean daily maximum temperature for each month in Khobar. The solid blue line shows the mean daily minimum temperature for each month. The broken red lines show the average hottest temperature in each month over the last thirty years and the broken blue line shows the average minimum.
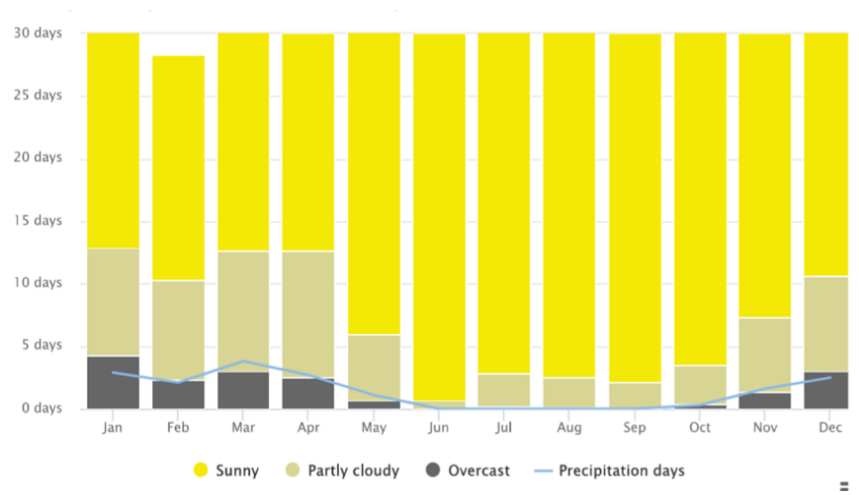
Figure 8.2: Cloudy, sunny and precipitation days

Figure 8.2 shows how many sunny days, partly cloudy and cloudy days plus days of precipitation there are per month. If the day has below 20% cloud cover, it is categorised as sunny. Partly cloudy refers to those days with 20–80% cloud cover.
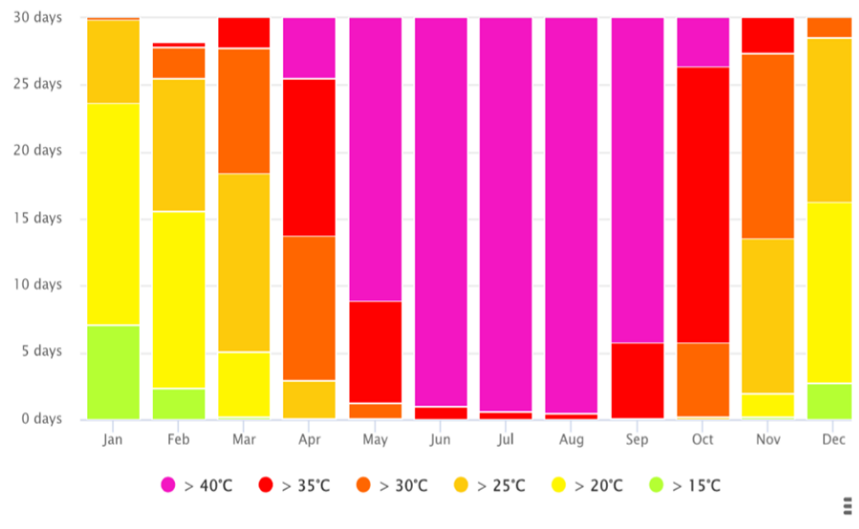
Figure 8.3: Maximum temperature across a year

Figure 8.3 shows how many days per month certain temperatures are reached in

Khobar.
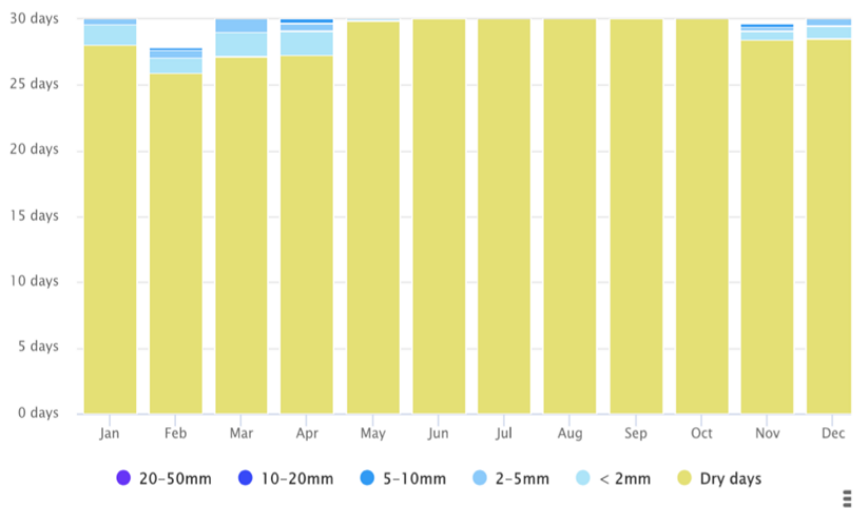
Figure 8.4: Precipitation levels

Figure 8.4 shows how many days per month certain amounts of precipitation are

achieved in Khobar.
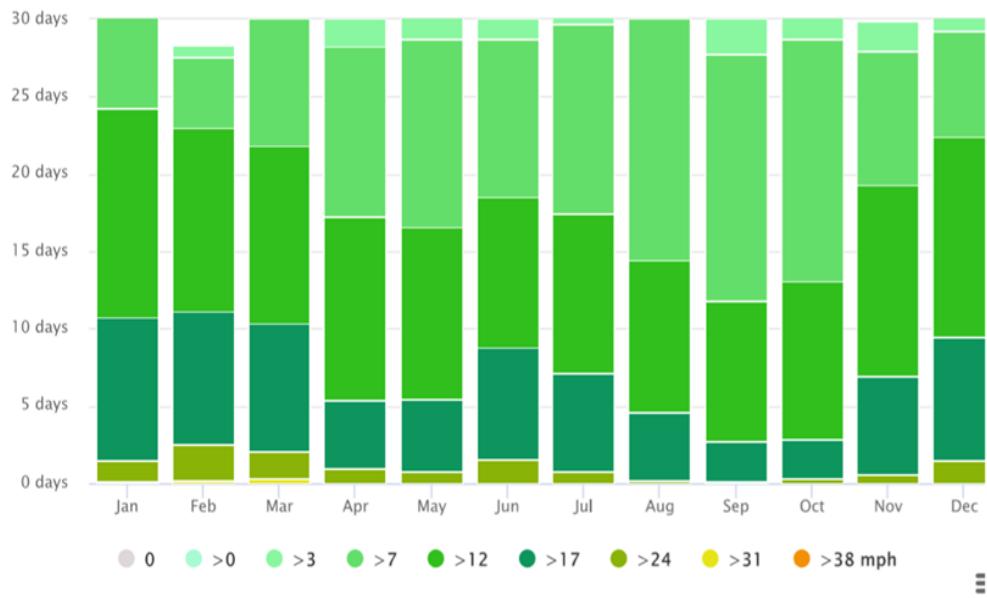
Figure 8.5: Wind speed

Figure 8.5 shows how many days per month certain wind speeds are reached.
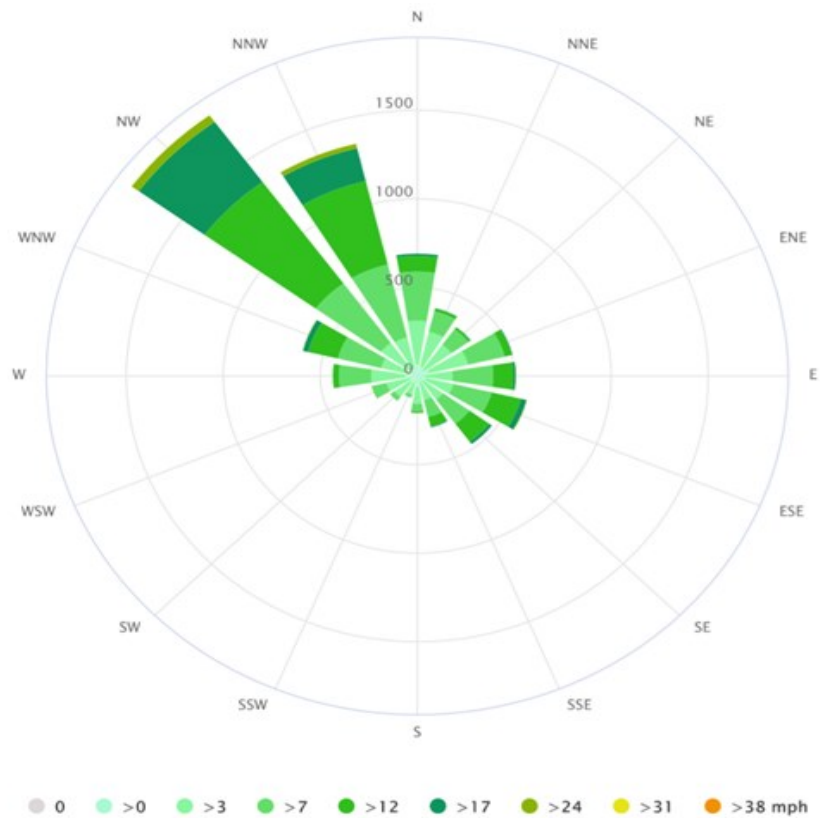
Figure 8.6: Wind direction

Figure 8.6 shows the number of hours per week the wind blows from the direction indicated.

8.3 Bdaia Tower
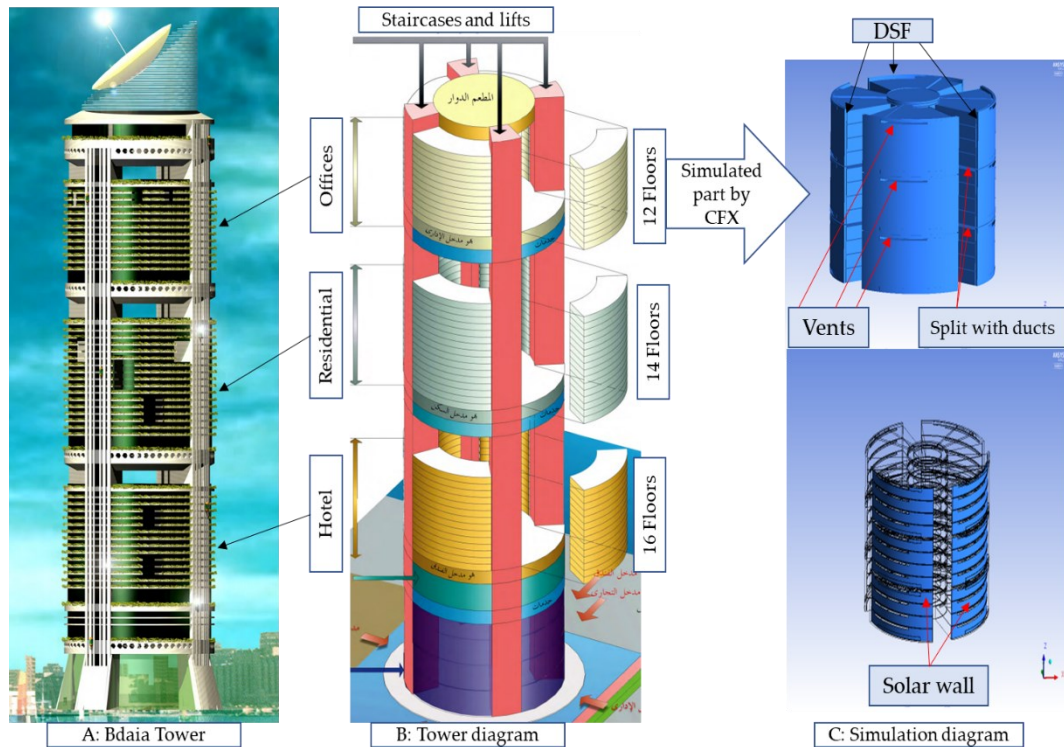
Figure 8.7: (A) Bdaia Tower, (B) A schematic diagram of tower layout, (C) A simulation design of the tower

Figure 8.7 (A) shows Bdaia Tower in the City of Khobar in the Kingdom of Saudi Arabia. The building sits on a 30,776 m² floor area and consists of three sections; a 14-storey hotel as the prime section, a 16-storey residential block in the middle and the final section of the building is a 12-floor office block as shown in the Tower diagram, figure 8.7 (B).

A prototype of the Multi-Storey DSF Pattern with Ducting, which was subjected to vigorous stimulations as previously discussed in Chapter 7, was created and applied to Section 3 of the building as per figure 8.7 (C).

The building was selected specifically due to its design complexity and its location in a city with hot weather.

8.3.1 Setting-up of numerical model

To set up a case study, a research prototype similar to section three (offices) of the Bdaia Tower was created. The model covered 27,564 m^2 of floor area, with a height of 3,75 m separating each of the 12 floors. It was divided into three sections of four floors each with ducting separating each section and a double-skin façade of 1m cavity surrounding the prototype as shown in figure 8.7 (C). Table 8.1 showing the number of nodes and elements of (Fig. 8.7C) domain.

Table 8.1 Mesh Information for CFX (Fig. 8.7C)

Domain	Nodes	Elements
Default domain	8948976	46351410
Option	Steady state	

8.3.2 Ambient temperature

To gauge the performance of the prototype in different weather temperatures, the model was tested against three different sets of temperatures, 25°C, 35°C and 45°C. The model internal temperature was set to 25°C accordingly.

> **Temperature and Airflow through the three parts of building area at 25°C**

This subsection shows the effect of an ambient temperature of 25°C on temperature and airflow within the three sections of the model space.
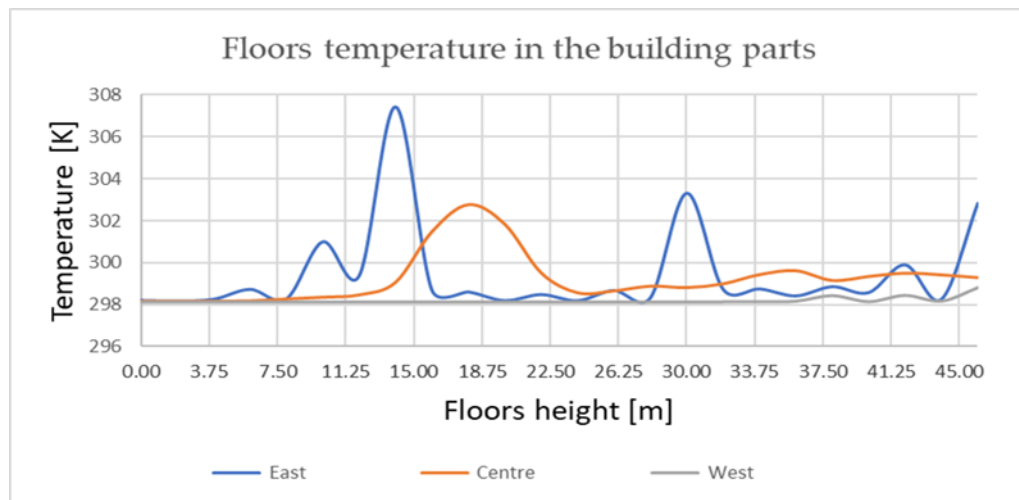
Figure 8.8: Floor temperature against floor height with 25℃ ambient temperature

Figure 8.8 shows the variation in temperature at the three sections of the model against floor height from three directions; East, Centre and West.

As the East direction was the sun facing side of the model, the temperature on each floor had no significant fluctuation apart from the voids of the sections. On the 4th floor, the sun-heated air in the cavity of the DSF moved through the void and the ducting and surpassed 37°C, the highest recorded temperature; the same thing happened at floor 8 and floor 12 levels, but the increase was lower. This movement of hot air affected the temperature level in the centre of the model while the air was moving up, noticeably opposite the ducting void of the 4th floor. However, in the West side of the model, no change in the temperature was

reported. Figure 8.9 shows temperature variations at the three parts of the building with 25°C ambient temperature.

Hence, there is no perceptible change in the temperatures internally.

Figure 8.9: Simulated temperature at three parts of the building with 25°C ambient temperature

Figure 8.10: Floor airflow against floor height with 25°C ambient temperature

Figure 8.10 shows the airflow across the three parts of building when the external temperature is 25°C. In the East and West parts of the building, the airflow shows a relatively convergent fluctuation, mostly below 0.5m/s, except for the upper floor of the East where the airflow had reached 1.2 m/s. This was because, due to the outlet vent opposite the 12th floor (the top floor), the increase in airflow through the centre part of the building caused an increase in air pressure at the

top, forcing air through the top floor. The centre part of the building was the highest in average airflow rate, especially on the first five floors, where it reached 1.1m/s, because it is an open and unsegmented area, and this part was affected by the hot air coming from the cavity of the double façades facing the sun. From the 6th floor, the airflow decreased significantly due to the reduction in the exterior airflow coming into the building. Figure 8.11 clearly shows airflow variations at the three parts of the building at 25°C ambient temperature.
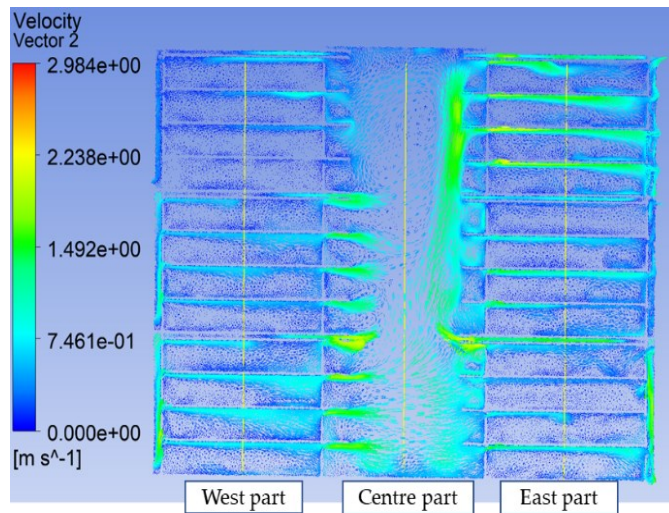
Figure 8.11: Simulated airflow at three parts of the building at 25°C ambient temperature

> **Temperature and Airflow at the three parts of building at 35°C**

Figure 8.12 shows the variation in temperature in the three sections of the model against floor height from three directions: East, centre and West while exterior temperature was 35°C.
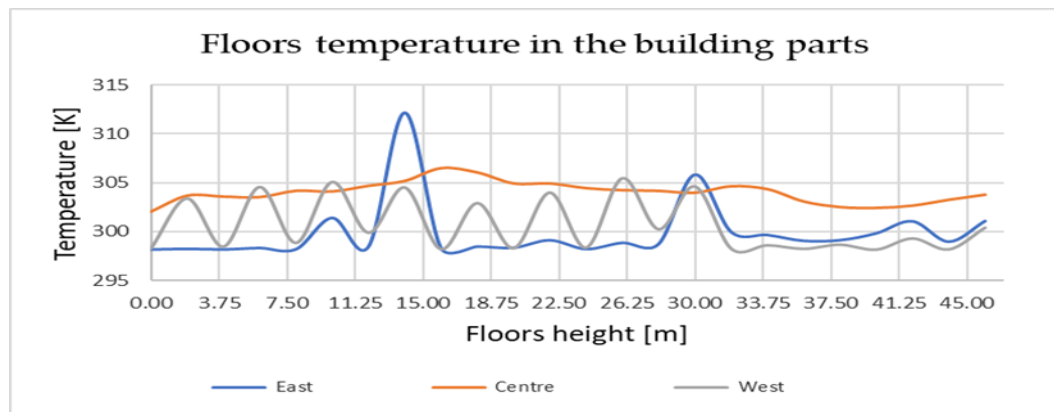
Figure 8.12: Floor temperature against floor height with 35℃ ambient temperature

The temperature on each floor showed significant fluctuation, apart from the voids of the sections. On the 4th floor the sun-heated air in the cavity of the DSF moved through the void and the ducting and surpassed 39°C, the highest recorded temperature. The same thing happened at floor 8 level, but the increase was lower. The movement of hot air increased the temperature level in the centre of the model by around 5°C while the air was moving up. Furthermore, on the West side of the model, the warm air from outside increased the internal temperature by around 5°C as well in an unstable chart until the 8th floor, which was due to the decrease of exterior airflow in the top section of the model. Figure 8.13 shows temperature variations at the three parts of the building at 35°C ambient temperature.

Hence, despite the fluctuations, the model preserved the internal temperatures at 5°C lower than the exterior on the West side, while the East side did not change significantly in temperature, apart from the top of the 3rd, 4th and 8th floors.

171

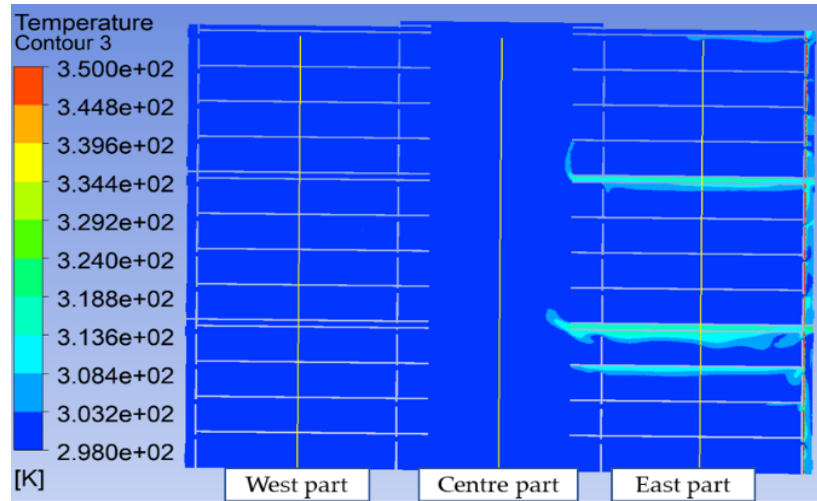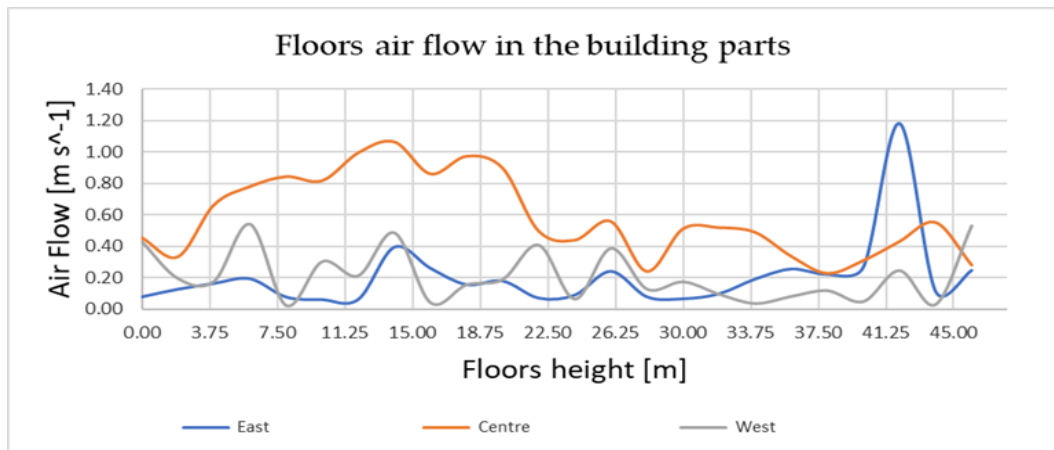Figure 8.13: Simulated temperature at three parts of the building at 35℃ ambient temperature
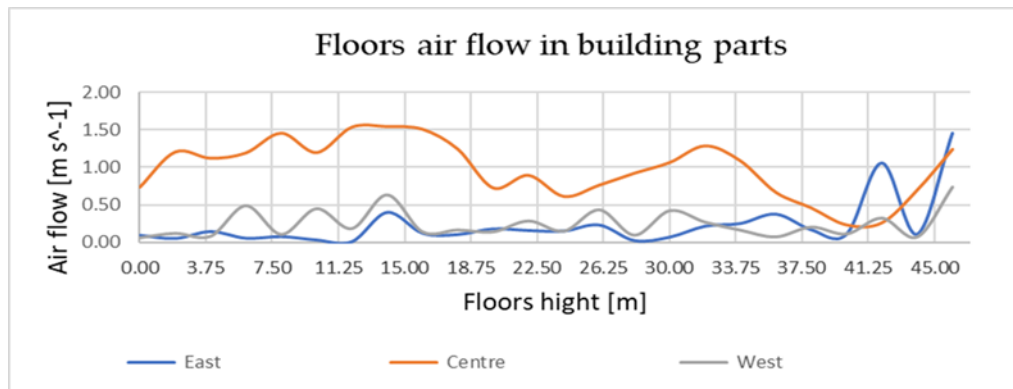
Figure 8.14: Floor airflow against floor height with 35℃ ambient temperature

Figure 8.14 shows the airflow across the three parts of building when the external temperature is 35°C. In the East and West parts, the airflow shows a relatively convergent fluctuation, being mostly below 0.6m/s, except for the upper floor of the eastern part where the airflow had reached 1.2 m/s. The centre was the highest in the average airflow rate, especially on the first five floors, where it reached 1.6m/s. This is because it is an open and unsegmented area, and this part was affected by the hot air coming from the cavity of the double façades facing the sun, and from the other side because the ambient temperature was 35°C. From the 6th floor, the airflow decreased significantly due to the reduction in the

exterior airflow coming into the building. Figure7.15 clearly shows airflow variations at the three parts of the building at 35℃ ambient temperature.

Figure 8.15: Simulated airflow at three parts of the building at 35℃ ambient temperature

➢ **Temperature and Airflow in the three parts of building area at 45°C**

Figure 8.16 shows that in the East of the model, the effect of the exterior temperature was similar to the previous section above, where the temperature on each floor showed significant fluctuation apart from the voids of the sections. On the 4th floor the sun-heated air in the cavity of the DSF moved through the void and the duct, reaching 45°C, the same as outside. The same thing happened at floor 8, but the temperature increase was lower.
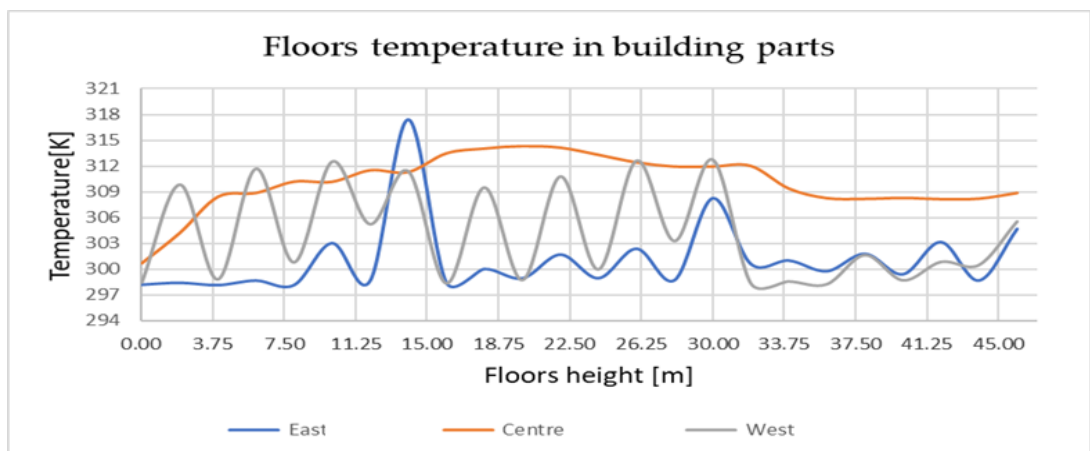
Figure 8.16: Floor temperature against floor height at 45℃ ambient temperature

The temperature level ranged between 36°C and 39°C at the centre of the model. The increase can be attributed to the movement of hot air from both sides. However, in the West side of the model, the warm air from outside caused a variation in the internal temperature up to the 8th floor and ranged between 28°C and 38°C. From the 9th floor, the temperature decreased significantly due to the reduction in the exterior airflow coming into the building, whereas in the East side it never exceeded 30°C, except on the 4th and 8th floors.

Figure 8.17 shows temperature variations in three parts of the building at 45°C ambient temperature.

Hence, despite the fluctuations, the model preserved the internal temperatures of occupied spaces (East and West sides) at an average of 15°C lower than the exterior. However, the centre was hotter this time, but that is not very important, because this part is not occupied.
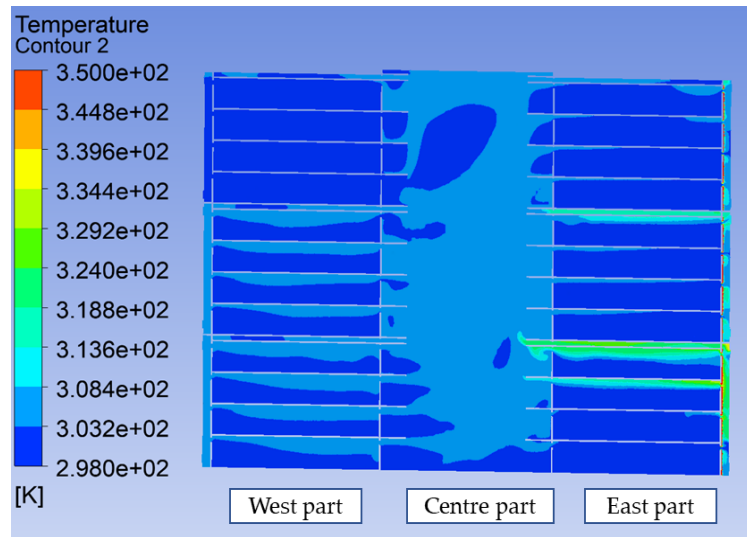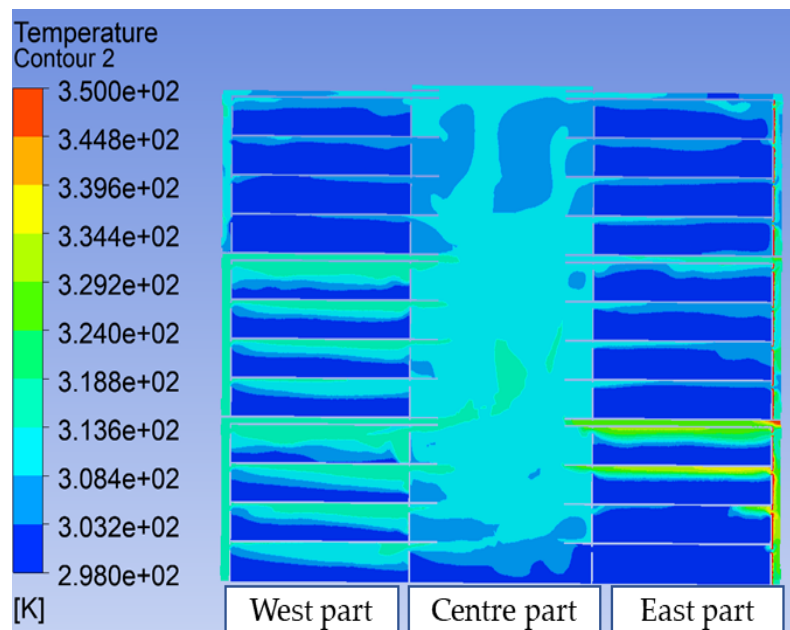

Figure 8.17: Simulated temperature at three parts of the building at 45℃ ambient temperature
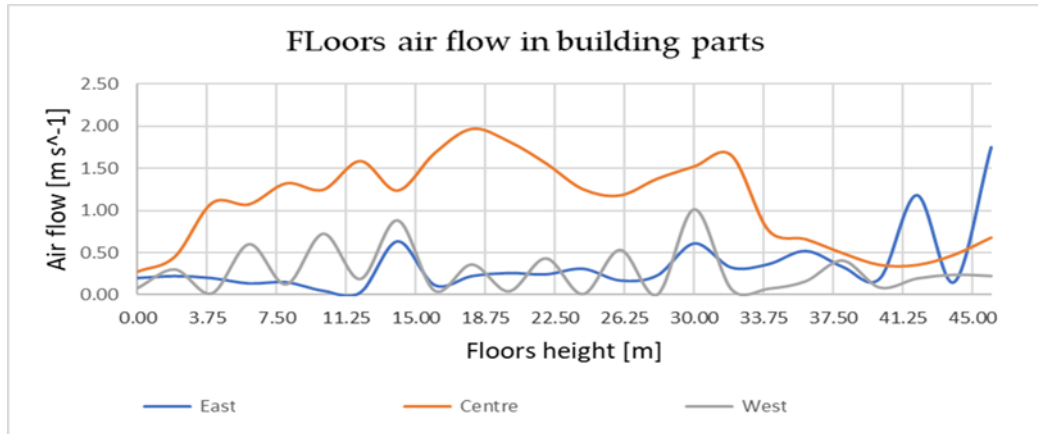
Figure 8.18: Floor airflow against floor height at 45℃ ambient temperature

Figure 8.18 shows the airflow across the three parts of building when the external temperature is 45°C. In the East and West parts, the airflow shows a relatively convergent fluctuation, mostly below 1m/s, except for the upper floor of the East where the flow reached 1.5 m/s. The Centre had the highest average airflow rate, especially on the 5th floor, where it reached 2m/s. This is because the heating of the DSF cavity is much higher given the hotter ambient temperature and because it is an open, unsegmented part of the building. Although the air speed inside the centre region is much greater than comfort threshold, the centre is not an occupation space.

From the 9th floor, the airflow decreased significantly due to the reduction in the exterior airflow coming into the building. Figure 8.19 clearly shows airflow variations at the three parts of the building at 45°C ambient temperature.
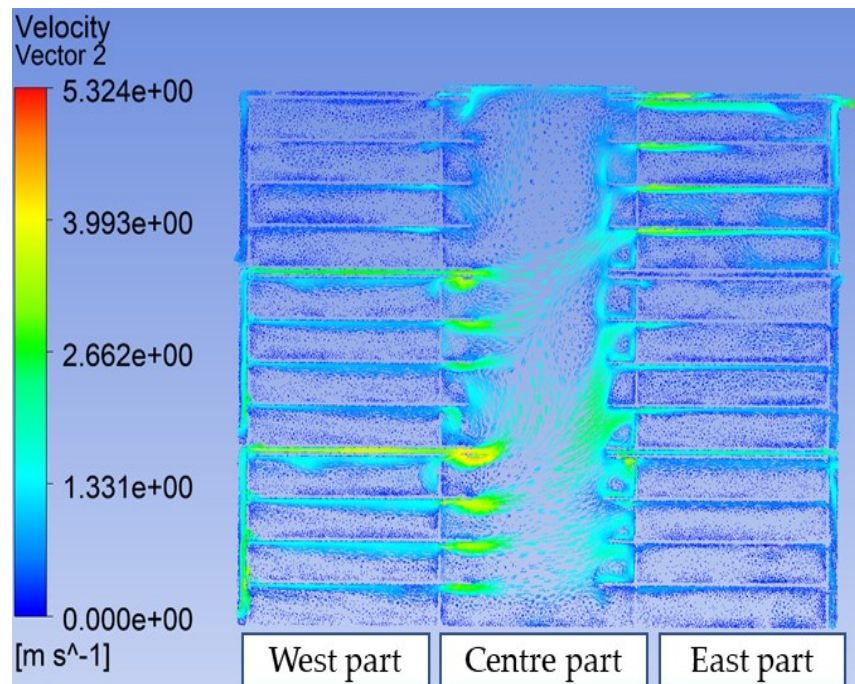
Figure 8.19: Simulated airflow at three parts of the building at 45℃ ambient temperature.

8.4 Conclusion

This chapter has shown the performance of a double-skin façade on the application of the study model to a real building in the city of Al Khobar in Saudi Arabia to measure its effectiveness in ventilating more complicated buildings, with both segmentation of DSF cavity and ducts.

The cavity was segmented in order to reduce the effect of elevation on airflow, because unsegmented cavities can generate a high level of airflow, as the cavity functions as a solar chimney. The purpose of introducing the ducts was to disperse the hot air produced by the solar heat within the cavity to other parts of the building far from the occupational spaces.

It can therefore be seen that ambient factors play an important role in the performance of this model. One of the most significant findings in this chapter is

the effectiveness of the ducts linking the DSF cavity to the other parts of building, which has a pronounced effect on airflow in the occupational spaces and on dispersing unwanted airflow. They also contribute to keeping the occupational space temperatures less than the ambient temperature by 10℃ at least, when the outside temperature is 35°C or more; however, there is no drastic change in the occupational space temperatures when the ambient temperature is 25℃.

The results support the main aim of this research of using natural ventilation in tall buildings, whether that be as part of a hybrid system or an entirely naturally ventilated arrangement. This contributes to the use of natural ventilation in high buildings to reduce the costs of conditioning systems. However, there are some features that need more investigation, such as the rise in temperature on the 4th floor in this case.

CHAPTER 9: Conclusions

As a form of natural ventilation, DSF has multiple advantages. However, a number of studies indicate DSF's viability as a passive cooling strategy is still problematic over the thermal effectiveness in hot weather. Admittedly, the DSF cavity and the adjacent interior spaces can overheat in summer, but segmentation of the cavity with ducts linking the cavity to the atrium along with appropriate ventilation configurations can solve the problem.

This study aimed to explore how the DSF system performs in office spaces with a variety of outside temperature scenarios. The study paid particular attention to how cavity-segmentation in conjunction with ducts affects the performance of the double-skin façades in internal spaces. Therefore, an intensive parametric study was conducted for a variety of design parameters of the model. In order to fulfil the objectives, various detailed computational models were developed and solved. As a result, the developed model was subjected to intensive validation against experimental data as well as well-established general expressions, such as dimensionless number Nu, Re. The developed model demonstrated significant aptitude for simulating the problematic conditions proposed, predicting a number of elements, including surface temperature values, air temperature and airflow rate.

The present study constitutes a key piece of research into office buildings that are naturally ventilated using DSF and their thermal performance with natural

ventilation mechanisms. DSF was used in high building models along with DSF cavity segmentation and ducts connecting the cavity segments to the atrium. With a view to building knowledge of natural ventilation in tall buildings for cost saving and potential developments to DSF, the present research sought to acquire an all-encompassing understanding of how to refine the technology, with particular emphasis on how it can be applied in buildings with natural ventilation.

The study suggests that segmentation of only the DSF cavity could present the safest option for envelope design of non-domestic high-rise buildings. This research is concerned with how segmentation affects consequent flow rates of associated office spaces. A DSF envelope flow was used for the study in order to assess the off-design conditions of three different configurations, namely non-segmented DSF cavity, segmented DSF cavity and segmented DSF cavity plus ducts (Figure 7.1).

The study pinpointed and assessed multiple factors affecting the performance of the double-skin façade, most significantly solar radiation, wind pressure and the building's internal configuration. Natural ventilation's reliance on thermal buoyancy means that designers require a greater understanding of how airflow behaves inside the DSF cavity, to better control ventilation in a building's internal spaces and make for better performance of buildings with DSF. The study was conducted using an office building as a reference model in order to examine how

the aforementioned design parameters affect thermal behaviour within a building. This involved using computer-aided simulation. In the first stage of the research, there was a parametric analysis. The resulting findings were used to develop and analyse optimised models, exploiting an amalgamation of solutions to achieve maximum thermal performance. Evaluation was also carried out for how wind availability, solar radiation and site conditions affect the DSF and the building's thermal performance. This was done with the objective of obtaining references for how DSF function can be bettered.

The ensuing sections provide a summary of the objectives set out in Chapter 1. There is also a discussion of the accomplishments, the research contribution and how DSFs perform under a variety of external temperature situations. Moreover, there is particular focus on the part played by segmented cavity with ducts on DSF performance. The chapter concludes with a discussion of the limitations of the research and possible directions for future research.

9.1 The Objectives of this Study

Objective 1: To investigate flow structure and behaviour in a DSF cavity with a range of openings and compartments—In this study, DSF was introduced to a building with a novel solar energy collection source constructed surrounding the building, causing natural convection patterns within the building to be modified.

Objective 2: To comprehensively investigate transfer of mass and heat caused by natural convection—Airflow within a building directly affects such transfers.

Thermal transfer leads to effects on thermal comfort for building occupants, and airflow relates to the way in which pollutants are dispersed. Both types of transfer are an essential part of measuring the impact of the DSF on the performance of the chosen building.

Toward these objectives, this study's results and findings support those of others: At 35°C external temperature (summer conditions), the interiors of buildings with a DSF are cooler than of those without, while at 10°C outside temperature (winter conditions), the interior of a building with a DSF is warmer than of those without. Thus, DSFs insulate in hot weather and warm the occupational spaces in cold weather. Buildings that have a unilateral façade are subject to the direct effects of wind and weather.

It has been seen that DSF has significant potential in the development of modern buildings. The oft-cited drawback of being more expensive is not necessarily true, due to DSF being more durable and consequently leading to long-term savings. Buildings with DSF have comfortable occupational spaces and are more environmentally friendly. In hot weather, DSFs serve to insulate and in cold weather, they cause heated air to move up to occupational spaces, ensuring that airflow is kept within acceptable limits (as mentioned in section 6.5). The result is less energy expenditure, meaning lower costs.

What this study has found corroborates many of the studies referenced in the literature review (Chapter 2), in that cavity depth has a major effect on how the

DSF performs. According to the present study, where the external temperature does not go above 35°C, the ideal depth of the DSF cavity is 0.7m to 1.0m. The first objective of this study, therefore, is met.

The basis of this study was development of a multi-storey DSF pattern wherein the DSF cavity is segmented into zones, each of which features a duct at the top linking the cavity and the atrium. This research sought to disperse the high load thermal buoyancy found at the top of each zone, reducing air speed and thus reducing its negative effects on the building's occupational spaces. Accordingly, the second objective of this study also is met.

Objective 3: To investigate the effectiveness of segmentation in conjunction with DSF in high-rise buildings—This is to increase the understanding of how DSF and segmentation can complement one another to improve airflow within a space in a high-rise building.

Objective 4: To investigate the impact of varied weather conditions on within-cavity airflow—surrounding temperatures and other factors depend upon climate and on specific weather patterns and constitute an important influence on natural convection within buildings. Therefore, convection is studied across a range of seasonal weather conditions, including hot and cold, including assessing wind as a factor which influences ventilation, etc. The study will contribute to knowledge about the way in which ventilation systems perform in general.

As regards objectives 3 and 4, the results of this research have demonstrated how DSF performs in three different configurations: Model A without segmentation, Model B with segmentation of the DSF cavity but without ducts and Model C with both segmentation and ducts (Chapter 7). The purpose of segmenting the cavity was to minimise the effect that elevation has on airflow; the fact that DSF cavities function as solar chimneys means that when unsegmented they can produce a high level of airflow. The ducts were thus intended to disperse the hot air, channelling it away from occupational spaces.

Ambient factors have a significant effect on how these three models perform. Significantly, the research revealed that ducts from the DSF cavity to the atrium are particularly effective in dispersing unwanted airflow away from occupational spaces. They also help warm the whole building when the weather is cold. The model containing ducts resulted in greater uniformity of temperature across the building. Thus, ducts can be effective in controlling airflow caused by external wind pressure and can help stop it impinging upon the comfort of those using the occupational spaces.

Segmentation has been shown to help create relatively uniform air pressure, airflow and temperature at the various elevations within the building, with the model developed in this study, containing ducts, combining the benefits of DSF cavity segmentation and ducts (Chapter 7).

The performance of this model was observed to be significantly affected by ambient factors. Ducts are particularly effective in controlling airflow and can help maintain temperatures in occupational spaces at least 10°C less than the external temperature when the latter is 35°C or higher. There is, however, no significant difference when external temperature is 25°C.

The results of this research support the main aim of using natural ventilation for high-rise buildings, whether as an entirely naturally ventilated system or as part of a hybrid system. This, therefore, boosts the case for naturally ventilating tall buildings in order to reduce costs.

9.2 Achievements of this Study

This work has addressed all the research objectives above. Its major contributions are summarised below:

1. Development of the multi-storey pattern of double skin façade was done by connecting its cavity to the atrium on the opposite side of the building via ducts. This model gives superior control over the airflow through the building, allowing air to pass through the occupational rooms when needed and excessive air to flow through the connecting ducts. The development of this pattern is unique and unprecedented in studies of natural ventilation of high-rise buildings. The notion of using these ducts was the inspiration for the concept of segmenting the DSF cavity and using ducts to connect it to the non-segmented atrium.

2. This is the first study involving partial segmentation wherein the DSF is segmented, with a duct at the top of each zone connecting the DSF cavity to the non-segmented atrium. Previous studies have looked at complete segmentation including the atrium; however, the present research is unique in that the atrium is non-segmented and connected to a segmented DSF façade via ducts. Splitting the cavity of the double-skin façades without splitting the rest of the building contributed to creating a balance between the floors in terms of temperature and airflow through them. The cavity was segmented in order to reduce the effect of elevation on airflow, because unsegmented cavities can generate a high level of airflow, as the cavity functions as a solar chimney. The purpose of introducing the ducts was to disperse the hot air produced by the solar heat within the cavity to other parts of the building far from the occupational spaces.

This new approach to segmentation has produced good results, similar to those of complete segmentation in terms of distributing airflow across the floors and the relative uniformity of air pressure from the top to the bottom of the building. This approach, therefore, has the advantages of segmented and non-segmented buildings, in that the effects are similar to those of complete segmentation, but with the cost being closer to that of non-segmented buildings. Moreover, the non-segmented atrium facilitates airflow within the building. It is, therefore, hoped that the

present study represents a significant contribution to knowledge of natural ventilation systems for application in high-rise buildings.

3. Previous studies have only explored segmentation of the entire building, whereas the present study is unique in that it has explored segmentation of just the DSF cavity according to floors. A model of five floors and four floors was studied and the results showed a match in performance. These results mean that, when a tall building is being designed, this can be done according to the number of floors in the building. Thus, if the number of floors can be divided by 5, the building can be constructed with zones, each containing five floors, which is the more economical of the two. The same is the case if the number of floors can be divided by 4. If it can neither be divided by 4 nor 5, a combination of the two can be used. For example, if a 27-storey building is to be constructed, it can be designed with three zones of five floors and three zones of four floors. This therefore demonstrates the effectiveness of segmentation in tackling the issue of thermal buoyancy and pressure differential in tall buildings. It also shows that segmentation is one of the most effective methods of naturally ventilating tall buildings.

4. The study model developed in this study has been shown to be suitable for hot climates. While previous studies had indicated that there is a thermal load as a result of double-skin façade, this study did not observe

such a feature. This is due to the fact that the DSF cavity in this model is segmented, thus dispersing the thermal load and preventing the load from becoming excessive. This model helped maintain temperatures at least 10°C lower in the occupational spaces in the building than the outside when the external temperature was 45°C.

9.3 Limitations of this Study

Given the timeframe, there were certain restrictions and limitations that hindered research outcomes, which ought to be avoided in any subsequent study. The majority of the limitations are associated with time and/or facilities. The limitations are outlined below:

1. Restrictions on time and facilities meant that a distinctive experimental work could not be carried out for this research.

2. Simulations were only carried out using steady state assumptions.

3. When the researcher faced difficulties with the simulations, a technician was not always available to assist.

4. For reasons beyond the researcher's control, his university account was disabled for a period of 18 months, thus delaying the research.

9.4 Future Work

Considering the outcomes and interpretations of the present study, the following is an outline of suggestions for future work:

1. Unsteady (transient) simulations should be used to acquire an understanding of the DSF system's dynamic performance.

2. A greater variety of sizes and locations of ducts for the DSF cavity should be examined.

3. Further consideration should be given to hot, humid weather.

4. Situations that require further investigation include the increase in temperature on the 4th floor of the first zone of the segmentation in the tests on the real building in Chapter 8.

References

Acharya, R. 2016. Investigation of Differences in Ansys Solvers CFX And Fluent.

Acred, A. & Hunt, G. R. 2014. Stack Ventilation in Multi-Storey Atrium Buildings: A Dimensionless Design Approach. *Building and Environment,* 72**,** 44-52.

Aflaki, A., Mahyuddin, N., Al-Cheikh Mahmoud, Z. & Baharum, M. R. 2015. A Review on Natural Ventilation Applications Through Building Façade Components and Ventilation Openings in Tropical Climates. Energy and Buildings, 101, 153-162.

Ahmed, M. M., Abel-Rahman, A. K., Ali, A. H. H. & Suzuki, M. 2016. Double-skin Façade: The State of Art on Building Energy Efficiency. *Journal of Clean Energy Technologies,* 4.

Alharbi, N. & Liu. 2015. A Multi-Scale Method for Large Eddy Simulation of Turbulence, 2015 ICMIDS Conference, Http://Www.Arl.Psu.Edu/Icmids/

Allard, F. and Santamouris, M., 1998. Natural Ventilation in Buildings: A Design Handbook (BEST (Buildings, Energy and Solar Technology).

Almohammadi, K.M., Ingham, D.B., Ma, L. and Pourkashan, M., 2013. Computational fluid dynamics (CFD) mesh independency techniques for a straight blade vertical axis wind turbine. Energy, 58, pp.483-493.

Anđelković, A. S., Gvozdenac-Urošević, B., Kljajić, M. & Ignjatović, M. G. 2015. Experimental Research of The Thermal Characteristics of a Multi-Storey Naturally Ventilated Double-skin Façade. Energy and Buildings, 86, 766-781.

Andersen, C. E., Bergsøe, N. C., Majborn, B. & Ulbak, K. 1997. Radon and Natural Ventilation in Newer Danish Single-Family Houses. *Indoor Air,* 7**,** 278-286.

Ansys, C. 2014. Theory Guide; Ansys. *Inc.: Canonsburg, Pa, USA*.

Arons, D. M. M., and L. R. Glicksman. "Double-skin, airflow Façades: Will the popular European model work in the USA." In Proceedings of ICBEST 2001, International Conference on Building Envelope Systems and Technologies, Ottawa, Canada, vol. 1, pp. 203-207. 2001.

ASHRAE 1992. Standard 55 - Thermal environmental conditions for human occupancy, Atlanta, USA, American Society of Heating, Refrigerating and Air-conditioning Engineers Inc.

ASHRAE 2001. ASHRAE 62 Ventilation for Acceptable Indoor Air Quality. Standard 62/2001. Atlanta.

ASHRAE 2009. Handbook—Fundamentals. Atlanta, Ga: American Society of Heating, Refrigerating and Air Conditioning Engineers.

ASHRAE 2013. ASHRAE 55 - Thermal Environmental Conditions for Humam Occupancy. Atlanta: Ame.

Aswani, A., Master, N., Taneja, J., Smith, V., Krioukov, A., Culler, D. and Tomlin, C., 2012, June. Identifying models of HVAC systems using semiparametric regression. In 2012 American Control Conference (ACC) (pp. 3675-3680). IEEE.

Atkinson, K. and Han, W., 2009. Numerical solution of fredholm integral equations of the second kind. In Theoretical Numerical Analysis (pp. 473-549). Springer, New York, NY.

Auliciems, A. and Szokolay, S.V., 1997. Thermal comfort. PLEA.

Awbi, H. B. 2003. Ventilation of Buildings, Taylor & Francis.

Awbi, H.B., 2007. Ventilation systems: design and performance. Routledge.

AWBI, H. B. (ed.) 2008. Ventilation systems: design and performance, London: Taylor& Francis.

Aynsley, R.M., Delta T Corp, 2007. Fan blade modifications. U.S. Patent 7,252,478.

Azarbayjani, M. 2010. Beyond Arrows: Energy Performance of a New, Naturally Ventilated Double-Skin Façade Configuration for a High-Rise Office Building in Chicago. University of Illinois At Urbana-Champaign.

Bahadori, M.N., 1978. Passive cooling systems in Iranian architecture. Scientific American, 238(2), pp.144-155.

Balocco, C. and Colombari, M., 2006. Thermal behaviour of interactive mechanically ventilated double-glazed façade: Non-dimensional analysis. Energy and Buildings, 38(1), pp.1-7.

Balocco, C., 2002. A simple model to study ventilated Façades energy performance. Energy and Buildings, 34(5), pp.469-475.

Barbosa, S. & IP, K. 2014. Perspectives of double skin façades for naturally ventilated buildings: A review. Renewable and Sustainable Energy Reviews, 40, 1019-1029.

BBRI 2002. Source Book for A Better Understanding of Conceptual and Operational Aspects of Active Façades.: Department of Building Physics, Indoor Climate and Building Services.

Betts, P L and Bokhari, 2000, Experiments on Turbulent Natural Convection in an Enclosed Tall Cavity, Int. J. Heat and Flow, Vol 21, Pp 675 – 683.

Blaser, W. 2004. Post Tower: Helmut Jahn, Werner Sobek, Matthias Schuler, Birkhauser.

Bordass, B., Cohen, R., Standeven, M. and Leaman, A., 2001. Assessing building performance in use 3: energy performance of the Probe buildings. Building Research & Information, 29(2), pp.114-128.

Boussinesq, J., 1903. Thōrie analytique de la chaleur mise en harmonie avec la thermodynamique et avec la thōrie mōanique de la lumi_re: Refroidissement et c̄hauffement par rayonnement, conductibilit̄ des tiges, lames et masses cristallines, courants de convection, thōrie mōanique de la lumi_re. 1903. xxxii, 625, [1] p (Vol. 2). Gauthier-Villars.

Brightman, R.I., Torres, J.J. and Donnelly, J., 1997. Energetics of larval red drum, Sciaenops ocellatus. Part II: Growth and biochemical indicators. Oceanographic Literature Review, 12(44), pp.1545-1546.

Brown, B., 2016. An introduction to the design and application of double skin facades in North American high-rise architecture (Doctoral dissertation, Cork Institute of Technology).

Celik, I. B. 1999. Introductory Turbulence Modeling. Western Virginia University.

CFX5 "User Menu Version 5.6" CFX International, Harwell, Uk, 2003.

Chan, A. L. S., Chow, T. T., Fong, K. F. & Lin, Z. 2009. Investigation on Energy Performance of Double-skin Façade in Hong Kong. Energy and Buildings, 41, 11351142.

Chan, A.L.S. and Chow, T.T., 2014. Calculation of overall thermal transfer value (OTTV) for commercial buildings constructed with naturally ventilated double skin façade in subtropical Hong Kong. *Energy and Buildings*, *69*, pp.14-21.

Chenvidyakarn, T. & Woods, A. W. 2010. On the natural ventilation of two independently heated spaces connected by a low-level opening. Building and Environment, 45, 586-595.

Chmielewski, M. and Gieras, M., 2013. Three-zonal wall function for k-ε turbulence models. Computational methods in science and technology, 19(2), pp.107-114.

Choi, W., Joe, J., Kwak, Y. & Huh, J.-H. 2012. Operation and Control Strategies for Multi-Storey Double-skin Façades During the Heating Season. *Energy and Buildings,* 49**,** 454-465.

Chou, S. K., Chua, K. J. & Ho, J. C. 2009. A Study on The Effects of Double-skin Façades on The Energy Management in Buildings. Energy Conversion and Management, 50, 22752281.

CIBSE 2005. Applications Manual Am10. Natural Ventilation in Non-Domestic Buildings. Great Britain: Chartered Institution of Building Services Engineers (CIBSE).

CIBSE 2006. Knowledge Series. Comfort. Great Britain: Chartered Institution of Building Services Engineers (CIBSE).

CIBSE 2010. Knowledge Series. How to Manage Overheating in Buildings: A Practical Guide to Improving summertime Comfort in Buildings. Great Britain: Chartered Institution of Building Services Engineers (CIBSE).

CIBSE 2015. Applications Manual Am11. Building Performance Modelling. Great Britain: Chartered Institution of Building Services Engineers (CIBSE).

Clements-Croome, D., 2006. Indoor environment and productivity. In Creating the productive workplace (pp. 53-82). Taylor & Francis.

Clements-Croome, D.J., Awbi, H.B., Bakó-Biró, Z., Kochhar, N. and Williams, M., 2008. Ventilation rates in schools. Building and Environment, 43(3), pp.362-367.

Compagno, A. 2002. Intelligent Glass Façades: Material, Practice, Design, Birkhauser, Basel.

Cook M.J., Ji, Y. & Hunt Gr. Cfd Modelling of Natural Ventilation: Combined Wind and Buoyancy Forces, International Journal of Ventilation, Vol. 1, Pp. 169180, 2003.

Daisey, J.M., Angell, W.J. and Apte, M.G., 2003. Abstract. Indoor air, 13(1), pp.53-64.

Daniels, B.J. and Crisinel, M., 1993. Composite slab behavior and strength analysis. Part II: Comparisons with test results and parametric analysis. Journal of Structural Engineering, 119(1), pp.36-49.

Darkwa, J., Li, Y. & Chow, D. H. C. 2014. Heat Transfer and Air Movement Behaviour In A Double-Skin Façade. Sustainable Cities and Society, 10, 130-139.

Day, J. K. & Gunderson, D. E. 2015. Understanding High Performance Buildings: The Link Between Occupant Knowledge of Passive Design Systems, Corresponding Behaviors, Occupant Comfort and Environmental Satisfaction. Building and Environment, 84, 114124.

De Gracia, A., Castell, A., Navarro, L., Oró, E. & Cabeza, L. F. 2013. Numerical Modelling of Ventilated Façades: A Review. Renewable and Sustainable Energy Reviews, 22, 539-549.

De Wit, S. & Augenbroe, G. 2002. Analysis of uncertainty in building design evaluations and its implications. Energy and Buildings, 34, 951-958.

Deardorff, J. W. A Numerical Study of Three-Dimensional Channel Flow At Large Reynolds Numbers, J. Fluid Mech., Vol. 41, Pp. 453-480, 1970.

Ding, W., Hasemi, Y. & Yamada, T. 2005. Natural Ventilation Performance of a Double-Skin Façade with A Solar Chimney. Energy and Buildings, 37, 411-418.

Djamila, H., Chu, C.-M. & Kumaresan, S. 2014. Effect of Humidity on Thermal Comfort in The Humid Tropics. Journal of Building Construction and Planning Research, 2, 109117.

Dutton, S. M., Banks, D., Brunswick, S. L. & Fisk, W. J. (2013), 'Health and economic implications of natural ventilation in california offices', Building and Environment 67, 34– 45.

Edagawa, A., Kimura, A., Tanaka, H., Tomioka, K., Sakabe, K., Nakajima, C., Suzuki, Y. et al. (2008), 'Detection of culturable and nonculturable legionella species from hot water systems of public buildings in japan', Journal of applied microbiology 105(6), 2104–2114.

Edwards M., Linden P.F. & Walker R.R. Theory and Practice – Natural Ventilation Modelling, Proc. Of Cibse National Conference, Pp. 102-108, 1994.

Eicker, U., Fux, V., Bauer, U., Mei, L. & Infield, D. 2008. Façades and Summer Performance of Buildings. Energy and Buildings, 40, 600-611.

Etheridge, D & Sandberg, M. Building Ventilation – Theory and Measurement. John Wiley and Sons Ltd, First Edition, 1996, Isbn 0-471-96087-X.

Etheridge, D. & Ford, B. Natural Ventilation of Tall Buildings–Options and Limitations. Proc., Ctbuh 8th World Congress, 2008. 226-232.

Ferreira, P., Ruano, A., Silva, S. & Conceio, E. (2012), 'Neural networks based predictive control for thermal comfort and energy savings in public buildings', Energy and Buildings 55, 238 – 251. Cool Roofs, Cool Pavements, Cool Cities, and Cool World.

Fisk, W.J., 2000. Health and productivity gains from better indoor environments and their relationship with building energy efficiency. Annual review of energy and the environment, 25(1), pp.537-566.

Fisk, W.J., 2002. How IEQ affects health, productivity. ASHRAE journal, 44(LBNL-51381).

Ford, B. and Schiano-Phan, R., 2005. Double-Skin Façades: Improving Performance and Reducing Costs. Proceedings of Passive and Low Energy Architecture Environmental Sustainability: The Challenge of Awareness in Developing Societies, Beirut, Lebanon, pp.13-16.

Gadi, M. B. 2010. 27 - Application of design and passive technologies for thermal comfort in buildings in hot and tropical climates A2 - Hall, Matthew R. Materials for Energy Efficiency and Thermal Comfort in Buildings. Woodhead Publishing.

Ghasemi, N. & Ghasemi, F. 2017. Double-Skin Façade Technology and Its Aspects In Field of Aesthetics, Environment and Energy Consumption Optimization. International Journal of Scientific Study, 5, 293–307.

Ghiaus, C., Allard, F., Santamouris, M., Georgakis, C., Roulet, C.A., Germano, M., Tillenkamp, F., Heijmans, N., Nicol, F., Maldonado, E. and Almeida, M., 2005. Natural ventilation of urban buildings–summary of URBVENT project. In Proceedings of the 1st International Conference on passive and low energy cooling for the built environment: PALENC (pp. 29-33).

Gratia, E. & De Herde, A. 2004a. Is Day Natural Ventilation Still Possible in Office Buildings with A Double-Skin Façade? Building and Environment, 39, 399-409.

Gratia, E. & De Herde, A. 2004b. Natural Cooling Strategies Efficiency in An Office Building with A Double-Skin Façade. Energy and Buildings, 36, 1139-1152.

Gratia, E. & De Herde, A. 2007a. Greenhouse Effect in Double-Skin Façade. Energy and Buildings, 39, 199-211.

Gratia, E. & De Herde, A. 2007b. The Most Efficient Position of Shading Devices in A Doubleskin Façade. Energy and Buildings, 39, 364-373.

Haase, M. and Amato, A., 2006. Design considerations for double-skin Façades in hot and humid climates.

Haase, M., Marques Da Silva, F. & Amato, A. 2009. Simulation of Ventilated Façades in Hot and Humid Climates. Energy and Buildings, 41, 361-373.

Hamza, N. 2008. Double Versus Single Skin Façades in Hot Arid Areas. Energy and Buildings, 40, 240-248.

Hamza, N. A. 2004. The Performance of Double-skin Façades in Office Building Refurbishment in Hot Arid Areas. Phd, University of Newcastle Upon Tyne.

Hazem, A., Ameghchouche, M. & Bougriou, C. 2015. A Numerical Analysis of The Air Ventilation Management and Assessment of The Behavior of Double-skin Façades. Energy and Buildings, 102, 225-236.

Heerwagen, J., 2000. Green buildings, organizational success and occupant productivity. Building Research & Information, 28(5-6), pp.353-367.

Heinberg, R., 2009. Blackout: coal, climate and the last energy crisis. New Society Publishers.

Hensen, J., Bartak, M. and Drkal, F., 2002. Modeling and simulation of a double-skin Façade system. ASHRAE transactions, 108(2), pp.1251-1259.

Hirsch, M.W., 1989. Convergent activation dynamics in continuous time networks. Neural networks, 2(5), pp.331-349.

Hong, N.H., Sakai, J. and Brizé, V., 2007. Observation of ferromagnetism at room temperature in ZnO thin films. Journal of Physics: Condensed Matter, 19(3), p.036219.

Hong, T., Kim, J., Lee, J., Koo, C. & Park, H. 2013. Assessment of Seasonal Energy Efficiency Strategies of a Double Skin Façade in a Monsoon Climate Region. Energies, 6, 4352-4376.

IEA, I. E. A. 2013a. Technology Roadmap Energy Efficient Building Envelopes Energy Technology Perspectives France: International Energy Agency.

IEA, I. E. A. 2013b. Transition to Sustainable Buildings: Strategies and Opportunities To 2050. Energy Technology Perspectives. International Energy Agency.

Irwin, P., Kilpatrick, J., Robinson, J. & Frisque, A. 2008. Wind and tall buildings: negatives and positives. The structural design of tall and special buildings, 17, 915-928.

Joe, J., Choi, W., Kwak, Y. & Huh, J.-H. 2014. Optimal Design of a Multi-Story Double-skin Façade. *Energy and Buildings, 76*, 143-150.

Kim, S. Y., and K. D. Song. "Determining photosensor conditions of a daylight dimming control system using different double-skin envelope configurations." *Indoor and Built Environment* 16, no. 5 (2007): 411-425.

Kim, Y.-M., Kim, S.-Y., Shin, S.-W. & Sohn, J.-Y. 2009. Contribution of Natural Ventilation in A Double-skin Envelope to Heating Load Reduction in Winter. Building and Environment, 44, 2236-2244.

Kleiven, T., 2003. Natural ventilation in buildings: architectural concepts, consequences and possibilities. Institutt for byggekunst, historie og teknologi.

Kragh, M. Monitoring of Advanced Façades And Environmental Systems. In: Keiller, A. & Ledbetter, S., Eds. Whole-Life Performance of Façades, 2001 Bath, Uk.

Lars Davidson. An Introduction to Turbulence Models. Chalmers university of technology, 2003.

Laustsen, J. 2008. Energy efficiency requirements in building codes, energy efficiency policies for new buildings. International Energy Agency (IEA), 2, 477-488.

Lienhard, J.H., 1966. Synopsis of lift, drag, and vortex frequency data for rigid circular cylinders (Vol. 300). Pullman, WA: Technical Extension Service, Washington State University.

Liu, W and Makhvilaze, G, 2008, An Implicit Finite Element Solution of Thermal Flows at Low Mach Number, J. Comput. Physics, Vol 227, Pp 2743 – 2757

Liu, W. 2009. A Triple Level Finite Element Method for Large Eddy Simulations. Journal of Computational Physics, 228, 2690-2706.

Lou, W., Huang, M., Zhang, M. & Lin, N. 2012. Experimental and Zonal Modeling For Wind Pressures on Double-Skin Façades of a Tall Building. Energy and Buildings, 54, 179-191.

Manz, H. 2004. Total Solar Energy Transmittance of Glass Double Façades with Free Convection. Energy and Buildings, 36, 127-136.

Marques Da Silva, F., Gomes, M. G. & Rodrigues, A. M. 2015. Measuring and Estimating Airflow in Naturally Ventilated Double-skin Façades. Building and Environment, 87, 292-301.

Mergi, C. & Al-Dawoud, A. 2007. Integration of ventilation in the design of commercial buildingsapplication to atrium buildings in hot/humid climate. Architecture and Environment, 6, 14-27.

Mingotti, N., Chenvidyakarn, T. & Woods, A. W. 2011. The Fluid Mechanics of The Natural Ventilation of a Narrow-Cavity Double-Skin Façade. Building and Environment, 46, 807-823.

Mingotti, N., Chenvidyakarn, T. & Woods, A. W. 2013. Combined Impacts of Climate and Wall Insulation on The Energy Benefit of An Extra Layer of Glazing in The Façade. Energy and Buildings, 58, 237-249.

Moosavi, L., Mahyuddin, N., Ab Ghafar, N. & Ismail, M. A. 2014. Thermal Performance of Atria: An Overview of Natural Ventilation Effective Designs. *Renewable and Sustainable Energy Reviews, 34,* 654-670.

Muhič, S. and Butala, V., 2004. The influence of indoor environment in office buildings on their occupants: expected–unexpected. Building and Environment, 39(3), pp.289-296.

Mulyadi, R. 2012. Study on Naturally Ventilated Double-Skin Façade in Hot and Humid Climate. Nagoya University.

Murakami, S. Overview of Turbulence Models Applied In Cwe-1997, 2nd, Eacwe, Italy, Pp.3-23, 1997.

Myhrvold, A.N., Olsen, E. and Lauridsen, O., 1996. Indoor environment in schools–pupils health and performance in regard to CO2 concentrations. Indoor Air, 96(4), pp.369-371.

Nasrollahi, N. & Salehi, M. 2015. Performance Enhancement of Double-skin Façades in Hot and Dry Climates Using Wind Parameters. Renewable Energy, 83, 1-12.

Nelson, N. A., Kaufman, J. D., Burt, J. & Karr, C. (1995), 'Health symptoms and the work environment in four nonproblem united states office buildings', Scandinavian journal of work, environment & health pp. 51–59.

Nguyen, A.T. and Reiter, S., 2014. A climate analysis tool for passive heating and cooling strategies in hot humid climate based on Typical Meteorological Year data sets. Energy and buildings, 68, pp.756-763.

Nguyen, T. M. N., Ilef, D., Jarraud, S., Rouil, L., Campese, C., Che, D., Haeghebaert, S., Ganiayre, F., Marcel, F., Etienne, J. et al. (2006), 'A community-wide outbreak of legionnaires disease linked to industrial cooling towershow far can contaminated aerosols spread?', Journal of Infectious Diseases 193(1), 102–111.

Nicol, F., Humphreys, M. & Humphreys, M. 2012. Adaptive Thermal Comfort: Principles and Practice, London, Routledge.

Nielsen, P. V. (ed.) 2007. Computational Fluid Dynamics in Ventilation Design, Brussels: Rehva.

Ochoa, C. E. & Capeluto, I. G. 2009. Advice Tool for Early Design Stages of Intelligent Façades Based on Energy and Visual Comfort Approach. Energy and Buildings, 41, 480488.

Oesterle, E., Lieb, R.-D., Lutz, M. & Heusler, W. 2001. Double-skin Façades – Integrated Planning, Munich, Prestel.

Oldewurtel, F., Parisio, A., Jones, C.N., Gyalistras, D., Gwerder, M., Stauch, V., Lehmann, B. and Morari, M., 2012. Use of model predictive control and weather forecasts for energy efficient building climate control. Energy and Buildings, 45, pp.15-27.

Ole Fanger, P., 2006. What is IAQ?. Indoor air, 16(5), pp.328-334.

Pappas, A. & Zhai, Z. 2008. Numerical Investigation on Thermal Performance and Correlations of Double-skin Façade with Buoyancy-Driven Airflow. Energy and Buildings, 40, 466-475.

Park, C.-S., Augenbroe, G., Sadegh, N., Thitisawat, M. & Messadi, T. 2004. Realtime Optimization of a Double-Skin Façade Based on Lumped Modeling And Occupant Preference. Building and Environment, 39, 939-948.

Pasquay, T. 2004. Natural Ventilation in High-Rise Buildings with Double Façades, Saving or Waste of Energy. Energy and Buildings, 36, 381-389.

Patankar, S. V. 1980. Numerical Heat Transfer and Fluid Flow, (1980). *Hemisphere, New York*, 25-73.

Pérez-Grande, I., Meseguer, J. & Alonso, G. 2005. Influence of Glass Properties on The Performance of Double-Glazed Façades. Applied Thermal Engineering, 25, 3163-3175.

Poirazis, H. 2006. Double-skin Façades: A Literature Review. Sweden: Iea Shc Task 34 Ecbcs Annex 43.

Poirazis, H., 2004. Double-skin façades for office buildings. Holland: Lund Institute of Technology.

Popescu, D., Bienert, S., Schtzenhofer, C. & Boazu, R. (2012), 'Impact of energy efficiency measures on the economic value of buildings', Applied Energy 89(1), 454 – 463. Special issue on Thermal Energy Management in the Process Industries.

Radhi, H., Sharples, S. & Fikiry, F. 2013. Will Multi-Façade Systems Reduce Cooling Energy in Fully Glazed Buildings? A Scoping Study of Uae Buildings. Energy and Buildings, 56, 179-188.

Rahmani, B., Kandar, M. Z. & Rahmani, P. 2012. How Double-skin Façade'S Air-Gap Sizes Effect on Lowering Solar Heat Gain In Tropical Climate? World Applied Sciences Journal 18, 774-778.

Rijal, H. B., Tuohy, P., Humphreys, M. A., Nicol, J. F., Samuel, A. & Clarke, J. 2007. Using Results from Field Surveys to Predict the Effect of Open Windows on Thermal Comfort and Energy Use in Buildings. Energy and Buildings, 39, 823-836.

Sadineni, S. B., Madala, S. & Boehm, R. F. 2011. Passive Building Energy Savings: A Review of Building Envelope Components. Renewable and Sustainable Energy Reviews, 15, 3617-3631.

Saelens, D. 2002. Energy Performance Assessments of Single Storey Multiple-Skin Façades. Phd, Catholic University of Leuven.

Safer, N., Woloszyn, M. & Roux, J. J. 2005. Three-Dimensional Simulation with A Cfd Tool of The Airflow Phenomena in Single Floor Double-Skin Façade Equipped with A Venetian Blind. Solar Energy, 79, 193-203.

Santamouris, M., 2013. Energy and climate in the urban built environment. Routledge.

Schiefer, C., Heimrath, R., Hengsberger, H., Mach, T., Streicher, W., Santamouris, M., Farou, I., Erhorn, H., Erhorn-Kluttig, H., Matos, M. D., Duarte, R. & Blomsterberg, Å. 2008. Best Practice for Double-skin Façades Intelligent Energy Europe.

Schlichting, H. Boundary-Layer Theory, 7th Ed., Mcgraw-Hill, New York, 1979.

Schneider, G.E. and Raw, M.J., 1987. Control volume finite-element method for heat transfer and fluid flow using colocated variables—1. Computational procedure. Numerical Heat Transfer, Part A Applications, 11(4), pp.363-390.

Seppanen, O., Fisk, W.J. and Lei, Q.H., 2006. Effect of temperature on task performance in officeenvironment (No. LBNL-60946). Ernest Orlando Lawrence Berkeley NationalLaboratory, Berkeley, CA (US).

Seppanen, O.A., Fisk, W.J. & Mendell, M.J. Association of Ventilation Rates and Co2 Concentrations with Health and Other Responses in Commercial and Institutional Buildings, Indoor Air, Vol. 9, Pp. 226-252, 1999.

Shameri, M. A., Alghoul, M. A., Elayeb, O., Zain, M. F. M., Alrubaih, M. S., Amir, H. & Sopian, K. 2013. Daylighting Characterstics Of Existing Double-Skin Façade Office Buildings. Energy and Buildings, 59, 279-286.

Shameri, M. A., Alghoul, M. A., Sopian, K., Zain, M. F. M. & Elayeb, O. 2011. Perspectives of Double-skin Façade Systems in Buildings and Energy Saving. Renewable and Sustainable Energy Reviews, 15, 1468-1475.

Singh, M. K., Mahapatra, S. & Atreya, S. K. 2011. Adaptive Thermal Comfort Model for Different Climatic Zones of North-East India. Applied Energy, 88, 2420-2428.

Smith, G.D., 1985. Numerical solution of partial differential equations: finite difference methods. Oxford university press.

Stec, W. & Paassen, D. V. Sensitivity of The Double-skin Façade on The Outdoor Conditions. International Conference on Air Quality and Climate; Indoor Air 2005 Beijing.

Streicher, W., Heimrath, R., Hengsberger, H., Mach, T., Waldner, R., Flamant, G., Loncour, X., Guarracino, G., Santamouris, H., Farou, I., Zerefos, S., Assimakopoulos, M., Duarte, R., Blomsterberg, A., Sjoberg, L. & Blomquist, C. 2007. On the Typology, Costs, Energy Performance, Environmental Quality and Operational Characteristics of Double-skin Façades in European Buildings. In: Santamouris, M. (Ed.) Advances in Building Energy Research Earthscan.

Sundell, J., Levin, H., Nazaroff, W.W., Cain, W.S., Fisk, W.J., Grimsrud, D.T., Gyntelberg, F., Li, Y., Persily, A.K., Pickering, A.C. and Samet, J.M., 2011. Ventilation rates and health: multidisciplinary review of the scientific literature. Indoor air, 21(3), pp.191-204.

Thomas, R. (2013), Environmental Design: An Introduction for Architects and Engineers, Taylor & Francis.

Torres, M., Alavedra, P., Guzmán, A., Cuerva, E., Planas, C., Clemente, R. & Escalona, V. Double-skin Façades - Cavity and Exterior Openings Dimensions for Saving Energy on Mediterranean Climate. Building Simulation, 2007 Beijing, China.

Versteeg, H. K. & Malalasekera, W. 1995. An Introduction to Computational Fluid Dynamics: The Finite Volume Method. Pearson Education. Longman Group Ltd. Isbn 0-470-23515-2.

Versteeg, H.K. and Malalasekera, W., 1996. An introduction to computation fluid dynamites.

Vincent, D., Annesi, I., Festy, B. & Lambrozo, J. (1997), 'Ventilation system, indoor air quality, and health outcomes in parisian modern office workers', Environmental research 75(2), 100–112.

Wang, L. & Chen, Q. 2008. Evaluation of Some Assumptions Used in Multizone Airflow Network Models. Building and Environment, 43, 1671-1677.

Weir, G. & MUNEER, T. 1998. Energy and environmental impact analysis of double-glazed windows. Energy Conversion and Management, 39, 243-256.

Wendt, J.F. ed., 2008. *Computational fluid dynamics: an introduction.* Springer Science & Business Media.

Wesseling, P. and Oosterlee, C.W., 2001. Geometric multigrid with applications to computational fluid dynamics. Journal of computational and applied mathematics, 128(1-2), pp.311-334.

Wong, P. C. 2008. Natural ventilation in double-skin façade design for office buildings in hot and humid climate. The University of New South Wales Australia.

Wong, P. C., Prasad, D. & Behnia, M. Methodology for Natural Ventilation Design for Highrise Buildings in Hot and Humid Climate. World Sustainable Building Conference, 2005 Tokyo.

Wong, P., Prasad, D. & Behnia, M. 2008. A new type of double-skin façade configuration for the hot and humid climate. Energy and Buildings, 40, 1941-1945

Wood, A. & Salib, R. 2013. Natural Ventilation in High-Rise Office Buildings. Council on Tall Buildings and Urban Habitat.

Wyon, D. (1993), 'Healthy buildings and their impact on productivity', proceedings of Indoor Air 93(6), 3–13.

Wyon, D. (1997), 'Indoor environmental effects on productivity', Proceedings of Paths to Better Building Environments.

Wyon, D.P., 2000, October. Enhancing productivity while reducing energy use in buildings. In Proceedings of the E-Vision 2000 Conference (pp. 11-13).

Wyon, D.P., 2004. The effects of indoor air quality on performance and productivity. Indoor air, 14(7), pp.92-101.

Wyon, D.P., Andersen, I.B. and Lundqvist, G.R., 1979. The effects of moderate heat stress on mental performance. Scandinavian journal of work, environment & health, pp.352-361.

Yeang, K., 2006. A Vertical Theory of Urban Design. In Urban Design Futures (pp. 153-158). Routledge.

Zhang, J., Christianson, L.L. and Riskowski, G.L., 1992. Detailed measurements of room air distribution for evaluating numerical simulation models. In ASHRAE Winter Meeting (pp. 58-45). Publ by ASHRAE.

Zhang, Y. & Barrett, P. 2012. Factors Influencing The Occupants'Window Opening Behaviour In A Naturally Ventilated Office Building. Building and Environment, 50, 125134.

Zhang, Y., Wang, J., Chen, H., Zhang, J. & Meng, Q. 2010. Thermal Comfort in Naturally Ventilated Buildings in Hot-Humid Area of China. Building and Environment, 45, 25622570.

Zienkiewicz, O.C. and Taylor, R.L., 1989. The finite element method: basic formulation and linear problems (Vol. 1, pp. 1-20). London: McGraw-Hill.